



UNIVERSIDADE D
COIMBRA

Gonçalo José Martins Afonso

IMPACT OF REBAUDIOSIDE A IN CANCER
CELL METABOLISM: POTENTIAL AS A SAFE
CHEMOTHERAPEUTIC ADJUVANT

Dissertação no âmbito do Mestrado em Bioquímica, orientada pela Professora Doutora Teresa Oliveira e pelo Professor Doutor Rui de Carvalho e apresentada ao Departamento de Ciências da Vida da Faculdade de Ciências e Tecnologia da Universidade de Coimbra.

Outubro de 2020



Faculdade de Ciências e Tecnologia | Departamento de Ciências da Vida
Mestrado em Bioquímica

**IMPACT OF REBAUDIOSIDE A IN CANCER CELL
METABOLISM: POTENTIAL AS A SAFE
CHEMOTHERAPEUTIC ADJUVANT**

Gonçalo J. M. Afonso

Coimbra
Outubro de 2020

The work presented in this dissertation was developed in the Mitochondrial Toxicology and Experimental Therapeutics group (MitoXT), at the Center for Neuroscience and Cell Biology of University of Coimbra, Portugal, under the supervision of Dr. Teresa Cunha-Oliveira (CNC-UC), as external supervisor, and by Dr. Rui Carvalho (FCTUC-UC), as internal supervisor.

Part of this work was presented in the ESCI Virtual Meeting 2020 | Covid19 edition, virtually held from 20-30th September 2020, under the title “Impact of Rebaudioside A in the metabolism of Breast Cancer cells and assessment of its chemotherapeutic potential” as a short presentation.

This work was financed by the European Regional Development Fund (ERDF), through the COMPETE 2020 - Operational Programme for Competitiveness and Internationalization and Portuguese national funds via FCT – Fundação para a Ciência e a Tecnologia, under projects POCI-01-0145-FEDER-029297; PTDC/BTM-SAL/29297/2017 (“MitoScreening - Development and validation of innovative screening methods for mitochondrial health modulators”) and UIDB/04539/2020

Supported by project “Summer Course in Interdisciplinary Research, Development and Innovation in Cellular and Molecular Metabolism” (15-20/7/245), funded by the Portuguese Foundation for Science and Technology (FCT) and Directorate General for Higher Education (DGES).



UNIÃO EUROPEIA
Fundo Europeu
de Desenvolvimento Regional



CENTER FOR NEUROSCIENCE
AND CELL BIOLOGY
UNIVERSITY OF COIMBRA
PORTUGAL



Aknowledgments

I would like to thank my supervisors, Dr. Teresa Cunha-Oliveira and Dr. Rui Carvalho, for their help throughout this remarkable year, and for believing in my capabilities.

To all my colleagues in the MitoXT group, to its PI, Dr. Paulo Oliveira, for his support, to Dr. Vilma Sardão for helping me with the Seahorse XF Analyser, to Inês Miranda-Santos and Sónia Pinho, for teaching me new techniques and for the help with the Mitoplate-S1 assays.

To all my family, the base of everything I achieve.

Table of Contents

Acknowledgements	vi
Table of Contents	viii
List of Acronyms and Abbreviations	xi
Abstract	xiv
Resumo	xv
1-Introduction	1
1.1 Stevia and Steviol Glycosydes	1
1.2 Known properties of SGs – an overview	3
1.3 SGs and cancer.....	4
1.4 Insulin in cancer	11
1.5 Metabolic profile in cancer treatment	11
1.6 Doxorubicin	13
1.7 Objectives	15
2-Materials and Methods	16
2.1.1 Reagents and materials list	16
2.1.2 Cell lines.....	18
2.2 Methods	19
2.2.1 Cell culture Media Composition	19
2.2.2 Cell culture Procedures	20
2.2.2.1 Cell adaptation to a different culture media.....	20
2.2.2.2 Protocols for cell viability	20
2.3 Resazurin assay.....	21
2.3.1 Background	21
2.3.2 Procedure.....	21
2.4 SRB assay	22
2.4.1 Background	22
2.4.2 Procedure.....	22
2.4.3 Data analysis.....	23
2.5 Metabolic profiling assays.....	23
2.5.1 Mitoplate S-1	23
2.5.1.1 Background	23
2.5.1.2 Procedure.....	26

2.5.1.3 Data analysis.....	26
2.5.2 NMR Metabolic Profiling	27
2.5.2.1 Background	27
2.5.2.2 Protocol.....	27
2.5.2.3 Data analysis.....	28
2.5.3 Seahorse Extracellular Flux Analyzer	29
2.5.3.1 Background	29
2.5.3.2 Protocol.....	31
2.5.3.3 Data analysis.....	32
2.5.4 H ₂ DCFDA oxidation assays	32
2.5.4.1 Background	32
2.5.4.2 Protocol.....	33
2.5.4.3 Data analysis.....	33
2.6 Timeline of all assays.....	34
3-Results and Discussion	35
3.1 Impact of RebA on cell viability	36
3.1.1.1 Details and objectives.....	36
3.1.1.2 IC ₅₀ values for RebA were higher than expected, with no difference in the presence of insulin.....	36
3.1.1.3 IC ₅₀ values retrieved by Resazurin assays were lower than those of SRB.....	38
3.1.1.4 IC ₅₀ values obtained for RebA were higher than those documented for other Steviol Glycosides	38
3.1.1.5 RebA alone seems to lack chemotherapeutic potential.....	41
3.1.2.1 RebA as a potential adjuvant for Doxorubicin – Considerations for the assays	42
3.1.2.2 Neither RebA nor Insulin decreased the IC ₅₀ of Doxorubicin	43
3.1.2.3 The effect of Doxorubicin was enhanced in HG medium.....	45
3.1.3 Choosing concentrations for the other assays	46
3.2 Characterization of metabolic changes induced by RebA	47
3.2.1 Analysis of mitochondrial metabolism by using Mitoplate S-1	47
3.2.1.1 Details and objectives of these assays	47
3.2.1.2 RebA promoted mitochondrial oxidation of substrates associated with the TCA cycle in OX, when compared to control, when in LG an overall increase was observed	48

3.2.1.3 RebA-treated Hs578t cells cultured in LG had metabolic profiles with similarities to those of control cells cultured in OX.....	51
3.2.2 Metabolic profiling through analysis of extracellular and intracellular metabolites.....	55
3.2.2.1 Details and objectives.....	55
3.2.2.2 Analysis of extracellular metabolites through ¹ H NMR assays ..	55
3.2.2.2.1 The spectrum resolved for the commercial sample of RebA was similar to the one obtained for the analytical one, indicating high degree of purity	55
3.2.2.2.2 Increased glucose uptake and lower production of lactate hints at a shift towards a more oxidative phenotype in the presence of RebA.....	57
3.2.2.3 ¹³ C NMR assays suggest an anabolic character of metabolism	62
3.2.3 Impact of RebA for OCR and ECAR	64
3.2.3.1 OCR values were higher in the presence of RebA for cells in LG medium. Spare respiratory capacity and non-mitochondrial respiration were tendentially enhanced.....	64
3.2.3.2 OCR values in the presence of RebA were lower in OX medium.	69
3.2.4 Study of the effect of RebA and correlation with changes in ROS levels. 73	
3.2.4.1 RebA significantly increased oxidation of DCFH into DCF.....	75
4-Conclusions	77
5-References	79
6-Supplementary data	90

List of Acronyms and Abbreviations

Ace	Acetate
Acetyl-Coa	Acetyl-Coenzyme A
Akt	Protein kinase B
ATP	Adenosine Triphosphate
DMEM	Dulbecco's Modified Eagle's Medium
DOX	Doxorubicin
ECAR	Extracellular Acidification Rate
FADH2	Flavin Adenine Dinucleotide
FBS	Fetal Bovine Serum
FCCP	Carbonyl Cyanide 4-(trifluoromethoxy)phenylhydrazone
Glu	Glutamate
GLUT	Glucose Transport Proteins
H ₂ O	Water
H ₂ O ₂	Hydrogen Peroxide
HG	High Glucose medium
IC50	Half Maximal Inhibitory Concentration
Ins	Insulin
IPT	Insulin Potentiation Therapy
Lac	Lactate
LG	Low Glucose medium
NADH	Nicotinamide Adenine Dinucleotide (reduced)
NADPH	Nicotinamide Adenine Dinucleotide Phosphate (reduced)
NHDF	Normal Human Dermal Fibroblasts
OCR	Oxygen Consumption Rate
OX	OXPHOS medium
OXPHOS	Oxidative Phosphorylation
PBS	Phosphate-buffered saline
PI3K	Phosphoinositide 3-kinase
RebA	Rebaudioside A
ROS	Reactive Oxygen Species
SGs	Steviol Glycosides
SRB	Sulforhodamine B
TCA	Tricarboxylic Acid
TNBC	Triple Negative Breast Cancer

Abstract

Steviol Glycosides (SGs) are molecules obtained from plants from the genus *Stevia* Cav. and are commonly used as natural sweeteners. New properties are still being discovered for these molecules, the most remarkable being an apparent behavior as insulin mimetic regarding modulation of GLUT transporters. More recently, several studies suggested a promising use in chemotherapeutic strategies. There is still much to uncover regarding those phenomena, especially related to an eventual use in anti-cancer therapies, with knowledge currently limited to a small number of SGs and an overall lack of non-tumoral cell lines used as control. One of the less studied SGs in this regard is Rebaudioside A (RebA), even though it is one of the most important in the food industry. In this work, effects of RebA in two breast cancer cell lines were tested, as well as in non-tumoral skin fibroblasts, focusing on studying the metabolic changes it might induce and its effects on cell viability. RebA was tested along with Doxorubicin, as a possible adjuvant for this chemotherapeutic drug. Results of Resazurin and SRB assays suggest that RebA had a IC₅₀ for cell viability dozens of times higher than those observed for other SGs, such as stevioside and steviol, and showed no potentiation of the effect of Doxorubicin for neither cell line addressed. On the other hand, NMR, Seahorse Extracellular Flux Analyzer assays and Mitoplate-S1 assays suggested that RebA induced a metabolic rewiring towards a more oxidative metabolism, while experiments with H₂DCFDA suggested an increase in the levels of Reactive Oxygen Species. Those results suggest that, unlike other SGs, RebA may not have an application in chemotherapy, neither on its own nor when used along doxorubicin, but its metabolic changes can be interesting and need to be further studied for application in other therapies.

Keywords: Steviol glycosides, metabolic reprogramming, oxidative phosphorylation, chemotherapy potentiation

Resumo

Glicosídeos de Steviol (SGs) são moléculas obtidas a partir de plantas do género *Stevia* Cav., sendo frequentemente utilizados como adoçantes naturais. Contudo, descobriram-se mais propriedades para essas moléculas, sendo as mais relevantes um aparente comportamento insulino-mimético, relacionado com a modulação de transportadores GLUT. Recentemente, vários estudos sugeriram a possibilidade de serem utilizados em estratégias quimioterapêuticas. Ainda há muito por desvendar sobre esses fenómenos, especialmente com um eventual uso em terapias anti cancro, com o conhecimento atual restringido a um número reduzido de SGs e falta de ensaios em linhas não tumorais como controlo. Um dos SGs menos estudado para estes fins é o Rebaudiosídeo A (RebA), apesar de ser um dos mais importantes na indústria alimentar. Neste trabalho, testaram-se os efeitos do RebA em duas linhas celulares tumorais de cancro da mama, assim como em fibroblastos da pele, empregues como controlo não tumoral, com foco no estudo de alterações metabólicas e efeitos na viabilidade celular. O RebA foi ainda testado em conjunto com a Doxorrubicina, para aferir se pode ser utilizado como adjuvante para este fármaco quimioterapêutico. Ensaio realizados de Resazurina e SRB sugerem que o RebA teve um IC50 para a viabilidade celular significativamente superior ao de outros SGs, tais como o steviol e steviosídeo, e não mostraram potenciação do efeito da Doxorrubicina para nenhuma linha celular testada. Por outro lado, ensaios de RMN, Seahorse e Mitoplate-S1 sugerem que o RebA induziu uma reprogramação metabólica para um metabolismo mais oxidativo, e ensaios com H₂DCFDA a sugerir um aumento nos níveis de espécies reativas de oxigénio. Estes resultados sugerem que, ao contrário de outros SGs, o RebA pode não ter aplicação em quimioterapia, pelo menos quando usado por si só ou em conjunto com a Doxorrubicina, mas as alterações metabólicas induzidas demonstram potencial para serem mais estudadas para aplicação noutras terapias.

Palavras-Chave: Glicosídeos de Steviol, Reprogramação metabólica, Fosforilação oxidativa, Potenciação de quimioterapia

1 - Introduction

Research aimed towards molecules that occur naturally in biological systems could reveal unforeseen insights into important mechanisms as well as new properties that can be extrapolated into biotechnological or clinical use, opening new windows for innovative treatments for a wide array of diseases or providing new alternatives to the existing drugs, which can sometimes be of difficult synthesis and, thus, very expensive. A widely important factor to have in consideration regarding the molecules used for a particular end is that they may possess unknown properties that, when uncovered, can lead to a repurposing towards a totally different area of application. Rebaudioside A (RebA) is a natural molecule commonly used as a sweetener, and, in this work, its effect in breast cancer and human dermal fibroblasts' metabolism was studied, while trying to uncover if it possesses any potential to be used in chemotherapeutic strategies or other therapeutic approaches.

1.1 Stevia and Steviol Glycosides

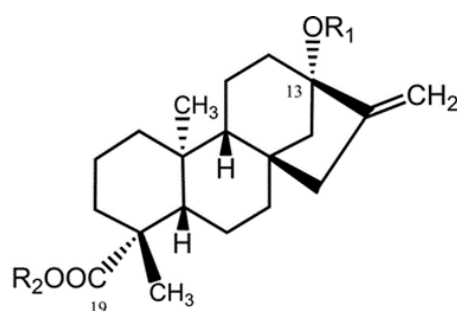
In current society, metabolic-related diseases are becoming more prevalent. Several factors are contributing to this, such as pollution, radiation, exposure to new chemicals with undiscovered properties but, above all, modern nutrition, with overly processed foods, plays a central role in this problem.

Often indiscriminate sugar usage in foods makes it harder for the average consumer to have an equilibrated diet in this regard and making them more prone to conditions such as obesity, diabetes and even cancer. With this in mind, several tries have been made over the recent decades to reduce those problems and allow people to live longer, healthier lives, without metabolic disorders, with one of the most noticeable approaches being the replacement of sugar with sweeteners. Most popular sweeteners are of artificial origin, namely aspartame and sucralose. There are, however, natural alternatives to such substances, the most prominent being stevia.

Stevia Cav. is a genus of plants of the Asteraceae family, native to tropical regions of the American continent. Its leaves have been used for centuries by Native Americans in

those regions for their sweetening properties, and currently its use is ever expanding worldwide, but it is still not established in the Western world as other artificial sweeteners.

From 200 to 400 times sweeter than sugar, while having zero calories (Esen, 2016), its importance in the food industry is growing as side effects for artificial sweeteners are being found, and inclusively some of them have been reported to have a negative impact not only in health (Tandel, 2011) but also in the environment, as it is the case for some synthetic sweeteners such as aspartame and cyclamate not being completely removed in current water treatment processes (Li et al, 2018). The molecules responsible for Stevia's sweetening properties are known as Steviol Glycosides (SGs). SGs all have in their composition steviol, a diterpene compound, and then different combinations of monosaccharides (Figure 1).



Compound name	R ₁ (C-13)	R ₂ (C-19)	Formula	Mass
Steviol	H	H	C ₂₀ H ₃₀ O ₃	318.22
Steviol mono-glucoside	β-Glc	H	C ₂₆ H ₄₀ O ₈	480.27
Steviol mono-glucosyl ester	H	β-Glc	C ₂₆ H ₄₀ O ₈	480.27
Rubusoside	β-Glc	β-Glc	C ₃₂ H ₅₀ O ₁₃	642.33
Steviolbioside	β-Glc-(2→1)-β-Glc	H	C ₃₂ H ₅₀ O ₁₃	642.33
Stevioside	β-Glc-(2→1)-β-Glc	β-Glc	C ₃₈ H ₆₀ O ₁₈	804.38
Rebaudioside A	β-Glc-(2→1)-β-Glc \ (3→1)-β-Glc	β-Glc	C ₄₄ H ₇₀ O ₂₃	966.43
Rebaudioside B	β-Glc-(2→1)-β-Glc \ (3→1)-β-Glc	H	C ₃₈ H ₆₀ O ₁₈	804.38
Rebaudioside C	β-Glc-(2→1)-α-Rha \ (3→1)-β-Glc	β-Glc	C ₄₄ H ₇₀ O ₂₂	950.44
Rebaudioside D	β-Glc-(2→1)-β-Glc \ (3→1)-β-Glc	β-Glc-(2→1)-β-Glc	C ₅₀ H ₈₀ O ₂₈	1128.48
Rebaudioside F	β-Glc-(2→1)-β-Xyl \ (3→1)-β-Glc	β-Glc	C ₄₃ H ₆₈ O ₂₂	936.42
Dulcoside A	β-Glc-(2→1)-α-Rha	β-Glc	C ₃₈ H ₆₀ O ₁₇	788.38

Figure 1: Structure of steviol, and composition of different steviol glycosides. Adapted from Wang et al, 2015

The process for obtention of SGs differ from manufacturer to manufacturer, but the scheme for its obtainment tends to follow the same points, with one first step where the leaves of the plant are subjected to water extraction and its extract purified by ion exchange chromatography, originating a primary extract, then followed by a second step consisting in the recrystallization of the SGs from ethanol or methanol, resulting in products with high purity of SGs, such as RebA and stevioside, the most abundant in the plant.

1.2 Known properties of SGs – an overview

SGs are well known for their sweetening properties, but hidden behind this well-known facet, they have been reported to possess a wide variety of attributes that can lead them to be promising therapeutic agents for several purposes. In the literature, there are several cases of SGs being described as anti-inflammatory, immunomodulators, antihyperglycemic, insulin mimetic, having wound healing potential, among other applications (Koyama et al, 2003; Esen, 2016; Geuns, 2003; Jeppesen et al, 2000; Boonkaewwan et al, 2006; Boonkaewwan et al, 2013). A noteworthy aspect is that SGs' properties are often not well explained nor consistent in the literature, leaving their study as an open area of investigation with a lot to decipher and to make clear, and that may be of particular relevance as they are consumed by a large population.

A particularly well studied aspect about SGs is their enhancement of glucose uptake and modulation of GLUT transporters, whose activity was linked to the PI3K/Akt pathway (Rizzo et al, 2013; Prata et al, 2017; Bhasker et al, 2015). For all those properties, even for the best-known ones, to our best knowledge, the exact protein that SGs activate is unknown. Overall, the explanations for the previously mentioned properties can be summed up as below:

a) Insulin mimetic / Antihyperglycemic properties – SGs increase the phosphorylation of the proteins PI3K and Akt. Furthermore, SGs were able to revert the reduction of the uptake of glucose caused by an inhibitor of the insulin receptor/PI3K/Akt pathway, methylglyoxal (Rizzo et al, 2013). It was observed that they induce the transport of several GLUTs, such as GLUT4, to the plasma membrane (Bhasker et al, 2015; Prata et al, 2017). SG and insulin were shown to cause similar changes in GLUT4 protein content and transcript levels (Bhasker et al, 2015). Due to these similarities, SGs are commonly referred as insulin-mimetic, regarding the uptake of glucose and GLUT modulation. SGs are also antihyperglycemic (Aghajanyan et al, 2017) as, due to their

previously described cellular effects, their presence leads to lower sugar levels in the bloodstream, as cells uptake more glucose.

b) Anti-inflammatory and immunomodulatory – Some studies have been made to understand the mechanisms behind these activities. Stevioside has been shown to suppress lipopolysaccharide-induced release of IL- β and TNF- α , mediated by TLR4, while suppressing nitric oxide without any observed toxic effect up to 1 mM. Furthermore, it was suggested that activation of IKK- β and transcription factor NF- κ B was attenuated (Boonkaewwan et al, 2006). Those results have been confirmed by the same authors in a later article where SGs diminished the lipopolysaccharide-induced pro-inflammatory cytokine gene expression through the I κ B α /NF- κ B pathway (Boonkaewwan et al, 2013).

c) Wound healing- some studies have suggested the potential for SG to enhance wound healing (Das, 2013; Babakhanyan et al, 2017). In these studies, wound healing was enhanced in the presence of SG, when compared with controls. However, no mechanisms to explain this phenomenon were presented.

1.3 SGs and cancer

In addition to the characteristics mentioned in the previous section, there are also suggestions that SGs may have chemotherapeutic potential (Chen, Jun-Ming, Jue Zhang et al, 2018; Chen, Jun-ming, Yongmei Xia et al, 2018; Gupta et al, 2017; Li et al, 2017; Paul et al, 2012; Ren et al, 2017; Yasukawa et al, 2002, Khare et al, 2019, Martínez-Rojo et al, 2020). However, further studies are needed, with the aim of establishing if they can be used as a chemotherapeutic drug, either on its own or as a safe adjuvant agent for already established anti-cancer drugs. Treatment of tumoral cell lines with some SGs such as stevioside and steviol can lead to apoptosis, associated with an arrest in the G1 and at the G2 phases of the cell cycle (Chen Jun-Ming, Jue Zhang et al, 2018; Chen, Jun-ming, Yongmei Xia et al, 2018; Gupta et al, 2017; Paul et al, 2012; Li et al, 2017; Ren et al, 2017). However, even if this conclusion was consensual, the mechanisms behind this are not. Tests in mice with skin cancer suggested that SG have inhibitory effects against the TPA-induced inflammation, thus inhibiting tumor promotion (Yasukawa et al, 2002). However, since SGs are also known to be anti-inflammatory, this method may not have been the most adequate. For an osteosarcoma cell line, U2OS, there was a downregulation of the ability of colony formation through activation of the mitochondrial apoptotic pathway, which was suggested by the increase of the Bax/Bcl-2 ratio and activation tumor protein 53, of cyclin-dependent kinase inhibitor 1 and cyclin-dependent kinase, in a mechanism

independent of Survivin and Caspase 3 (Chen, Jun-ming, Yongmei Xia et al, 2018). The same authors further studied this potential chemotherapeutic activity in six different gastrointestinal cancer cell lines (Chen, Jun-Ming, Jue Zhang et al, 2018) and their results agreed with the previous study. Furthermore, a concentration-dependent overexpression of p21 and p53 and downregulation of Cyclin D1 was observed. This adds further evidence for the activation of the mitochondrial apoptotic pathway. Regarding cytotoxicity, steviol had similar efficiency as 5-fluorouracil at 100-200 µg/mL and had stronger effects at 250 µg/mL (Chen, Jun-Ming, Jue Zhang et al, 2018). Steviol also caused miRNA regulation. Results from a different study were also consistent with the apoptotic behavior observed previously, but this time in colon cancer cells (Ren et al, 2017). In this study, cell cycle arrest has been associated with the MAPK signaling pathway, along with high levels of phosphorylated p38. By inhibiting this pathway and ROS production, the presence of stevioside did not cause any response, suggesting that those may not be necessary for the occurrence of apoptosis. This time, the dose that inhibited cancer cell growth was 5 µM of stevioside. The growth inhibitory effect of stevioside was also documented for ovarian cancer cells through the Akt/ERK pathway (Li et al, 2017). A decrease in mitochondrial transmembrane potential was also observed. These authors suggest an inactivation of the PI3K/Akt signaling pathway, which goes against the previous claims of activation of this pathway by SGs. So, during the apoptotic process, if these results are correct, the regulation of the PI3K/Akt pathway can be reduced. Finally, two studies by different groups were made in MCF-7 breast cancer cells. (Gupta et al, 2017; Paul et al, 2012). For both cases, the previous cell-cycle arrest and apoptotic mechanisms induced by SGs were confirmed. In one case, the IC₅₀ of steviol was 185 µM (Gupta et al, 2017), while for the other case, the IC₅₀ was 5 µM (Paul et al, 2012). Also, it has been suggested that a metabolite of some SGs, Isosteviol, may act as DNA polymerase and DNA topoisomerase inhibitor, which can be another possible explanation for its chemotherapeutic potential (Mizushima et al, 2005).

Finally, in a more recent study by Martínez-Rojo et al, 2020, it was suggested that an extract from two genera of stevia reduced prostate cancer cells migration and proliferation, indicating that the extract of these plants contains molecules capable of this effect, possibly SGs, but further studies are required to identify the exact origin of this phenomenon, before it can be applied to clinical approaches. It was also used along enzalutamide, but without improvement of the efficiency of enzalutamide in the toxicity towards prostate cancer cells.

An important observation that further suggests that SG can become a potential chemotherapeutic agent is that its tolerance is greater than those of some common

chemotherapeutic drugs, like 5-fluorouracil, and also that steviol appears minimally in the plasma during metabolism, while having a shorter half-life in the human body than 5-fluorouracil and doxorubicin (Chen, Jun-ming, Yongmei Xia et al, 2018; Chen, Jun-Ming, Jue Zhang et al, 2018). This would be translated into higher levels of tolerance to this drug, as well as possible fewer side effects. One must not forget that stevia's extract is regularly consumed by millions of people throughout the world, being considered safe, so if it ends up having any therapeutic potential, there would be less barriers towards its implementation.

Regarding the current literature concerning all the above properties presented by SGs, we find the following observations noteworthy:

a) For all the above chemotherapy-related studies, no non-tumoral cell lines were used as a control, except for Martínez-Rojo et al, 2020, where neo natal human fibroblasts were compared against prostate cancer cells, but no pure SG was tested, being a possibility of the presence of other molecules that might be counteracting eventual toxic effects, such as polyphenols and other antioxidants found in the extract. So, there is an urgent need to determine if SGs' toxicity is higher for tumoral cells than for healthy ones. If SGs happen to have the same (or lower) IC50 for healthy cells than for tumoral cells, this might argue against a potential chemotherapeutical use, at least as a single drug.

b) The exact protein that SG activate is not known for any of the above cases. However, some potential signaling pathways have been reported, in a relatively consistent way, to be activated, such as the PI3K/Akt pathway (Rizzo et al, 2013).

c) Inflammation, immunomodulation (Hawkins and Stephens, 2015; Abu-Eid et al, 2014) and wound-healing (Yu et al, 2017; Abdelkader et al, 2016), also have a connection to the PI3K/Akt pathway, as well as the already discussed antihyperglycemic and anti-tumoral effects (Figure 2). Thus, we suggest that those effects may be partially due to the stimulation of different ramifications of the PI3K/Akt pathway that is known to happen in the presence of SGs. Consequently, the proteins that SGs activate should be upstream of PDK1, the last common protein described to be activated by SG. It is also possible that the entirety of the PI3K/Akt pathway's ramifications will be activated. That link has not yet been made in the literature.

d) Some SGs were shown to pass through membrane transporters, entering into the cell, namely the aglycone form, steviol, often resultant from the metabolism of other SGs, through hOAT1 and hOAT3 transporters, to which it had high affinity (Srimaroeng et al, 2005). Even if this may not be an indicator of the location of their target, their action

might not necessarily be dependent of insulin receptors but perhaps it can directly affect other proteins of the PI3K/Akt pathway, activating it somewhere in the middle, potentially bypassing regulatory mechanisms. Since upstream the PDK1 the only non-protein molecule is PIP3, it is a potential candidate for being mimicked by SG.

e) The source of the increased levels of ROS after exposure to SGs has not been determined. However, we believe that it comes from changes in the metabolism, potentially due to the increase in glucose uptake, connected to the GLUTs modulation that has been observed to be caused by SG. A potential shift from glycolysis to OXPHOS was also suggested as a cause for the increase in ROS (Afonso et al, 2020). Also, as SGs interfere with several signaling pathways, such as the PI3K/Akt and p53 pathway, they may cause further functional changes that may contribute to an enhanced ROS production, even related with the mitochondrial apoptotic pathway.

f) Regarding the increase in glycolysis, it is possible that there is also an abnormal increase in OXPHOS, with a theoretical cause for it being a lactic acidosis resulting from augmented glycolysis fluxes, even countering the pro-glycolytic Warburg effect (Wu et al, 2016), characterized by a preference of glycolysis in cancer cells over aerobic respiration that non-tumoral cells tend to adopt, which could result in even higher production of ROS and in elevated oxidative stress (Afonso et al, 2020), suggesting antioxidant imbalance in the cell, in the mitochondria and in the cytoplasm. In mice brain slices at the CA3 area of the hippocampus, ROS are also known to increase in the presence of Rebaudioside A, with increases in both the rate of oxidation of the ROS indicator H₂DCFDA and increases in FAD-linked autofluorescence, a redox-active coenzyme (Afonso et al, 2020). ROS cause a reduction in the levels of PTEN (Leslie, 2003) a protein which is already downregulated in some cancers (Noh et al, 2011) further increasing PI3K/Akt activation, despite the Warburg effect (Icard et al, 2018). It is well known that excessive ROS can cause damage to critical macromolecules, and they could be one of the main causes for apoptosis (Comporti et al, 1989; Redza-Dutordoir and Averill-Bates, 2016).

g) In the literature, SGs concentration ranges for chemotherapeutic activity differ from paper to paper, even in the same cell line and the same SG (Gupta et al, 2017; Paul et al, 2012). So, the conditions in which the cells are grown may have influence in this outcome, as possibly the origin of the sample and methods of extraction or purification.

h) Regarding the combination of SG and insulin, if it is proven to be cumulative, and once Rebaudioside A (RebA) itself enhances the production of insulin in pancreatic

β cells (Jeppensen et al, 2000; Phillipaert et al, 2017), a mixture of both could have the potential to be used for diabetes as an alternative for the traditional insulin injections. While our work is not geared towards diabetes, if the data confirms our predictions, this study can also back up this claim.

i) To our knowledge, the study of the chemotherapeutic potential of SGs, not counting the cases where the whole extract was used such as in Martínez-Rojo et al, 2020, has only been tested for a limited number of SGs, namely steviol and stevioside. As such, there is an opportunity to study the effect of different SGs (Chen, Jun-Ming, Jue Zhang et al, 2018; Chen, Jun-ming, Yongmei Xia et al, 2018; Gupta et al, 2017; Li et al, 2017; Paul et al, 2012; Ren et al, 2017; Yasukawa et al, 2012, Khare et al, 2019).

j) It is also important to note that all those properties described for SG, and not only the well-known modulation of GLUTs transport and increase in glycolysis, are also shown by insulin in some degree: anti-inflammatory / immunomodulatory (Sun et al, 2014); wound healing (Yu et al, 2017; Abdelkader et al, 2016); chemotherapeutic potential (Damyanov et al, 2012) used in Insulin Potentiation Therapy, a controversial approach to chemotherapy where insulin is administrated along with conventional chemotherapeutic drugs, administered in lower dosage than the usual, with the claim that they retain the same effect because insulin potentiates its uptake by the tumoral cells. Regarding the dubious chemotherapeutic potential of insulin, if it in fact exists, it must be dose dependent, since different studies suggested that in some cancers it may even act against chemotherapeutic drugs (Wei et al, 2015). So, this last point is at an urgent need of being addressed, as a way to either confirm or debunk Insulin Potentiation Therapy, which is currently being used by some clinics (Damyanov et al, 2012), exposing it as untrustworthy. Thus, our suggestion is that SGs are insulin mimetic agents not only regarding the increase in glycolysis, but also in every other pathway in which insulin has a role. However, through an extensive analysis of the literature, joining information from different articles, we suggest that either SGs bypass the insulin receptors and overcome the mechanism of regulation for insulin, or the chemotherapeutic activity that SGs may present may come from a different source, such as from an increase in ROS, activation of the PI3K/Akt pathway, by inhibiting DNA polymerase and Topoisomerase (Mizushina et al, 2005) or even lactic acidosis due to aerobic glycolysis overcharge, and then increasing the OXPHOS, due to the effect described by Wu et al, 2016. For the case of high levels of ROS, it could lead to the activation of mitochondrial apoptotic pathways that were described above. If there is any truth to the Insulin Potentiation Therapy, if SGs really are insulin-mimetic, then stevia could be also used for this end with the same mechanism, possibly even combining both for a maximum response. However, the drug

dosage should be maintained close to 100% to avoid an increased probability of development of resistance like it is observed in current Insulin Potentiation Therapy (Geeraert et al, 2019). This would be one of the, if not the first, cases where a direct overstimulation of a metabolic pathway would be used in order to directly kill cancer cells or, at least, to potentiate the effects of chemotherapeutic drugs, according to our knowledge. If this would be the case, overloading cells with glucose would create a metabolic imbalance in cancer cells, thus explaining the chemotherapeutic effects of SGs. So, it would be crucial to test the IC50 of SGs, insulin and their combination, in cells with different metabolic profiles – from more glycolytic to more oxidative - in order to try to assess the previous claim. If proven correct, this method would go against the canonical idea of using only inhibitions for cancer treatment or other ways of impairing a specific cellular function and may open new ways of approaching oncotherapy.

Since different SGs exhibit similar effects but with different potencies, for example, for the increase in glucose uptake (Rizzo et al, 2013), we suggest that the pharmacophore group for the GLUT modulation is within the steviol part of these molecules, also for the eventual chemotherapeutic potential, as steviol showed toxicity towards cancer cells. (Chen, Jun-ming, Yongmei Xia et al, 2018; Chen, Jun-Ming, Jue Zhang et al, 2018; Gupta et al, 2017). Eventually, the different sugar moieties coordinated to this molecule in the different SG may cause different stereochemical properties, resulting in different areas of the steviol being exposed, which may increase or decrease its effects, depending on the SG. Also, the different combinations of sugars possible in SGs lead to molecules with different sizes, which can impact their transport into the cell, leading to a higher or lower uptake. The presence of a glucose molecule as a constituent group of some SG, like RebA, may have some effects on its own.

If our results suggest that cancer cell lines are more vulnerable to the eventual chemotherapeutic potential of SG than healthy cells, this could be due to several factors, such as the Warburg effect, since a lactic acidosis would be easier to achieve and then the overactivation of OXPHOS would theoretically occur first in tumor than in healthy cells. Also, basal levels of ROS in cancer cells are usually higher in tumoral cells (Cantor et al, 2012; Icard et al, 2018; Sayed et al, 2013; Vaupel et al, 2019). Due to this, antioxidant proteins tend to be overexpressed, therefore there is a possibility that cancer cells may not respond so well to an increase in oxidative stress. Also, cancer cells exhibit an elevated level of glucose uptake, with the rate-limiting step being GLUTs-mediated transport of glucose (Adekola et al, 2012) - SGs may attenuate this limitation leading to higher levels of intracellular glucose than the ones that cancer cells can cope with.

1.4 Insulin in cancer

The impact of insulin in cancer might be of special relevance due to the high prevalence of metabolic syndrome worldwide, and thus in the cancers that may arise (Pothiwala et al, 2009). Insulin has been reported to have a direct impact on tumors and their treatment – however with contradicted outcomes in the literature. It has been suggested that high levels of insulin contributed for resistance to oxaliplatin in colon cancer cell lines (Chen et al, 2011) In addition, chemo resistant cells displayed an increased proliferative response to insulin (Djiogue et al, 2013). Also, insulin enhances tumor cell proliferation and might contribute to chemoresistance of gastric cancer cells to 5-fluorouracil, probably due to upregulation of p-glycoprotein (Wei et al, 2015), capable of pumping drugs against the concentration gradient which is powered by ATP. There is a wide amount of data regarding a synergism between insulin and p-glycoproteins towards chemoresistance, with overexpression of this transporter being associated with upregulations of different pathways, such as PI3K / mTor and MAPK (Wang et al, 2013). These outcomes suggest that obesity-related metabolic disorders' effects on chemoresistance at may at least be partly due to insulin. Insulin has also a strong connection with some proteins capable of conferring some kind of resistance to chemotherapeutic agents, such as Caveolin-1, linked to a chemoresistant profile of several cell lines such as the Hs578t (Cai et al, 2004).

However, insulin itself has been used in cancer treatments, some of those quite controversial, such as the Insulin Potentiation Therapy (IPT) (Damyanov et al, 2012). As described in the previous section, this study and other of the same authors suggest that combining insulin with the drugs used in chemotherapy requires smaller dosages of these drugs in order to achieve the same effect. However, despite the alleged promising results, the explanations provided for this phenomenon are not convincing: it is claimed that this is due to insulin increasing membrane permeability (Damyanov et al, 2012). Due to this lack of explanation and shortage of publication of long-term survival rates, this method is controversial (Geeraert et al, 2019). Despite this, it is still being used in some clinics as an alternative method for cancer treatment.

1.5 Metabolic profile in cancer treatment

Metabolism can be everything in cancer. Even some authors suggest that cancer is a metabolic disease (Coller et al, 2014). Thus, it is of highest importance to trace relations between tumor cells metabolism and enhancement of chemotherapeutic strategies, which may lead to the use of tools of metabolic rewiring to be used to treat this disease.

Usually, a healthy cell has a certain requirement of ATP in order to maintain the usual homeostatic processes. But this is not enough for cancer - cancer cells do not only require ATP, but also must meet demands for macromolecular biosynthesis for replication, as well as producing proteins to cope with the increase in ROS originated as byproducts of their metabolism. The response to this is based in the consumption of glucose and glutamine, and in the pathways behind their processing (Coller et al, 2014).

The Warburg effect can be considered a hallmark for most cancers. It was discovered almost a century ago but prevails relevant to this day (Potter et al, 2016). It consists of the fact that cancer cells tend to have glycolysis activated even if the conditions would be more favorable for OXPHOS. Through this, the rate with precursors for other biomolecules are produced is higher, *de novo*, hastening the supply of molecules necessary for fueling cellular division, with enough lipids for new membranes and nucleotides for DNA replication. Uncoupling of glycolysis with OXPHOS, though, may lead to high levels of lactate, which may be toxic in high quantities if the lactic fermentation process is not able to handle high levels of this molecule – it has been observed that lactic acidosis can cause a reversion of the Warburg effect (Wu et al, 2016).

Cancer cells are also dependent on glutamine, the most abundant amino acid in serum, which is used to synthesize cellular biomolecules such as nucleic acids and non-essential amino acids. It is also used as a carbon source to supplement the Krebs cycle through anaplerosis.

Several signaling pathways are of high importance in cancer metabolism. The PI3K/Akt pathway has a crucial role – it is overactivated in a wide array of cancer types (Khan et al, 2013). Its activation is related to the activation of cell growth regulators, mTORC1, that regulates many cellular processes, such as an increase in the synthesis of several proteins, like transcription factors that regulate metabolic gene expression, such as HIF1 α , SREBP-1, c-Myc and p53 (Coller et al, 2014). The PI3K/Akt pathway is also known for the modulation of glycolysis, through the translocation of GLUT transporters promoted by Akt and activation of glycolytic enzymes, such as phosphofructokinase and hexokinase. Production of other biomolecules, such as lipids, are also stimulated through Akt, by stimulating *de novo* fatty acid synthesis.

Mitochondria are the primary source of energy in normal cells, through OXPHOS. However, some types of cancer cells might downregulate mitochondrial activity due to the preference for glycolysis, the Warburg Effect, relegating this organelle to a secondary role, generating the misconception that mitochondria are impaired in most cancers.

Despite this, mitochondria are in fact important in tumors, playing an important role in most of its phases, from malignant transformation (conversion of a normal cell into a neoplastic precursor) to tumor progression and even response to treatment (Porporato et al, 2018). For example, it has been shown that often tumor cells have resistance to mitochondria-mediated regulated cell death, and due to this some drugs are already being used in chemotherapeutic strategies to sensitize the tumors for further treatments (Ashkenazi et al, 2015). Along with this, the mitochondrial metabolism itself might be crucial, since it can be rewired to fulfill the anabolic needs of tumor cells, widening the metabolic options for biosynthesis of required biomolecules for cell proliferation (Zong et al, 2016). For example, metabolic rewiring from glycolysis to fatty acid oxidation or OXPHOS can be achieved in response to microenvironment alterations, such as a lactic acidosis, that will inhibit glycolysis and stimulate those other pathways (Wu et al, 2016).

In addition, it has been suggested that the existence of certain mitochondrial metabolites might be enough for promoting oncogenesis (Gisbergen et al, 2015). Furthermore, mutations in mitochondrial DNA have been reported to have a potential to lead to changes in the electron transport chain (Carew et al, 2002), thus interfering with the OXPHOS, and increasing the levels of ROS. A mechanism to control the levels of those species is by mitophagy, but mitophagy itself can be altered in cancer, through under expression of key genes to this process, being another promoter for oncogenesis. Thus, through a mentality of interfering with mitochondrial function, such as the mechanisms mentioned previously, development of new chemotherapeutic strategies could be achieved.

1.6 Doxorubicin

Doxorubicin (DOX) (Figure 3), also known as Adriamycin, is a chemotherapeutic drug used to treat diverse types of cancer, one of them being breast cancer. It is a non-selective class I antitumor antibiotic (anthracycline) and it acts by inhibiting topoisomerases I and II and intercalating with nucleic acids in DNA, interfering with its uncoiling and thus leading to apoptosis. DOX also causes an increase in ROS, that leads to further DNA damage. However, its use is often limited to a specific dose, due to its severe toxicity towards certain organs, most noticeably, the heart, characterized by an enlargement of the cardiomyocytes with impairment of the mitochondria in the cardiac muscle (Wallace et al, 2020). Furthermore, it may have and an impact in the immune system, in the brain (through production of ROS, despite being unable to cross the blood-brain barrier), in the kidney (through effects in the complexes I and IV of the

mitochondria) and in the liver (also though an increase in ROS) (Ferreira et al, 2018). Those effects can lead to life-threatening conditions. Thus, several strategies are being used in order to make its action more specific towards cancer, such as drug delivery systems (Zhao et al, 2018).

Regarding its pharmacokinetics in plasma, it has a distribution half-life of 5 to 10 minutes, and a terminal phase elimination half-life of 30 hours (Speth et al, 1988). DOX enters the cell through passive diffusion (Speelmans et al, 1994). After it enters the cell, it concentrates within the nuclear compartment rather than in the cytoplasm. However, tumor cells can develop resistance to DOX, for example, through changes in the autophagic pathway (Chen, Chao et al, 2018). In breast cancer, it was observed that DOX increases the levels of ceramide, a cellular lipid messenger, that leads to anti-apoptotic effects, through a mechanism yet to be discovered (Liu et al, 2008).

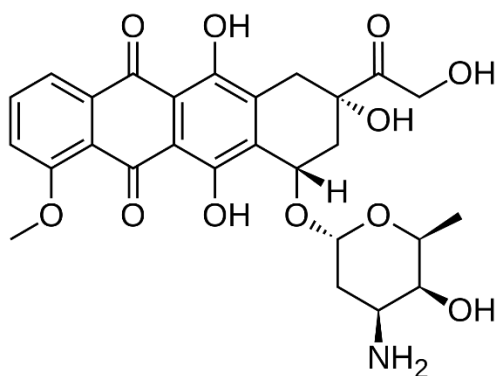


Figure 3- Molecular structure of Doxorubicin. Image obtained from <https://en.wikipedia.org/wiki/Doxorubicin>. Access date: 29/10/2020

1.7 Objectives

The current thesis is focused on the study of the effect of RebA in two different breast cancer cell lines as well as in non-cancer cells, in the form of human skin fibroblasts, and has the following objectives:

- a) Study the effect of RebA on the viability of tumor and non-tumor cells and compare them with the results for steviol and stevioside present in the literature. Determine if RebA has any potential to be used alone in chemotherapy
- b) Assess the IC50 for cell viability of Doxorubicin in the presence of RebA, to determine if this SG can be used as an adjuvant to potentiate the cytotoxicity of this chemotherapeutic drug. Test the cytotoxicity effect of Doxorubicin also in the presence insulin and for cells grown in different media with different metabolic profiles, to try establishing correlations between those conditions.
- c) Try to identify and understand the mechanism behind an eventual potentiation of the action of chemotherapeutical drugs
- d) Analyze the effects of RebA on cancer and non-cancer cells' metabolism, with a focus on the mitochondria and OXPHOS, and compare the results against insulin
- e) Based on the results, suggest other therapeutic applications for RebA

2 – Materials and Methods

2.1.1 Reagents and materials list

Information regarding the main reagents used throughout the assays are compiled in Table 1, with indication of the lot, catalog number and brand, when applicable. The list of materials in present in table 2

Table 1: List of reagents

Name of Reagent	Lot	Catalog Number	Brand
Cell culture			
D-(+)-Glucose	SLBG2661V	G7021-1KG	Sigma-Aldrich
D-Galactose	BCBM1928V	G5388-500G	Sigma-Aldrich
DMEM	SLBF6043V	D5030	Sigma-Aldrich
Fetal Bovine Serum	42F968K	10270-106	Gibco
HEPES	SLBB1143V	H3375-250G	Sigma-Aldrich
Hydrochloric acid (HCl)	1090102	131020	PanReac
L-Glutamine	SLBQ4624V	G3126	Sigma-Aldrich
PBS		BP399-20	Fischer BioReagents
Penstrep (Penicillin/Streptomycin/Amphotericin B)	2051350	15240-062	Gibco
Sodium bicarbonate	010M00291V	S6297-1KG	Sigma-Aldrich
Sodium hydroxide (NaOH)	BCBF6857V	S8045-1KG	Sigma-Aldrich
Sodium pyruvate	SLBB5884V	P2256 - 25G	Sigma-Aldrich
Trypsin	2091244	253-062	Gibco
Viability assays			
Doxorubicin hydrochloride	143376	D1515-10MG	Sigma-Aldrich
Glacial acetic acid	491223	131008.1611	PanReac
Insulin	SLBC1253V	I9278-5ML	Sigma-Aldrich
Methanol	SZBD318SV	32213-2.5L	Sigma-Aldrich
Rebaudioside A 98% (analytical)		TCIAR0095-5G	TCI Europe
Rebaudioside A 98% (commercial)			Provital
Resazurin sodium salt	MKBQ3226V	R7017-5G	Sigma-Aldrich
Sulphorhodamine B sodium salt	MKBD3195	S9012	Sigma-Aldrich
Tris-EDTA	13032	MB01601	NZYTEch
Trypan Blue		T8154	Sigma-Aldrich

Mitoplate S-1			
Biolog MAS		72303	Biolog
Mitoplates S-1		14105	Biolog
Redox dye MC		74353	Biolog
Saponin			Biolog
NMR Metabolic Profiling			
[U ¹³ C] Glucose			
Fumarate			
Sodium Azide			
Seahorse Extracellular Flux Analyzer			
Antimycin A	1397-94-0	A8674-25mg	Sigma-Aldrich
FCCP	95H4053	C2920-10mg	Sigma-Aldrich
Oligomycin	SZBD1680V	sc203342	SCBT
Rotenone	MKBS1062V	R8875-5G	Sigma-Aldrich
H₂DCFDA oxidation assays			
H ₂ DCFDA	1087822	C6827	Thermo Fischer

Table 2: List of materials

Material	Reference	Brand
Disposable syringes, 5 mL	SYRI-005-100	LabBox
Dual chamber counting slides	145-011	Bio-Rad
Seahorse XF Cell Mito Stress Test Kit	HPA103015100	Agilent Technologies
Seahorse XF96 V3 PS Cell Culture Microplates	101085-004	Agilent Technologies
Syringe filter, 0.2µm	10462200	GE Healthcare
T175 cell culture flask	734-2315	VWR
T25 cell culture flasks	734-2311	VWR
T75 cell culture flasks	734-2313	VWR
Tissue Culture 96-well plate	10062-900	VWR
XFe96 sensor cartridges	102418-000 B	Agilent Technologies

2.1.2 Cell Lines

Three different cell lines were used throughout the different assays: MCF-7, Hs578t and NHDF (Figure 4).

MCF7 is one of the most used breast cancer cell lines. It is an adenocarcinoma, positive for receptors for estrogen and progesterone. It belongs to the luminal A molecular subtype, which tend to be low-grade, to grow slowly and have the best prognosis (Comşa et al, 2015). It was used to serve as a model of breast cancer cells that are more vulnerable to DOX, even if they have been reported to become resistant to this drug if its doses are not adequate (Tsou et al, 2015).

Hs578t is a triple negative breast cancer cell line. It has origin in the mammary epithelium and is aneuploid. Has carcinosarcomatous features and is a metaplastic cancer, which is harder to treat (Chavez et al, 2010). It was chosen to serve as a model for a subtype of breast cancer that can become resistant to DOX through mechanisms such as an overexpression of Caveolin-1 (Cai et al, 2004).

NHDF (normal human dermal fibroblasts) are skin cells from the dermis and are responsible for creating connective tissue (Sarker et al, 2014). They were used as a model for a non-tumoral cell line in the present work as a way to test if RebA has in fact a specificity towards tumor cells, both on its own and as a potentiator of the effects of DOX.

The choice of NHDF as the non-tumoral control was motivated by several factors. Hs578bst cells were available, which are non-tumoral breast cancer cells, isogenic with the Hs578t cells, obtained from the same patient. Tries were made to grow these cells, but they presented a doubling time higher than one month. Furthermore, media had to be supplemented with Epidermal Growth Factor and insulin, which may cause metabolic changes that could influence the results. Finally, when those cells were passed into another flask, most of them died during the process. MCF12A cells were also available, from the epithelium of the breast, but they required a different medium to grow, as well as a necessity to supplement it with cholera toxin. Given all these factors, since NHDF cells can grow in the same medium and in the same conditions as Hs578t and MCF7, it was believed that they would provide a reliable comparative model of normal cells, despite having an origin in a different organ from where the tumor cells originate.

NHDF cells were obtained from Lonza, and both tumoral lines were obtained from ATCC.

The cells that were used were defrost at passages #4 (Hs578t), #5 (NHDF) and #24 (MCF7). Depending on the types of assays, and specially conditioned by whether or not a habituation to a different medium had to be performed, the assays were executed with cells from passages #3 to #10 after unfreezing.

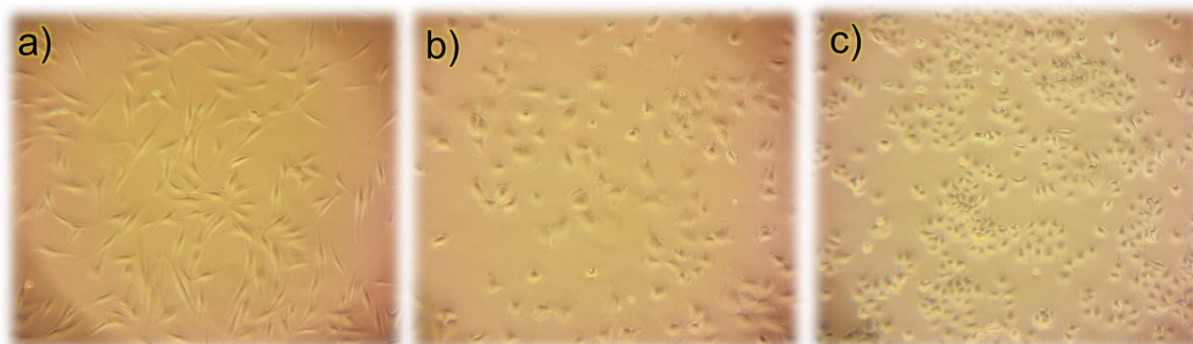


Figure 4: Images of the three cell lines used throughout the assays: a) NHDF; b) Hs578t; c)MCF7. Those specific images correspond to the cells used for the NMR assays at the moment of addition of the drugs.

2.2 Methods

2.2.1 Cell Culture Media Composition

Three different types of cell culture media were used: High-Glucose Medium (HG), Low-Glucose Medium (LG) and OXPHOS Medium (OX).

HG was composed by Dulbecco's Modified Eagle's Medium D5030 (DMEM), which was supplemented with 4.50 g/L (25 mM) of D-glucose, 0.98 g/L (6 mM) L-glutamine, 0.11 g/L (1 mM) sodium pyruvate, 3.7 g/L (44 mM) sodium bicarbonate, 100 U/ml penicillin, 100 µg/ml streptomycin, 250 ng/ml amphotericin B and fetal bovine serum 10% (v/v). pH was adjusted to 7.2 using hydrogen chloride (HCl) or sodium hydroxide (NaOH); LG had a similar composition to the HG medium, but with a lower quantity of glucose added of 0.9 g/L (5 mM); OX was based on the other media, but, instead of glucose, 1.8 g/L (10 mM) of D-galactose were added (Costa, 2017).

2.2.2 Cell Culture Procedures

Cells were unfrozen into T25 flasks in HG medium and were expanded into T75. If the experiment required a larger number of cells, further expansion was made into T175. At least four flasks of each cell line were grown simultaneously, in order to achieve a biological N (independent experiments) equal to four for all the performed assays. Cells were kept in an incubator with a humidified atmosphere with 5% CO₂ at 37°C. Passages were performed by submitting the cells to trypsin (0.5%) when their confluence was around 80%. The amounts of trypsin added were of 1, 2 or 3 mL for T25, T75 and T175 flasks, respectively. When the cells were in suspension, an equal amount of media was added to the flask in order to inactivate the trypsin. Those cells were then passed into 15 mL falcon tubes and centrifuged at 250 g for 5 min, to allow the cells to form a pellet. The supernatant was aspirated, the cells resuspended in 2 mL of medium and then passed into another flask. When the cells were collected for assays requiring a specific number of cells per well, the number of cells was determined by suspending 10 µL of those resuspended cells with 10 µL of trypan blue, and then 10 µL of that mix inserted into a slide and counted in a cell counter. Dilutions were then made with medium to achieve the desired cell concentration.

2.2.2.1 Cell adaptation to a different culture media

A gradual procedure was carried out to adapt cells grown in HG to either LG or OX media. Four passages were carried out in order to perform such adaptation, each using a different ratio of HG medium to the new one (75%-25%; 50-50%; 25-75%; 0-100%), as performed by Serafim (2011) for Hs5787 cells and for MCF-7 cells. A similar procedure was done for the NHDF cells' adaptation, but with daily changes in the ratio of media, in the same flask, as performed by Costa (2017), thus completing the adaptation in one passage.

2.2.2.2 Protocols for cell viability assays

Cells were added to 96 wells plates at a concentration of 8000 cells/well in 150 µL of medium and were left there for 24 h, to promote surface adherence. Then, the medium was removed and a similar volume of fresh medium with the drugs of interest was added and kept for 24 h for the viability curves for RebA and insulin, and for 72 h for the assays using DOX. Medium without drugs was added for the controls at the same timepoint.

2.3 Resazurin assay

2.3.1 Background

Resazurin is a phenoxazine dye, fluorescent, that has low toxicity towards cells. It has applications several types of assays in biological systems, as it is cell-permeable and sensitive to redox environments. Its most well know use is in cell viability assays, frequently used to test the cellular response to a certain substance, as in the presence of metabolic active cells it is reduced into resorufin, changing its color and causing alterations in its excitation and emission spectra, making this reaction easy to detect by readings of its fluorescence. This reaction occurs in exposure to substrates synthesized during the process of aerobic respiration in cells with an active metabolism, with NADH or NADPH being the reducing agent, by the dehydrogenase enzymes of these molecules (Chen, Jian Li et al, 2018). Figure 5 represents this reaction.

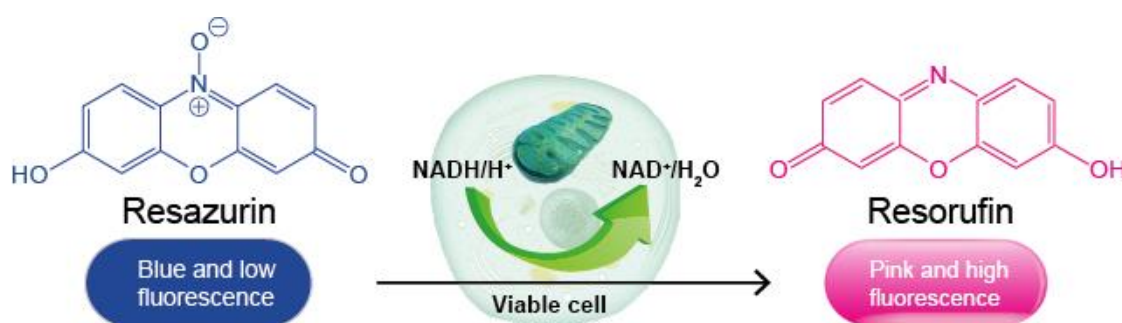


Figure 5: Representation of the resazurin assay. From <https://www.creative-bioarray.com/support/resazurin-cell-viability-assay.htm>, Date of access: 29/10/2020

2.3.2 Procedure

After the incubation time, the assay medium was removed, and 80 μ L of fresh medium with resazurin (10 μ g/mL) was added and let for 1 h. Then, the fluorescence in each well of the plates was read at the plate reader Cytation 3 with excitation/emission wavelengths of 355/455 (reference signal) and 560/590nm (resorufin), giving an indication of the metabolic viability of these cells. Procedure was based on Silva et al, 2016.

2.4 SRB assay

2.4.1 Background

Sulforhodamine B (SRB) (Figure 6) is a fluorescent dye, used to determine the relative amounts of cells, based on the measurement of the protein content of a given sample, which information can be extrapolated into a measure of cellular viability. It is often used to gauge effects of a certain drug in cell proliferation and drug-induced cytotoxicity. The property of SRB that make this possible is its ability to bind on basic residues of amino acids of cells fixed in a well, by methods such as exposure to ice-cold methanol, trichloroacetic acid or others.

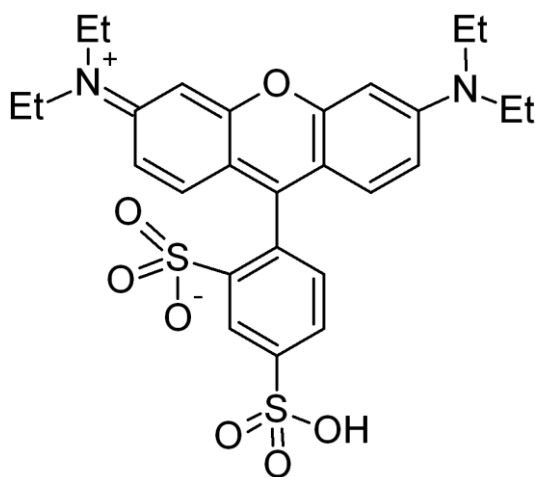


Figure 6 – Molecular structure of SRB. Image obtained from https://en.wikipedia.org/wiki/Sulforhodamine_B, assessed in the 29/10/2020

2.4.2 Procedure

Following the resazurin readings, the same plates were also used for the SRB assays. The medium was removed, the plates washed with PBS 1x (200 μ L/well) and then let to freeze in -20°C for at least 4 h in the presence of ice-cold 100% methanol / 1% acetic acid solution (100 μ L/well). Then, such solution was removed and 50 μ L/well of SRB were added and incubated for 1 h at 37°C . Following this step, SRB was removed and the plate washed with a solution of 1% acetic acid to remove the unbound SRB. Finally, 100 μ L/well of Tris-EDTA (10 mM) was added, and the plates read in the Cytation 3 multiplate reader at the wavelengths of 510 and 620 nm, giving us an indication of the amount of cellular proteins (cell mass) in each well and, indirectly, a measure of cellular viability. Procedure was based on Silva et al, 2016.

2.4.3 Data analysis

Data was obtained using the Cytation 3 Multi plate reading software, GEN5. The results of both resazurin and SRB readings were exported from the GEN5 into Microsoft Excel. Normalization was made by dividing the values of each well by the controls of the same row, containing medium without drugs. The relative values for each condition were exported into GraphPad Prism 8 and plotted into an XY table, with all the replicate values. A dose-response curve was then elaborated using those numbers, for each individual N (independent experiment), and a non-linear regression with variable slope (four parameters) was performed, to calculate the IC50 for cell viability for each curve. The results of this process were then inserted into another table, with conditions sorted by columns, and bar graphs with the IC50 values were made. Kruskal-Wallis test followed by Dunn's post-test for multiple comparisons were performed, between all the conditions that were intended to be compared, as to determine if there was statistical significance, established for p values lower than 0.05. Results were expressed as the mean, with error bars for the standard error of the mean, SEM.

2.5 Metabolic profiling assays

2.5.1 Mitoplate S-1

2.5.1.1 Background

Mitoplate S-1 consist in a 96 well plate pre-coated with a specific mitochondrial substrate in each well (Figure 7). They can be classified as a metabolic phenotype microarray that tests mitochondrial function. It is based on the principle that by measuring the rates of flow of electrons throughout the electron transport chain in mitochondria from substrates producing either FADH₂ or NADH after action of specific dehydrogenases, the activity of these organelles can be measured. Those substrates have a connection with specific transporters, dehydrogenases, and components of the electron transport chain. Thus, once the cells are inserted into the assay mix in the plate, without any substrate other than the one on each well, the rate of reduction of the redox dye used in this assay gives us an indication of the rate of oxidation of the substrate in each well and, thus, provides a hint about the capability of the cells to consume that substrate. This is linked to higher levels of expression of the transporters and enzymes correlated with that specific substrate, thus hinting at how active the pathway it is associated to is. The assay uses a tetrazolium redox dye (Dye MC) that changes from being transparent to purple when reduced by electrons from the cytochrome C, allowing its detection though measure at 590 nM, due to acting as the terminal electron acceptor for the electrons traveling throughout the electron transport chain (Figure 8).

A1	No Substrate	A2	α -D-Glucose	A3	Glycogen	A4	D-Glucose-1-PO4	A5	No Substrate	A6	α -D-Glucose	A7	Glycogen	A8	D-Glucose-1-PO4	A9	No Substrate	A10	α -D-Glucose	A11	Glycogen	A12	D-Glucose-1-PO4
B1	D-Glucose-6-PO4	B2	D-Gluconate-6-PO4	B3	D,L- α -Glycerol-PO4	B4	L-Lactic Acid	B5	D-Glucose-6-PO4	B6	D-Gluconate-6-PO4	B7	D,L- α -Glycerol-PO4	B8	L-Lactic Acid	B9	D-Glucose-6-PO4	B10	D-Gluconate-6-PO4	B11	D,L- α -Glycerol-PO4	B12	L-Lactic Acid
C1	Pyruvic Acid	C2	Citric Acid	C3	D,L-Isocitric Acid	C4	cis-Aconitic Acid	C5	Pyruvic Acid	C6	Citric Acid	C7	D,L-Isocitric Acid	C8	cis-Aconitic Acid	C9	Pyruvic Acid	C10	Citric Acid	C11	D,L-Isocitric Acid	C12	cis-Aconitic Acid
D1	α -Keto-Glutaric Acid	D2	Succinic Acid	D3	Fumaric Acid	D4	L-Malic Acid	D5	α -Keto-Glutaric Acid	D6	Succinic Acid	D7	Fumaric Acid	D8	L-Malic Acid	D9	α -Keto-Glutaric Acid	D10	Succinic Acid	D11	Fumaric Acid	D12	L-Malic Acid
E1	α -Keto-Butyric Acid	E2	D,L- β -Hydroxy-Butyric Acid	E3	L-Glutamic Acid	E4	L-Glutamine	E5	α -Keto-Butyric Acid	E6	D,L- β -Hydroxy-Butyric Acid	E7	L-Glutamic Acid	E8	L-Glutamine	E9	α -Keto-Butyric Acid	E10	D,L- β -Hydroxy-Butyric Acid	E11	L-Glutamic Acid	E12	L-Glutamine
F1	Ala-Gln	F2	L-Serine	F3	L-Ornithine	F4	Tryptamine	F5	Ala-Gln	F6	L-Serine	F7	L-Ornithine	F8	Tryptamine	F9	Ala-Gln	F10	L-Serine	F11	L-Ornithine	F12	Tryptamine
G1	L-Malic Acid 100 μ M	G2	Acetyl-L-Carnitine	G3	Octanoyl-L-Carnitine	G4	Palmitoyl-D,L-Carnitine	G5	L-Malic Acid 100 μ M	G6	Acetyl-L-Carnitine	G7	Octanoyl-L-Carnitine	G8	Palmitoyl-D,L-Carnitine	G9	L-Malic Acid 100 μ M	G10	Acetyl-L-Carnitine	G11	Octanoyl-L-Carnitine	G12	Palmitoyl-D,L-Carnitine
H1	Pyruvic Acid	H2	γ -Amino-Butyric Acid	H3	α -Keto-Isocaproic Acid	H4	L-Leucine	H5	Pyruvic Acid	H6	γ -Amino-Butyric Acid	H7	α -Keto-Isocaproic Acid	H8	L-Leucine	H9	Pyruvic Acid	H10	γ -Amino-Butyric Acid	H11	α -Keto-Isocaproic Acid	H12	L-Leucine

+ L-Malic Acid 100 μ M

Figure 7: Configuration of Mitoplate S-1 regarding the mitochondrial substrates within each well and their location in the plate.

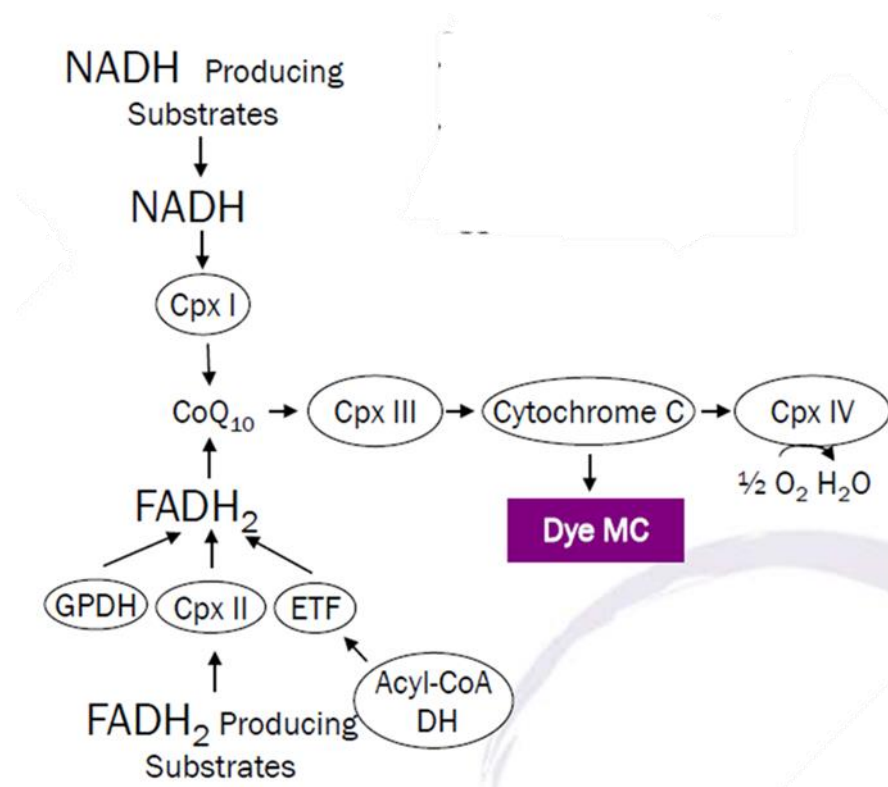


Figure 8: Schematic representation of the mechanisms behind the Mitoplate S-1 assay. Image obtained from the Biolog Mitoplate Instructions Guide, at www.biolog.com. Access date: 29/10/2020

2.5.1.2 Procedure

Mitoplates S-1 require one hour of incubation with an activation solution, to resuspend the substrates pre-loaded onto each well. For this, the plates were supplemented with the activation mix composed of sterile water, 24x Saponin (5µg/ml), 2x Biolog Mitoplate Assay Solution (BMAS), 6x Redox Dye MC obtained from Biolog, and added in proportion so the final concentration for each one was 1x, and let for 1 h in the incubator, in order to activate the plate by resuspending the substrates inside each well. The cells used were grown in the same conditions as for the viability assays, with replacement of the medium with a fresh one with 10 mM of RebA, or without it for the controls, in the day preceding the experiments, thus with an incubation time of 24 h. The procedures described in section 2.2.2 were followed to harvest the cells and get them into the desired concentration. Then, 30000 cells were added to each well. The plate was then immediately measured in the Omnilog system (Biolog), for 12 h. Procedure was based on the user manual provided by Biolog, and on Kuzniewska et al, 2020.

2.5.1.3 Data analysis

After the readings in the Omnilog equipment, its software retrieved the results in D5E files. Those were then imported into the program Data Analysis 1.7, from Biolog, and within it, the maximum rate of the oxidation of the dye was calculated, within the first 45 minutes where the curve was steeper. Those values were exported into CSV files, which were then imported into Microsoft Excel. The values of the negative control wells were subtracted to the ones with the mitochondrial substrates of interest. Those values were then inserted into XY tables in GraphPad Prism 8, from which Scatter Plots, plotting the test conditions against its respective control, used as a reference, were obtained.

2.5.2 NMR Metabolic Profiling

2.5.2.1 Background

Nuclear magnetic resonance spectroscopy (NMR) is a spectroscopic technique based in the presence of local magnetic field characteristic of nuclei. It works by exposing the sample in a magnetic field, where waves of specific wavelengths induce excitation of the nuclei of the sample, causing a phenomenon of nuclear magnetic resonance, then detected by sensors within the instrument. The magnetic field around specific nuclei is influenced by both its inherent characteristics, as well as the surrounding groups, giving information about the composition of molecules and even discriminating the presence of different molecules within a sample, especially those of organic nature, from sugars to proteins. There are several types of NMR techniques, the most relevant being proton NMR (or ^1H NMR) and carbon 13 NMR (or ^{13}C -NMR).

2.5.2.2 Protocol

T75 flasks were prepared with all the three cell lines, aiming at an initial confluence of 60%, to have an approximate confluence of 80% by the end of the assay. Following this passage, cells were kept in normal LG medium for 24 h. By the end of this time, the medium was removed, the flasks washed with 1X PBS and a different LG medium was added, with $[\text{U}^{13}\text{C}]$ glucose replacing the normal ^{12}C glucose in its entirety, either on its own or with 10 mM of RebA, 3 nM of insulin of both simultaneously. Cells were then incubated for one day. In the end of this period, samples of 200 μL of the medium in the flasks were obtained, to measure the concentration of extracellular metabolites, and then supplemented with 50 μL of a solution containing 10 mM of Fumarate (final concentration of 2 mM), to serve as a reference to calibrate the signal, and sodium azide, to keep the sample free of contaminations. These samples were then kept at -20°C and later analyzed in the RMN Varian and a ^1H NMR spectroscopy read was performed, at 599.73 MHz.

For the ^{13}C NMR analysis of intracellular metabolites, further steps were made, based on the protocol described by Warheit and Heinzle, 2014. Modifications made to it to compensate for difference in the experimental conditions. So, once the samples of medium for ^1H NMR analysis were collected, the remainder of the medium was removed, and the T75 flasks washed with warm 5 mL of PBS 1x. The PBS was then removed, and 4 mL of 80% methanol at -20°C were added to the flasks. These steps were performed as fast as possible, in order to make a more accurate metabolic quenching, with the

desired metabolites with less noise from other molecules synthesized in the response to the stress induced by this procedure. The flasks were immediately placed on top of a bed of dry ice, and cell scrapers were used to separate the cells, by then adherent to the bottom of the flask. Those samples were then centrifugated at 10000g for 10 min, at 4°C. The resultant supernatant, containing the extracellular metabolites, was collected into falcon tubes, which was then left overnight in a warm water bath, at 40°C, to allow the methanol to evaporate, inside a hotte. When the volume was lesser than 1 mL, the samples were transferred into 2 mL Eppendorf tubes, and inserted into a Thermoblock at 50 °C and left to finish the drying process, overnight, in a hotte. The dry samples, still inside its respective Eppendorf tubes, were then stored at -20°C. For the ¹³C reading, 200 µL of miliQ H₂O were added, as well as 50 µL of a solution of sodium azide and fumarate, at 10 mM. The final concentration of fumarate was 2 mM, and it was used to calibrate the signal in the NMR analysis. ¹³C NMR readings were performed at 150.81 MHz. Procedure for the assays was based in Tavares et al, 2015.

2.5.2.3 Data analysis

NUTS software was used for treatment of the spectra and calculation of the concentrations of the desired metabolites for each sample. Area below the peaks corresponding to ¹³C lactate, at 1.4 ppm, and ¹³C α-glucose at 5.35 ppm were calculated through integration and normalized through the area obtained for fumarate, with the known concentration of 2 mM. Those values were then adjusted, having in consideration that the ratio of sample to the standard was 80:20.

The values obtained were then inserted into column tables in GraphPad Prism 8, and bar graphs were drawn, with the desired conditions side by side non-parametric Kruskal-Wallis test followed by Dunn's post-test for multiple comparisons were performed, comparing each condition with the control, as to determine if there was statistical significance, for p values lower than 0.05. Results are expressed as a mean, with error bars for the standard error of the mean, SEM.

OXPHOS index was calculated according to equation (1), and it provides an indication about how oxidative the cells' metabolism is.

$$(1) \quad OXPHOS \text{ Index} = 1 - \frac{[Lactate]}{2} \div (5 - [Glucose])$$

2.5.3 Seahorse Extracellular Flux Analyzer

2.5.3.1 Background

Seahorse XF Analyzers are instruments used for the measurement of energy metabolism of live cells in real time. The main parameters that they read are oxygen consumption rate (OCR) and extracellular acidification rate (ECAR). OCR measures cellular oxygen consumption and, as such, provides direct information about mitochondrial respiration, while ECAR is linked with glycolysis, as it analyses small changes in the pH of the assay medium originated due to proton excretion linked to this metabolic pathway. Reading of such parameters is due to the presence of sensor that come in close proximity with the samples, being able to detect those small differences. Special 96 well plates are used, with the assay medium being similar to the one used in cell culture, but without FBS nor bicarbonate. Plates come with a cartridge, to which can be loaded specific quantities of desired drugs, making possible to measure its impact in real time. One of the most common Seahorse assays is the Mito Stress test (Figures 9 and 10), where sequential injections of oligomycin, Carbonyl cyanide-4-(trifluoromethoxy)phenylhydrazone (FCCP) and Rotenone + Antimycin A are performed. In a standard protocol of this test, a baseline is first obtained, corresponding to values of basal respiration and non-mitochondrial oxygen consumption. Then, oligomycin is injected. It inhibits the complex V, ATP synthase, decreasing the OCR levels due to a reduction in the flow of electrons, in proportion with the ATP production lost. FCCP is an uncoupler of respiratory chain, eliminating the normally present proton gradient and directly affecting the membrane potential of the mitochondria. This causes a maximum activity of the complex IV, increasing the OCR values to a maximum, indicating the maximum respiratory capacity of the cell sample and, by subtracting the levels of the previously determined basal respiration, it allows the calculation of spare respiratory capacity. The final injection consists of both rotenone and antimycin A, inhibitors of the complexes I and III, respectively, stopping mitochondrial respiration, leaving only non-mitochondrial oxygen consumption as the only factor contributing to the OCR.

Seahorse XF Cell Mito Stress Test Profile Mitochondrial Respiration

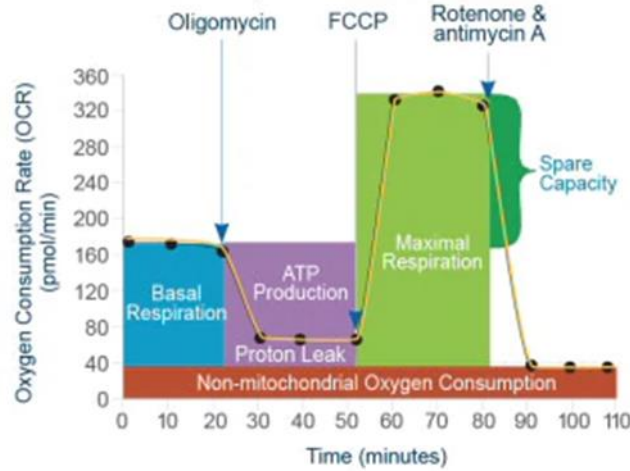


Figure 9: Representation of the typical output profile of the Seahorse Mito Stress test, regarding the OCR values, with indication of the parameters that can be determined through this assay. Image obtained from <https://www.agilent.com/en/product/cell-analysis/real-time-cell-metabolic-analysis/xf-assay-kits-reagents-cell-assay-media/seahorse-xf-cell-mito-stress-test-kit-740885>. Access date: 29/09/2020

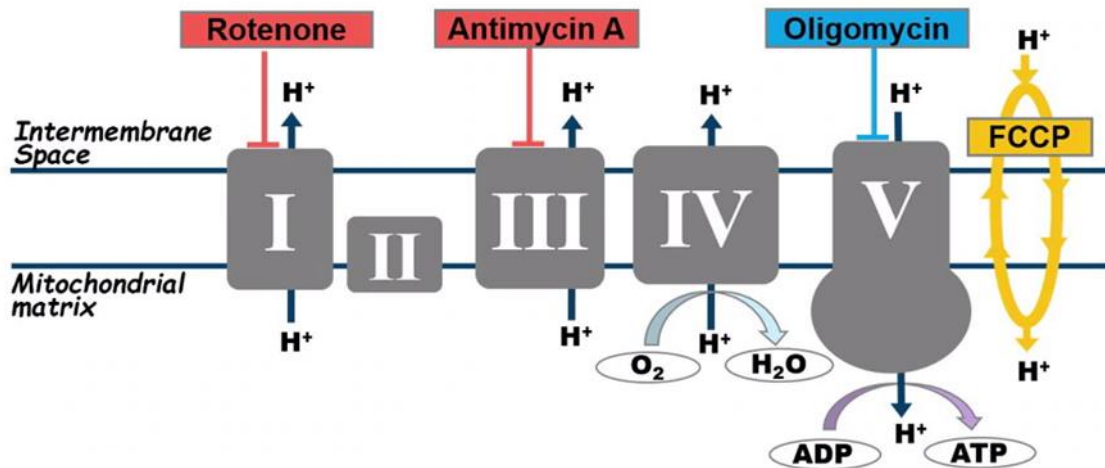


Figure 10- Representation of the electron transport chain and targets of the different mitochondrial drugs injected in the Mito Stress Test. Image obtained from <https://www.agilent.com/en/product/cell-analysis/real-time-cell-metabolic-analysis/xf-assay-kits-reagents-cell-assay-media/seahorse-xf-cell-mito-stress-test-kit-740885>, assessed on 29/09/2020

2.5.3.2 Protocol

Cells were grown in T75 in either LG or OX medium and harvested as described in section 2.2.2. Cells were then plated into Seahorse plates, at a density of 8000 cells per well for the NHDF cells, and with a density of 10000 cells per well for both Hs578t and MCF7, concentrations determined to be optimal in previous assays, and were kept in medium of the same type they were adapted to. After 24 hours, this medium was replaced with fresh one, with either 1 or 10 mM of RebA, or without it for the controls. Following 24 hours of exposure, the Mito Stress XF96 Analyzer protocol was executed. Two special media for this assay were made, Mitostress LG and Mitostress OX, with equal composition to both LG and OX, but without FBS and sodium bicarbonate, were elaborated. Its pH was set to 7.4, using 0.1 mM NaOH and 0.1 mM HCl. The media in the plates, with the drugs, was removed. The plates were then washed two times with 175 μ L of the corresponding Mito Stress media and then 175 μ L of it were kept in the wells. Solutions of 16 μ M of Oligomycin, 9 and 2.25 μ M of FCCP and 10 μ M of Rotenone + 10 μ M of Antimycin A, diluted in the adequate Mito Stress, media were prepared. The concentration of 9 μ M of FCCP was used for NHDF cells, as 2.25 μ M were used for the tumoral cells. Those values were resultant from previous assays and were found to be optimal for those cell lines, to provide a measurable response that did not kill or cause unwanted impairments the cells in the process. Then, 25 μ L of each was loaded into an individual slot in the cartridge of the Mito Stress assays. The cartridge was left in the previous day to hydrate and calibrate, in a utility plate with calibration media, in an incubator at 37°C. This utility plate was replaced by the Seahorse plates, containing the cells in the assay medium, and the assay was executed in an Agilent Seahorse XFe96 Analyzer. The protocol for this assay was based Agilent Seahorse XF Cell Mito Stress Test Kit user manual and from Costa et al, 2017,

The Wave software was used to program the protocol of the experiment. The protocol run was based in the standard Mito Stress protocol, with readings for the baseline and following the injections with Oligomycin, FCCP and Rotenone + Antimycin A, each with 3 measurement cycles, lasting 18 minutes for each condition. For each injection cycle, 25 μ L of the correspondent mitochondrial inhibitors were injected into each well.

After the procedure and respective readings in the Agilent Seahorse XFe96 Analyzer were finished, the plates were centrifuged at 250g for 5 minutes and then the assay medium in was removed. The wells were washed once with 150 μ L of PBS 1x and then 100 μ L of 100% methanol / 1% acetic acid and were stored at -20°C for several days. Then, the content of the plates was discarded, and they were washed with PBS 1x and

left in an incubator, at 37°C, to dry. Then, 30 µL of 0.05% SRB were added to each well for one hour and left in the same incubator for one hour. The SRB was then removed and the plates washed three times with 1% acetic acid. After drying, 200 µL of Tris-NaOH were added to the Seahorse plates. In a different, conventional multi well plate, 100 µL of Tris-NaOH were added. After performing up and down in the Seahorse plates, 100 µL of its content were transferred into the other plate, using a multichannel pipette, keeping the same order for all the wells. This plate was then read in the Cytation 3, at 510 and 620 nm. The results of this reading were used for normalization purposes.

2.5.3.3 Data analysis

Normalization was made directly in the Wave Software, using the results from the SRB readings. The results were exported from Wave into Microsoft Excel, through the tools of exportation “Seahorse XF Cell Energy Phenotype Test Report Generator” and “Seahorse XF Cell Mito Stress Test Report Generator”. The data in those files related to the parameters intended to be analyzed was then inserted into GraphPad Prism 6. OCR and ECAR results are expressed as a mean, with error bars corresponding to the SEM. In the energy maps, results are expressed with the Standard Deviation, SD, instead.

2.5.4 H₂DCFDA oxidation assays

2.5.4.1 Background

2',7'-dichlorodihydrofluorescein diacetate (H₂DCFDA) is a reduced form of the highly fluorescent 2',7'-dichlorofluorescein (DCF). It is used as an indicator of ROS within a sample. Even if it is not specific to a particular molecule, neither gives information about the origin of the source of those reactive species, its use can give important information about oxidative stress, especially when used along other assays to complement this cons.

H₂DCFDA is cell permeable and once it diffuses into the cells, it can be deacetylated into 2',7'-dichlorodihydrofluorescein (H₂DCF) by cellular esterases. Then, in the presence of ROS, predominantly, but not exclusively, H₂O₂, it is oxidated into DCF, with excitation wavelengths of 485 nm and emission wavelength of 528 nm.

2.5.4.2 Protocol:

The procedure was based in the one used by Branco et al, 2013. Cells were previously cultivated in LG medium in T75 and harvested following the procedure at section 2.2.2. Cells were then plated onto 96 wells plates, at a concentration of 8000 cells per well for the NHDF cells, and 10000 cells per well for the Hs578t and 20000 cells per well for the MCF7 and let for 24 h in the incubator in an humified atmosphere of 5% CO₂ at 37°C. By the end of this time, the media was replaced by a fresh one, containing different concentrations of RebA, depending on the well, or without it, for the controls. For another 24 h the plate was left to incubate. Then, the media was replaced with new one containing H₂DCFDA and incubated 1 h. Later, that media was removed, and a fresh one added, with the composition of Mito Stress LG medium, without FBS and bicarbonate. The plates were immediately inserted in the Cytation 3 plate reader, under an excitation wavelength of 485 nm, and its emission measured at 538 nm for 2 h. The generated GEN5 files were then exported into Microsoft Excel and the data points exported to GraphPad Prism 8.

2.5.4.3 Data analysis

The period with the highest slope for all the cell lines was determined to be between 8-36 min, as the first minutes were correlated with stabilization of the cells and after approximately 40 minutes after the beginning florescence levels started to halt its increase, possibly due to most of the probe in the system being already oxidized. So, a linear regression of the curves was performed in this interval, and the resulting slope was calculated. This value provides a direct indication of the rate of probe's oxidation, and thus provide an indication of the levels of ROS, such as, but not limited to, H₂O₂. This was performed for each N, with the results of the slope being inserted in a column table, from which bar graphs were elaborated.

Considering the low sample size (<30 independent data points/condition), non-parametric Kruskal-Wallis test followed by Dunn's post-test for multiple comparisons were performed, comparing each condition with the control, as to determine if there was statistical significance, for p values lower than 0.05. Results are expressed as a mean, with error bars for the SEM.

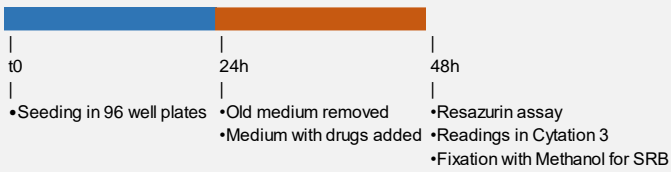
2.6 Timeline of all assays

The timelines for all the assays were planned to be as similar as possible, in order to allow for more reliable comparisons between all the different tests (Figure 11). For all the assays, cells were harvested from flasks with levels of confluence ranging from 75 to 90%, in order to allow them to keep a more proliferative phenotype, followed by seeding. After this step, cells were always kept for one day in fresh medium, in order to allow them to become adherent. As metabolism plays a key factor in this work, concentrations of substrates in the media should be similar between all the conditions in the moment of addition of the drugs. So, the previous medium was removed, and new one containing the drugs were added. Incubation times with the drugs were always 24 h, except for the assays with DOX, where such time was not enough for this anthracycline to fully exert its effect. So, in the assays with this chemotherapeutic drug, cells were exposed to it for 72h. After the end of the incubation time, the medium with the drugs was removed, and, depending on the experiment, medium for that assay was added.

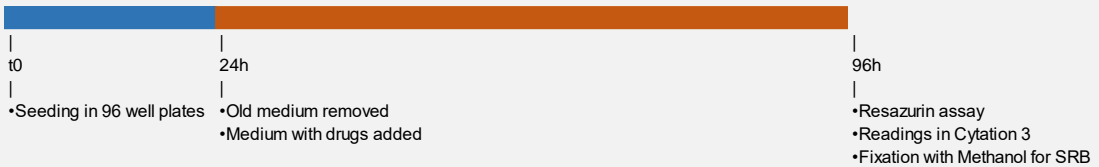
TIMELINES

Cell viability assays

Viability curve for RebA and RebA + Insulin

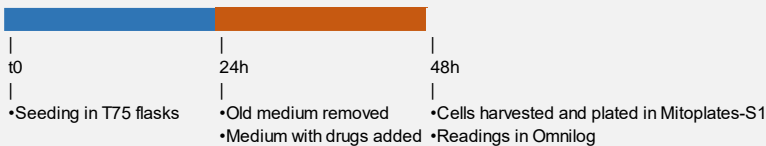


Viability curve for DOX and combinations with RebA and insulin

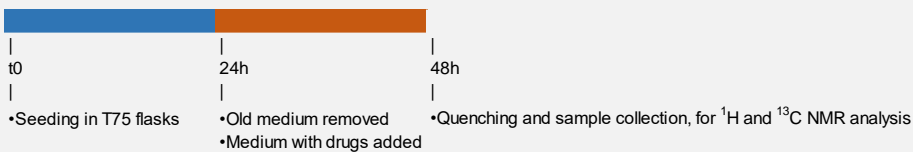


Metabolic profiling assays

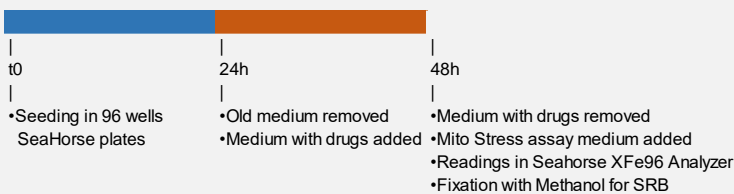
Mitoplates



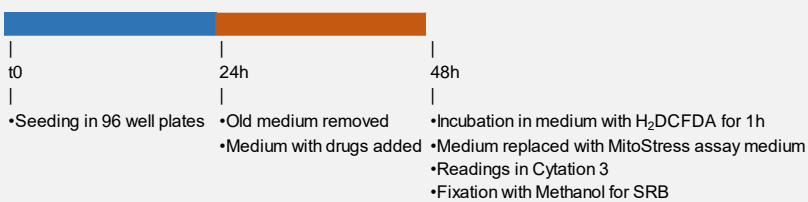
NMR

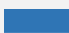


SeaHorse



H₂DCFDA



 Cells in medium similar to the one they were grown into, to become adherent


 Cells in medium containing the drugs of interest

Figure 11: Representation of the timeline for all the assays.

3 – Results and Discussion

3.1 Impact of RebA on cell viability

3.1.1.1 Details and objectives

The main objective was to assess if RebA had any potential to be used as a chemotherapeutic drug on its own, which would be the case if it was more toxic towards tumoral cells than to non-tumoral ones. It was also relevant to assess whether this eventual effect would have an underlying metabolic origin, being modulated by the addition of insulin or by prior cell culture in different metabolic contexts. Viability curves after 24 h of exposure to RebA alone (1.25-60 mM), to RebA at the same concentrations but combined with 3 nM insulin, or to insulin supplementation (0.46 – 11.12 mM) alone were performed for NHDF, Hs578t and MCF7 cells, each cultured in OX, LG and HG media. It is important to note that FBS present in the culture media already contains insulin, and its concentration may depend on the lot. In this work, the same FBS lot was used for all experiments, except for some of the assays for the viability curve of RebA.

3.1.1.2 IC₅₀ values for RebA were higher than expected, with no difference in the presence of insulin

For the tests with insulin supplementation alone, the results retrieved a horizontal line, parallel to the X axis, indicating no response to this hormone at the concentrations tested. In contrast, for both the conditions containing RebA, a curve was obtained, and the IC₅₀ values for cell viability for resazurin and SRB assays were calculated and plotted in Figure 12.

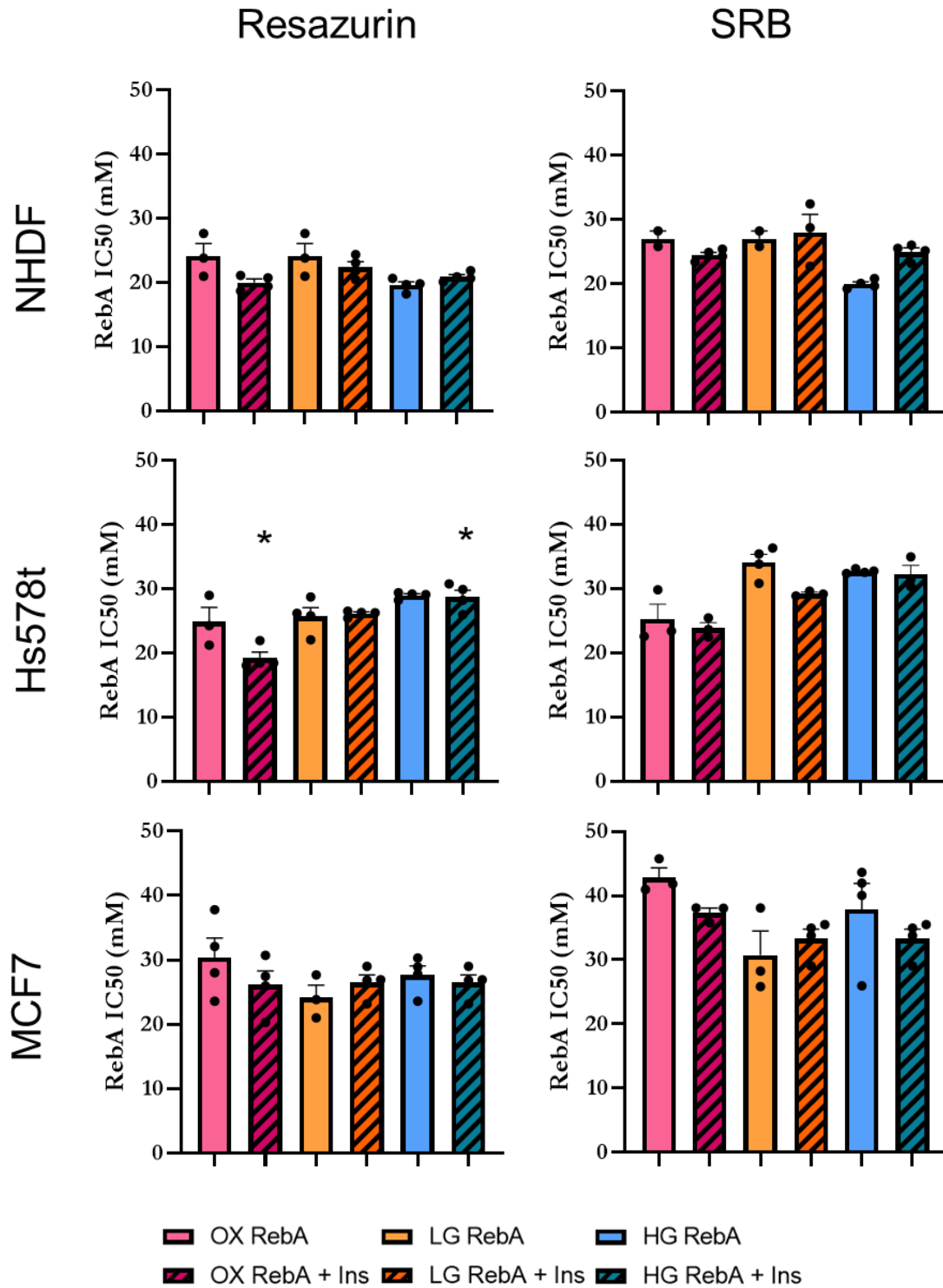


Figure 12: IC50 values for cell viability in the presence of either Reba or Reba+3nM of insulin, obtained through resazurin and SRB assays, for NHDF, Hs578t and MCF7 cells in OX, LG and HG medium. Non-parametric Kruskal-Wallis test followed by Dunn’s post-test for multiple comparisons were performed, comparing each condition of the same medium and each condition with its equivalent in the other mediums, within the same cell line and assay type, as to determine if there was statistical significance. *: $p < 0.05$. Results are expressed as a mean, with error bars for the SEM. N for each condition: 3-4

IC50 values obtained for cell viability varied from 20 to 40 mM, with the lowest IC50 for RebA being found in NHDF and the highest in MCF7. When we compare the results of the IC50 for RebA with those for RebA + 3 nM of Insulin, there appears to be no consistent tendency towards neither an increase nor a decrease in the IC50 values. Also, results were similar between all the media tested and showed no statistical significance when compared through the Kruskal-Wallis multiple comparison test, except for the case of the conditions OX RebA + Ins vs HG RebA + Ins for the Hs578t cell line, in the resazurin assays. As this was not replicated in the LG medium nor in the other two cell lines, this may be a false positive, possibly originated by a technical error, such as an addition of a lower number of cells than those intended in the OX condition, leading to a higher ratio of molecules of RebA per cell and, thus, to artificially higher toxicity. This needs to be confirmed by repeating the experiments.

3.1.1.3 IC50 values retrieved by Resazurin assay were lower than those of SRB

Overall, for most cases, the IC50 values for cell viability that were calculated based on the viability curves obtained from the SRB assays were tendentially higher than those obtained through the resazurin assays. This can be due to the nature of the assays, as one is based in the levels of proteins present (SRB), while the other is based in the cells' metabolism (resazurin). So, even if those assays are complementary to each other, slight differences such as the ones verified are common. The differences that are observed in our case, imply that cell metabolism was affected at lower concentrations than their total protein levels. Autophagy and cell death can also be a source for such differences.

3.1.1.4 IC50 values obtained for RebA were higher than those documented for other Steviol Glycosides

The most important aspect of this set of experiments was that the obtained IC50 values for cell viability were, for all the cases, higher than those of other SGs found in the literature (Table 3). Even with most of those studies being performed in different conditions, with different cell lines, different times of exposure and different methods, the MCF7 cell line was also used in the works of Gupta et al, 2017, and of Paul et al, 2012, for steviol and stevioside, respectively. As MCF7 cells were also used in the present work, it is fair to compare our results with those papers, and this indicates that RebA is by far less toxic than those SGs. This hints that RebA does not possess some of the

properties that lead to toxicity and cell death, that brings to the suggestion of the use of those other SGs glycosides on their own as chemotherapeutic agents in the previously mentioned studies.

Table 3: Comparison of the results of cell viability assays for RebA with assays for other SG in the literature show that RebA had the highest IC50

Paper	Cells	SG tested	Exposure time	Cells per well	Medium	Assay	IC50
Chen, Jun-Ming, Jue Zhang et al, 2018	U2OS (Osteosarcoma)	Steviol	48h	5000	DMEM	MTT assay	1 mM
Chen, Jun-ming, Yongmei Xia et al, 2018	HGC-27 (Human gastric cancer)	Steviol	48h	5000	DMEM	MTT assay	1 mM
Gupta et al, 2017	MCF-7 (Breast cancer)	Steviol	48h	10000	DMEM	SRB	185 μM
Li et al, 2017	OVCAR-3 (Human ovarian cancer)	Stevioside	24, 48 and 72h	500	DMEM	MTT assay	10 μM
Paul et al, 2012	MCF-7 (Breast cancer)	Stevioside	24, 48 and 72h	3000000	DMEM	Trypan Blue	15 μM
Ren et al, 2017	HT-29 (Human colon cancer)	Stevioside	24, 48 and 72h	20000	RPMI	MTT assay	5 μM
Khare et al, 2019	SKBR3 and MDA-MB-231 (Breast cancer)	Stevioside	4h	?	DMEM	MTT assay	60 μM
Our Results	NHDF Hs578t MCF7	RebA	24h	8000	DMEM (OX, LG, HG)	Resazurin and SRB	20-40 mM

As such, the sweetening properties have no correlation with toxicity, as RebA is the sweetest SG from the ones with available data on this regard and apparently the least toxic. Possible explanations for this evident difference in the results may be due to many reasons, most notoriously based in the nature of the molecules of the Steviol Glycosides. Since both Stevioside and Steviol itself (being present in the composition of all SGs) both exhibited cytotoxicity at low concentrations, it is very possible that this pharmacophore group is within the steviol core of these molecules. As Stevioside is more toxic than steviol, according to the literature, we deduce that the monosaccharides moieties attached to the core may play an important role, either by creating some sort of stereochemical impediment or even facilitating the orientation of the pharmacophore towards the target, or by facilitating the transport of the molecule to its eventual acting place – it has been reported, at least for some SGs, that they can be transported into cells by hOAT1 and hOAT3 transporters (Srimaroeng et al, 2005). If their target is inside the cell, this could prove to be a determinant factor in the toxicity. The molecule of RebA, when compared with Steviol and Stevioside, it is the largest, having one more glucose moiety than Stevioside (Figure 13).

Size may play a role in the noticeable differences in IC50 values. It is, however, not a synonymous of less toxicity, as Stevioside showed, consistently, to have a lower IC50 than steviol (Table 3). According to this, the sugar moieties in stevioside may play an important role in enhancing the toxicity of the steviol core. This could be, for example, due to stereochemical impediments in certain parts of its core, hiding some groups while exposing the pharmacophore in steviol towards its target. The sugar moieties can also interact with some undetermined transporter, potentially increasing its affinity towards this molecule, incrementing its uptake. However, too many monosaccharide moieties coordinated to the steviol core can be too much, hindering the transport of the molecule, which can be the case of RebA. These points are, however, of speculative nature, and further work would be necessary to determine the transporters with affinity towards SGs such as stevioside, and to see if RebA has, in fact, a size large enough to hamper its transportation. This would go along with the hypothesis established in the section 1.3, however with negative consequences for the case of RebA.

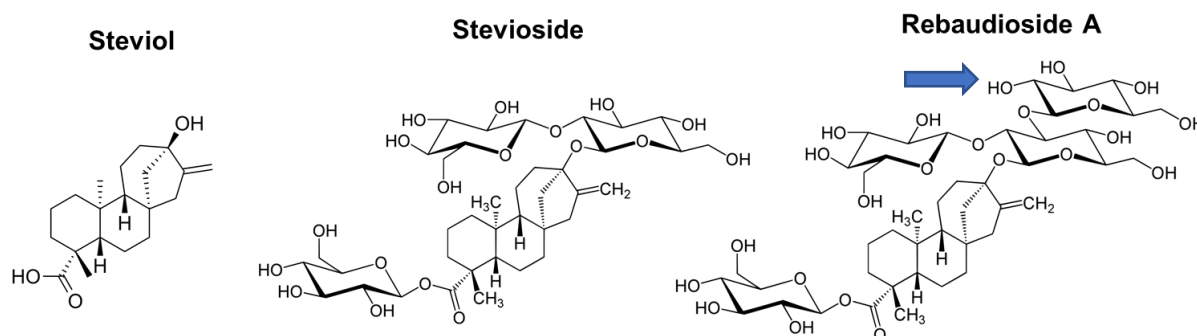


Figure 13: Representation of the molecules of Steviol, Stevioside and Rebaudioside A. Additional moiety of RebA, when compared with stevioside, in evidence. Images for the molecules were obtained from <https://en.wikipedia.org/wiki/Steviol>, <https://en.wikipedia.org/wiki/Stevioside> and https://en.wikipedia.org/wiki/Rebaudioside_A, respectively. Access date: 29/10/2020

3.1.1.5 RebA alone seems to lack chemotherapeutic potential

One of the main objectives was to determine if whether RebA could have a chemotherapeutic potential on its own. One remarkable result is that the IC₅₀ for cell viability appears to be lower for the non-tumoral cells, NHDF, than for the tumoral ones. This suggests that there is no targeted toxicity for cancer cells, as it would be desired for a chemotherapeutic drug, favoring the opposite scenario. Another factor that hinders the chemotherapeutic potential of RebA when administered alone are the high values for IC₅₀ for cell viability that were obtained. In the literature, studies for the toxicological effect of RebA in mice observed that a chronic administration of RebA at 15 g/kg was not enough to achieve the LD₅₀, although side effects were presented, especially in the kidneys. Not knowing the exact rate of absorption into the bloodstream, even if the entirety of the RebA was absorbed, the concentration that we determined for the IC₅₀ could be higher than that, discarding the use for the ends we were testing.

A possible explanation for the cell death observed in our assays is the precipitation of RebA itself, as it was noticeable for concentrations higher than 40 mM, specially at 60 mM. Thus, the toxicity observed could arise from media saturation with RebA, and possibly not having the same mechanisms as were reported for the other SG, such as interference with the cell cycle and growth arrest. High levels of this molecule can also interfere with transporters, receptors, or other molecules essential for cell survival.

The cytotoxicity results may suggest that RebA may be safer for food consumption than Steviol and Stevioside, the latter also widely used as a natural sweetener in the food industry.

3.1.2.1 RebA as a potential adjuvant for Doxorubicin – Considerations for the assays

Once RebA appears to have no chemotherapeutic potential on its own, a question is raised if it could help to potentiate chemotherapeutic drugs. Potentiation of such drugs by both pure SGs or for the whole stevia's extract has limited information in the literature. A small number of papers addressed this eventual potentiation, such as Martínez-Rojo et al, 2020, where the whole extract was used along with enzalutamide, which activates of androgen receptors and caspases 8 and 3, but the stevia's extract did not show potentiation for this drug. However, the extract alone inhibited the migration and proliferation of prostate cancer cells. As the whole extract was used in this paper, the SGs responsible for this are not determined. As for assessing if RebA could potentiate the toxicological effects of a chemotherapeutic agent, the effect of two concentrations of RebA in combination with DOX was tested to determine if RebA could be used as a safe chemotherapeutic adjuvant, at least for this anthracycline and cancer antibiotic.

Since RebA has been described as insulin mimetic, insulin was also used as comparison, to assess if their responses would be similar, while, at the same time, testing the controversial Insulin Potentiation Therapy, as described by Damyanov et al, 2012. The concentrations that were selected for RebA were 1 and 5 mM, based on the IC₅₀ observed for steviol of 1 mM in Chen, Jun-ming, Yongmei Xia et al, 2018 and Chen, Jun-Ming, Jue Zhang et al, 2018, while 5 mM was used due to the higher IC₅₀ that was observed for this SG in our previous assays. For the assays with insulin, additional quantities of this hormone were added to achieve the concentration of 3 nM (which would be added to the insulin already present in the medium due to FBS supplementation, which was an unknown, but constant amount since the same lot of FBS was used for all these assays). The amount of insulin supplementation was based on the values that can be naturally achieved in the blood 1 h after glucose consumption (Buppajarntham et al, 2019).

The concentrations of Doxorubicin were chosen based on pilot assays, from 0.02 to 10 μ M in NHDF and from 0.005 to 5 μ M in Hs578t and MCF7 cell lines, in order to achieve a viability curve.

Cells were grown in both OX and HG medium, to assess if the observed effects were related with cellular metabolic profile.

3.1.2.2 Neither RebA nor Insulin decreased the IC50 of Doxorubicin

A chemotherapeutic adjuvant is a drug that increases the effect of a given chemotherapeutic drug towards the desired target, without affecting the non-tumoral cells. As seen in Figure 14, this behavior was not found for the concentrations of RebA and insulin used alongside DOX, arguing against their use as chemotherapeutic adjuvants, at least for DOX.

In all cases, for assays carried out both in OX and HG conditions, neither Insulin nor both concentrations of RebA had any appreciable effect in the IC50 of Doxorubicin, backed by the lack of statistical significance between the comparisons that were made against the IC50 for cell viability for Doxorubicin alone within the same medium. The slight, non-statistically significant increase in the doxorubicin IC50 for cell viability in the presence of RebA can be due to the rate of cellular proliferation, as the exposure to 1 and 5 mM of RebA induced a slight decrease in cell proliferation for all the cell lines (Figure S3 supplementary data), and thus a lower rate of cell proliferation is expected to negatively influence the effectiveness of Doxorubicin, with the other eventual changes evoked by RebA not being enough to counteract this. With only this assay, it is not possible to say that this decrease in cell proliferation is backed by metabolic alterations induced by RebA, but this will be addressed in the next sections.

Regarding the lack of effect of insulin when used along Doxorubicin, the absence of effect cannot be credited to a lack of expression of GLUT 4, at least for the tumoral cell lines, as microarray data from Neve et al, 2006, suggests the existence of transcripts. This argues against Insulin Potentiation Therapy, where lower drugs of chemotherapeutic drugs than those applied in common chemotherapeutic approaches were proposed. So, based in the results that were obtained, it is suggested to avoid this therapy.

As RebA is commonly used as a sweetener, it is relevant to point out that its consumption may not affect the efficiency of chemotherapeutic therapies, even having in consideration that the concentrations that were used are hard to achieve by this means, especially with lower quantities of RebA being applied to food when compared to sugar, as RebA is hundreds of times sweeter (Esen, 2016).

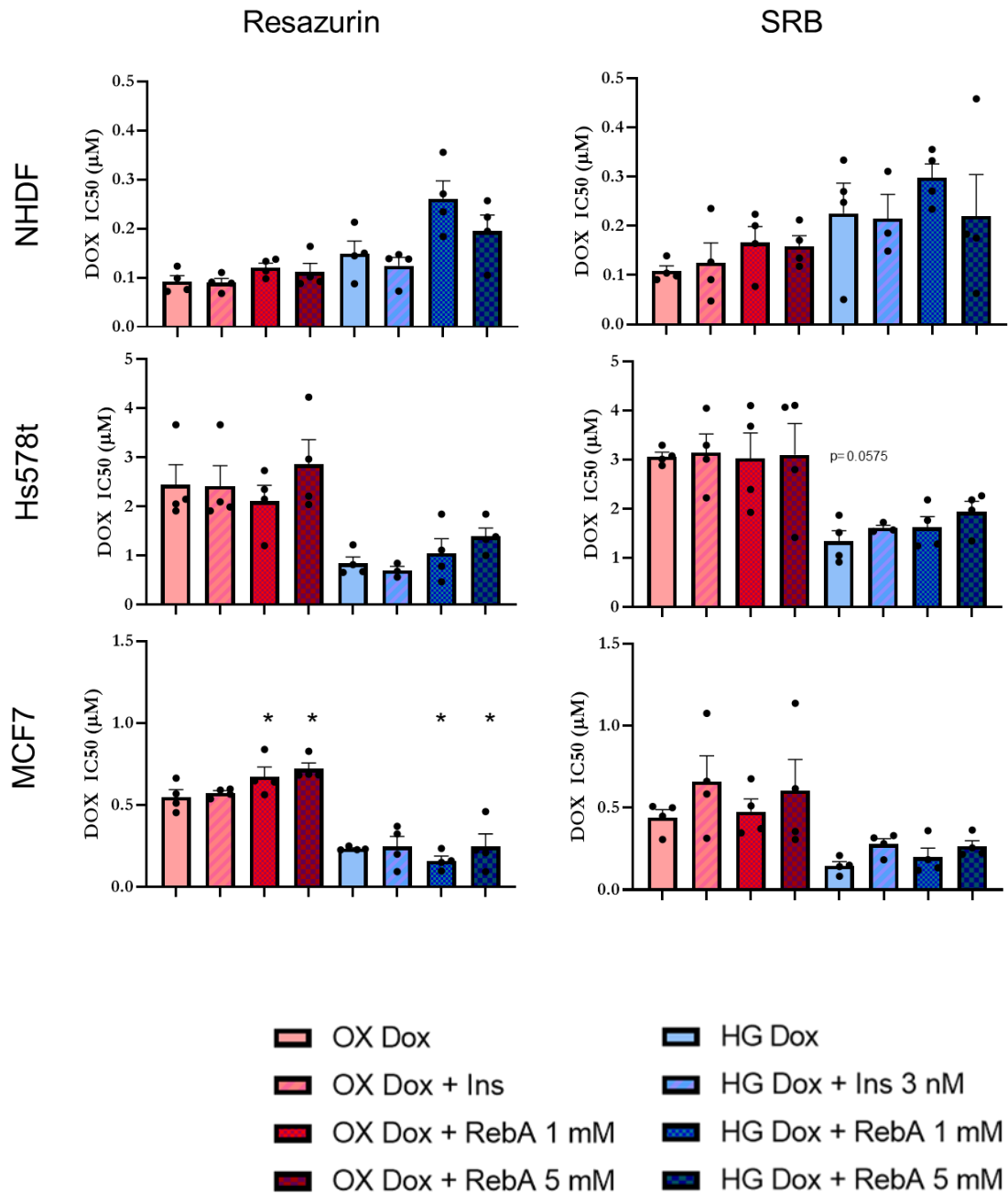


Figure 14: IC₅₀ values for cell viability in the presence of DOX, either on its own or in combination with 3 nM of insulin, 1 and 5 mM of RebA, obtained through resazurin and SRB assays, for NHDF, Hs578t and MCF7 cells in OX and HG medium. Non-parametric Kruskal-Wallis test followed by Dunn's post-test for multiple comparisons were performed, comparing each condition with the control of the same medium and each condition with its equivalent in the other media, within the same cell line and assay type, as to determine if there was statistical significance. *: $p < 0.05$. Results are expressed as a mean, with error bars for the SEM. N for each condition: 3-4

3.1.2.3 The effect of Doxorubicin was enhanced in HG medium

Despite the lack of potentiation of DOX toxicity in the presence of RebA and insulin, it can be argued that there was a significant trend for a decrease in the IC₅₀ of doxorubicin in tumoral cell lines in HG medium when compared to the values obtained for cells grown in OX medium. This only occurred for the tumoral cell lines, where the IC₅₀ for each condition was tendentially decreased by more than half when compared to their OX counterpart, with some cases achieving statistical significance, despite the overall spread of the data points. The main effects induced by the different media were of metabolic origin, hinting that the more glycolytic cells cultured in the HG media were more prone to being afflicted by DOX, possibly due to the more proliferative nature of these cells.

The HG medium contains high concentrations of glucose, 25 mM, close to the blood concentrations achieved during hyperglycemia. With abundance of this sugar, the cells prefer to consume it despite the existence of other substrates in the medium, such as glutamine, especially since the cells used have a proliferative nature, principally the tumoral cells, characterized by the Warburg Effect (Potter et al, 2016). This glucose is consumed through glycolysis, to provide intermediates for the synthesis of biomolecules, such as DNA and lipids, necessary for cellular proliferation, even if glycolysis is not the most efficient way to generate energy ATP-wise. Thus, cells grown in HG are conditioned to have a more glycolytic, proliferative phenotype. On the other hand, cells in OX medium are more oxidative in nature, since in this medium glucose was replaced by galactose, which is primarily metabolized through the Leloir pathway. However, glutamine is also present in the medium, and this substrate is preferentially consumed in this condition (Costa, 2017, Rossignol et al, 2004).

Depending on the composition of the medium regarding pyruvate supplementation, in lower quantities or absence of this substrate, glutamine is the most notorious contribution to the Krebs cycle, after being converted into glutamate, in the mitochondria, and then into α -Ketoglutarate, thus feeding this mitochondrial pathway (Rossignol et al, 2004). As in the case of this work Pyruvate was supplemented in a low concentration of 1 mM, its contribution may not be as expressive as the one described for glutamine (6 mM). In this case, there is a lower synthesis of biomolecules associated to a lower rate of cell proliferation, in the case of the tumoral cells. In addition to this, as the metabolism becomes more focused in the mitochondria, tumoral cells may have more difficulties in generating energy, with changes in its bioenergetic and biosynthetic state (Wallace, 2012).

As it was the case for the previous set of experiments, the SRB assays retrieved slightly higher IC50 values for all the cases, but the results had similar behavior.

Cell culture in HG or OX media led to relevant differences, regarding the cells doubling time, which was lower for all the cell lines cultured in OX, but affecting particularly the tumoral cells, which presented significantly slower growth rate.

With this in mind, and having in consideration the mechanisms of doxorubicin, the differences in cell proliferation rate caused by the conditioning to the different media may be the key factor regarding the enhancement of doxorubicin toxicity observed for cells grown in HG medium versus those grown on OX medium. In contrast, for the non-tumoral NHDF cells, its growth rate was not as hindered as for their tumoral counterparts. Furthermore, along with other factors, such as eventual higher ROS levels generated from mitochondrial activity, may play a role in the higher doxorubicin toxicity in cells cultured in OX medium. In this assay, the medium happened to be the best adjuvant, as it enhanced the DOX toxicity towards tumoral cells but not for the non-tumoral control, unlike insulin and RebA, that did not manifest this characteristic.

So, the metabolic manipulation that was achieved by growing the cells in the different media shows promise for further studies, through alteration of the levels of key substrates in the microenvironment may have potential for potentiation of chemotherapeutic drugs that target cells based on their growth rate.

3.1.3 Choosing concentrations for the other assays

The assays with resazurin and SRB for cell viability suggested that RebA does not possess the necessary requirements to be used as neither a chemotherapeutic drug on its own nor as chemotherapeutic adjuvant, at least for doxorubicin and, potentially, to other drugs with a similar mechanism, results that were unexpected when we have in consideration those previously obtained for other SGs such as Steviol and Stevioside, (Chen, Jun-Ming, Jue Zhang et al, 2018; Chen, Jun-ming, Yongmei Xia et al, 2018; Gupta et al, 2017; Li et al, 2017; Paul et al, 2012; Ren et al, 2017; Khare et al, 2019). The results so far were not as expected (high IC50 values for cell viability), but with time constraints due to the COVID19 pandemic and the resultant restrictions to the laboratorial work during most of the time available for the development of this thesis, choices had to be made regarding the priorities of the work. Having in consideration the low number assays that were possible to carry out, it was chosen to prioritize testing higher concentrations of RebA, when only one concentration was possible to be tested.

This aimed to increase the probability of detecting eventual RebA-induced responses. Other studies trying to replicate possible plasmatic concentrations of SGs, such as Srimaroeng et al, 2005, chose concentrations up to 1 mM of SGs to better reflect eventual physiological applications. So, as a proof of concept for the effects of RebA, when more concentrations were not possible to be tested, a higher concentration was preferred.

As such, a concentration of 10 mM of RebA was used for the Mitoplate-S1 and NMR assays. This concentration was also used for the H₂DCFA and Seahorse assays, however with the safeguard that lower, more plausible concentrations should be eventually used in a therapeutic scenario.

3.2 Characterization of metabolic changes induced by RebA

3.2.1 Analysis of mitochondrial metabolism by using Mitoplate S-1

3.2.1.1 Details and objectives of these assays

Mitoplates S-1 were used to study the effect of RebA in mitochondrial metabolism. NHDF and Hs578t cells were tested, both grown in both LG and OX medium. Cells were subjected to 10 mM of RebA, present in the cell culture medium, for 24 h, and compared against their control, allowing the drawing of scatter plots, shown in Figures 15 to 18. Cells were subjected to 10 mM of RebA for 24 h. Eventual results would be due to conditioning of the cells to a different state in the presence of RebA, as during the readings of Mitoplate S-1, RebA was not present in the assay medium (described in the section 2.5.1.2).

3.2.1.2 RebA promoted mitochondrial oxidation of substrates associated with the TCA cycle in OX, when compared to control, while in LG an overall increase was observed

Observing first the NHDF cells in OX medium in the control situation (absence of RebA), it is noticeable that there are substrates linked to a higher rate of dye reduction (higher distances to the diagonal), those being D-L-Isocitric acid, L-Malic acid, α -Keto-Glutaric acid, Succinic acid, Pyruvic acid, Fumaric acid and Citric acid. All those substrates are correlated with the TCA cycle, thus indicating that at the moment of the assay, this part of the mitochondrial metabolism was predominant. On the other hand, substrates such as tryptamine, g-Amino-Butyric Acid, α -Keto-Isocaproic, Acetyl-L-Carnitine and L-Leucine were the ones associated with a lower rate of reduction of the dye.

Most substrates appear in the scatter plot as a cluster, between 0 and 5 units of the axes.

In the presence of 10 mM of RebA, it is noticeable that, while some substrates present similar rates of dye reduction, there are some notable increases, such as the cases of Pyruvic acid, Succinic acid, α -Keto-Glutaric acid, when compared to control condition. Those substrates, which were originating a higher rate of probe reduction in the control, were associated to further increases in the signal, suggesting that RebA further enhanced the activity of the TCA cycle. Other remarkable enhancements induced by RebA were the cases of Acetyl-L-Carnitine, α -Keto-Isocaproic acid and Tryptamine, the ones associated with the lowest values in the control condition. Overall, the comparison of this pair of conditions points towards an enhancement of the oxidative profile of those cells, with higher mitochondrial activity and, thus, higher consumption of mitochondrial substrates.

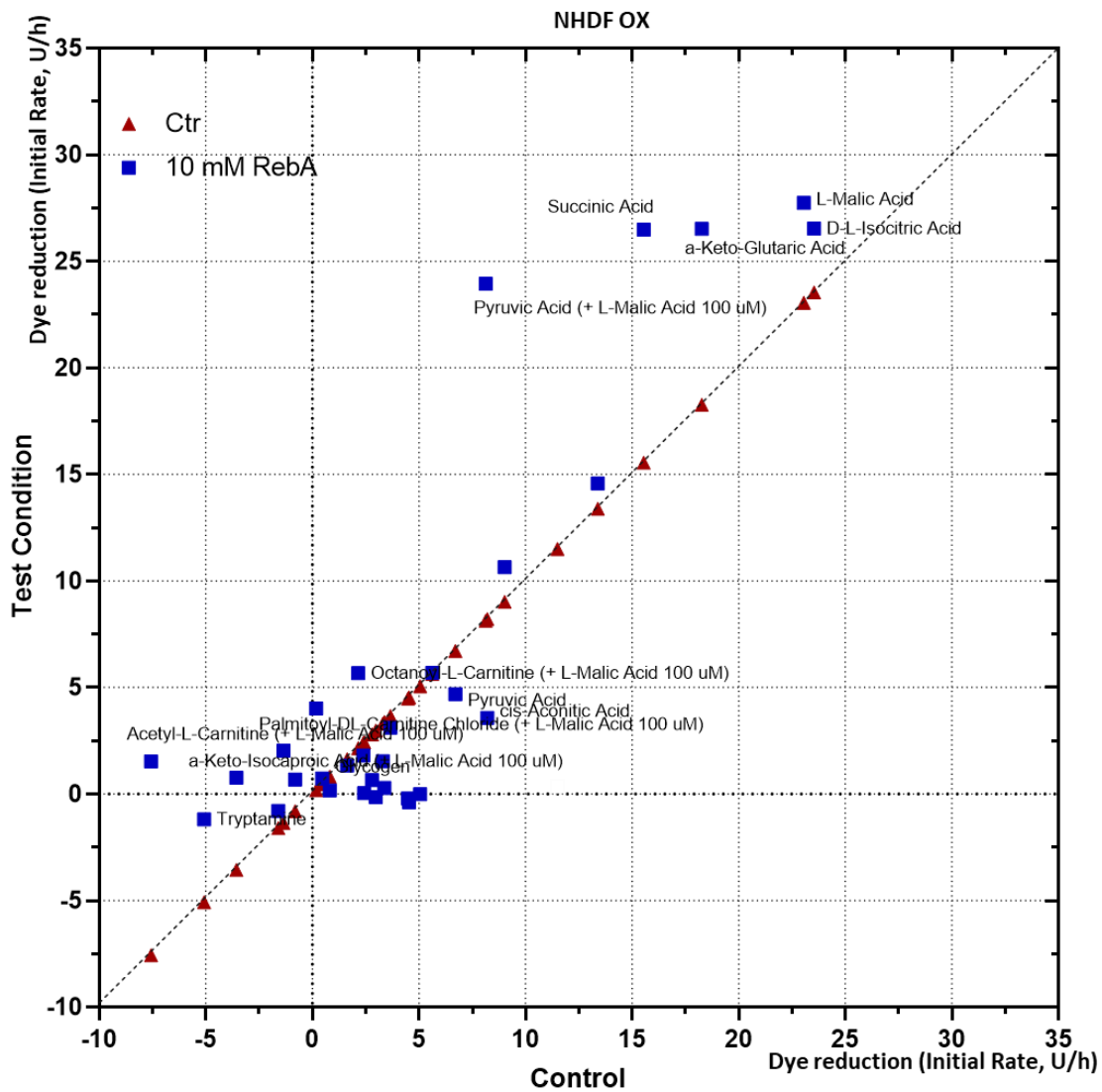


Figure 15: Scatter plot for the average of the results obtained through Mitoplate S-1 for NHDF cells grown in OX medium in the presence of 10 mM of RebA plotted against the control condition. N=3 for each condition.

In LG medium, NHDF cells still show a preference for substrates of the TCA cycle in control conditions. However, the cluster comprising most of the mitochondrial substrates appears at values lower than 2.5 U/h, suggesting an overall lower mitochondrial activity compared to their equivalent in OX. When these cells were exposed to RebA, the rate of the dye's reduction for all the substrates was enhanced compared to control, bringing those values closer to the ones observed in the OX assays, with the main cluster of substrates averaging the 5 U/h. There were some individual substrates associated to a significant enhancement of dye reduction rates when exposed to RebA, such as Succinic acid, L-Malic Acid, D-L-Isocitric Acid and cis-Aconitic acid, once more the ones

associated with the TCA cycle. There was also a noteworthy increase in the rate of dye reduction for Octanoyl-L-Carnitine. Similarly, there were also the cases of the enhancement of the consumption of Leucine and α -Keto-Isocaproic acid, a deaminated Leucine. Leucine is a ketogenic amino acid, forming acetyl-CoA and acetoacetate.

Having all those occurrences into consideration, RebA appears to stimulate the cells to adopt a more oxidative profile, enhancing the mitochondrial activity in this non-tumoral model.

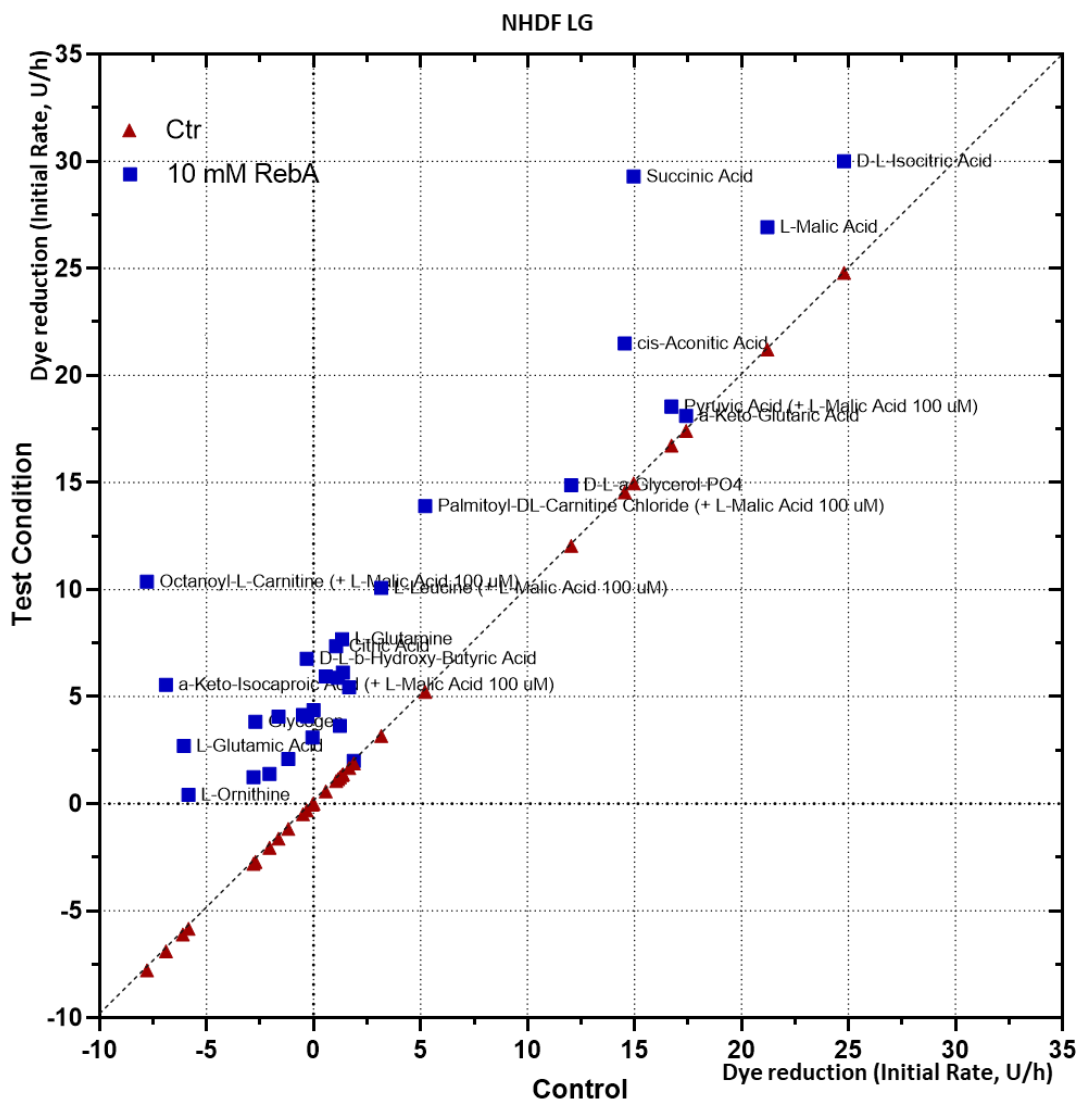


Figure 16: Scatter plot for the average of the results obtained through Mitoplate S-1 for NHDF cells grown in LG medium in the presence of 10 mM of RebA plotted against the control condition. N=3 for each condition

3.2.1.3 RebA-treated Hs578 cells cultured in LG had metabolic profiles with similarities to those of control cells cultured in OX

Hs578t cells were subjected to the same conditions as the NHDF cells, and comparisons were made between Hs578t cells exposed to RebA with their control, either in LG or OX media (Figures 17 and 18). In this tumoral model, the rates of probe reduction had higher levels than those observed in the NHDF cells. This is not synonymous, however, that those cells in culture consume those substrates at a higher rate, as there are other factors that can be behind these differences, such as different responses to the concentration of saponin in the assay media, which can make the cells more or less permeable to the substrates based on their inherent characteristics, and there is a possibility that the concentration of saponin that was used, despite being the same for both cell lines, had more impact in the Hs578t cells than in NHDF. So, comparisons of absolute values of rate of oxidation of the dye between those different cell lines may not be directly comparable. However, comparisons are possible within the same cell line, subjected to different conditions.

For the Hs578t cells grown in OX medium, it can be seen that for both the control and for the treated cells, most substrates are correlated with a low rate of dye reduction. Then, analyzing the control, around ten substrates possess rates over the 25 U/h, with three of them having higher rates than the others, those being Palmitoyl-DL-Carnitine, cis-aconitic and L-Malic acid. This data implies that the TCA cycle may be, once again, the most active pathway, with other of its substrates still being consumed at an above average rate, such as Fumaric acid and D-L-Isocitric acid. Regarding the high signal originated by Palmitoyl-DL-Carnitine, implies that the cells are also consuming fatty acids, possibly being used in beta-oxidation to fuel the cycle. In cells exposed to RebA, it is noticeable a slight increase in the consumption of L-Malic Acid and cis-Aconitic acid, while there was a slight decrease for Palmitoyl-L-Carnitine. In the other hand, there were very noticeable increases in the rate of dye reduction associated with α -Keto-Glutaric acid, as well as pyruvic acid. Overall, this suggests at least a partial enhancement of the oxidative profile of the cells, even if some substrates of the TCA cycle were associated with a slight decrease in the signal, such as Fumaric acid and D-L-Isocitric acid. This may be due, for example, to the existence of anaplerotic reactions within the pathway, suggesting the higher need of some of these substrates for other ends.

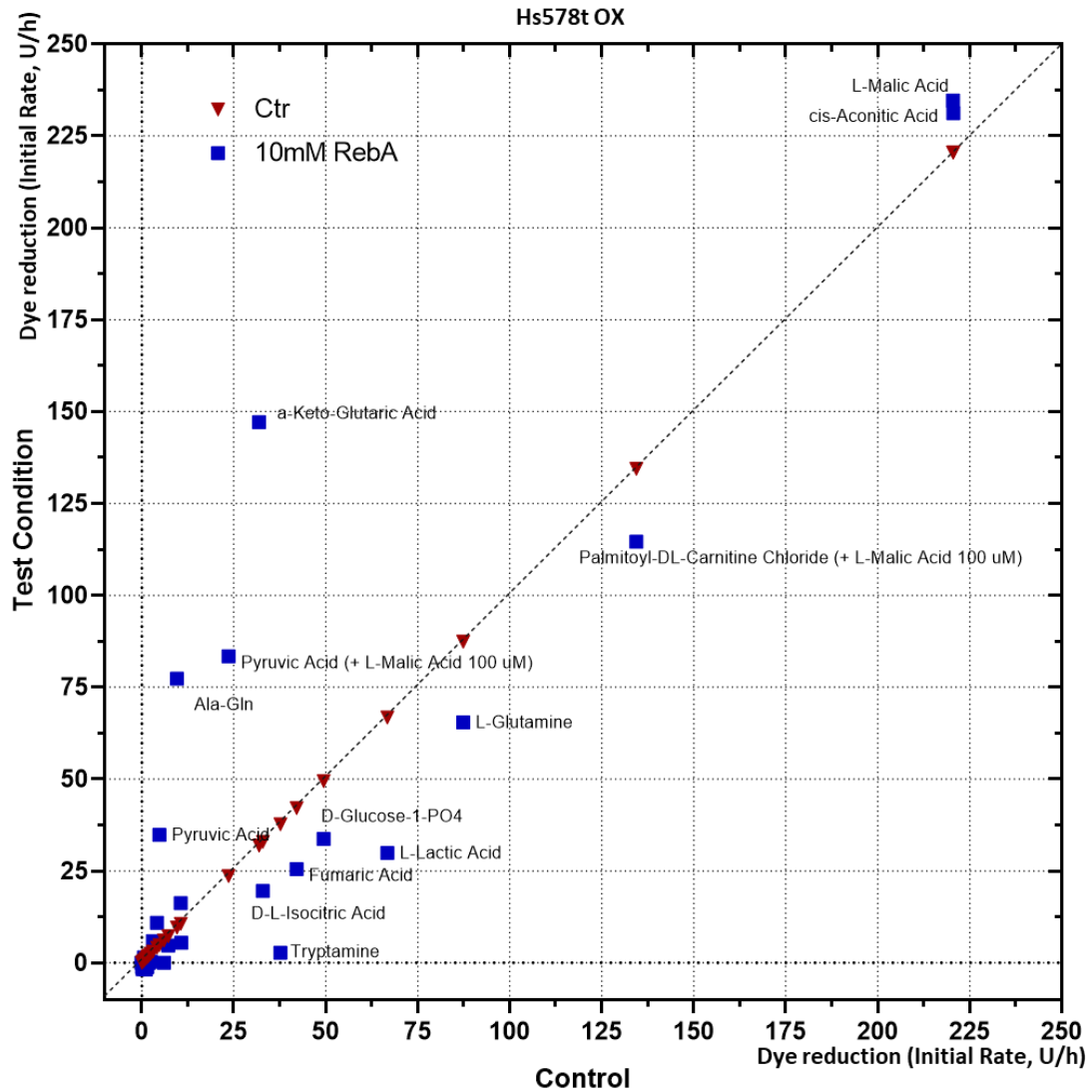


Figure 17: Scatter plot for the average of the results obtained in the Mitoplate S-1 assay for Hs578t cells grown in OX medium in the presence of 10 mM of RebA plotted against the control condition. N=3 for each condition

Regarding the assays carried out for Hs578t cells in LG medium, it can be seen that the average values obtained for the signals related to the rate of probe reduction was lower than for their OX counterparts, suggesting a decrease in mitochondrial activity, which is consistent with the fact that, in the presence of glucose, the tumoral cells present a more glycolytic phenotype, relying less in mitochondria for ATP production. The third substrate with higher rate of probe oxidation was D-Glucose-1-PO4, while the rate for D-Glucose-6-PO4 was also high. Glycogen was also being consumed at high rates, indicating a

possible activation of glycogenolysis. Still, Fumaric acid and D-L-Isocitric acid were the most consumed substrates, suggesting a still significant activity of the TCA cycle. For the cells exposed to RebA, there were some remarkable alterations regarding the most consumed substrates. First of all, the rate of probe reduction was increased for L-Malic and Cis-Aconitic acids, which were the two substrates that stood out with the highest values in the assays with Hs578t cells in OX medium. Opposite to this, Fumaric acid and D-L-Isocitric acid's rate of substrate oxidation were much lower than those of the control and, once again, going toward the rates occurring for those substrates in OX conditions. Along with this, there were big decreases also associated with Glycogen and D-Glucose-6-PO₄ (but not for D-Glucose-1-PO₄). This suggests a loss in the glycolytic profile of those cells in the presence of RebA, at least partially. There was also an increase in Lactic acid consumption, which can be related to its conversion into Pyruvic acid, also more consumed in the presence of RebA. There were contrary effects for both fatty acids in this assay, Octanoyl-L-Carnitine and Palmitoyl-DL-Carnitine, with the consumption of the latter being increased, while the other was decreased. When those values are compared with the ones for this cell line in OX condition, the rate of consumption for Palmitoyl-DL-Carnitine was the third highest for all substrates, while Octanoyl L-Carnitine had the 9th lowest rate. Putting all this information together, Hs578t cells in LG medium that were exposed to RebA shifted towards a metabolic profile with high degree of similarity with those cells grown in OX medium, suggesting a higher reliance in mitochondrial activity, thus inducing a more oxidative phenotype.

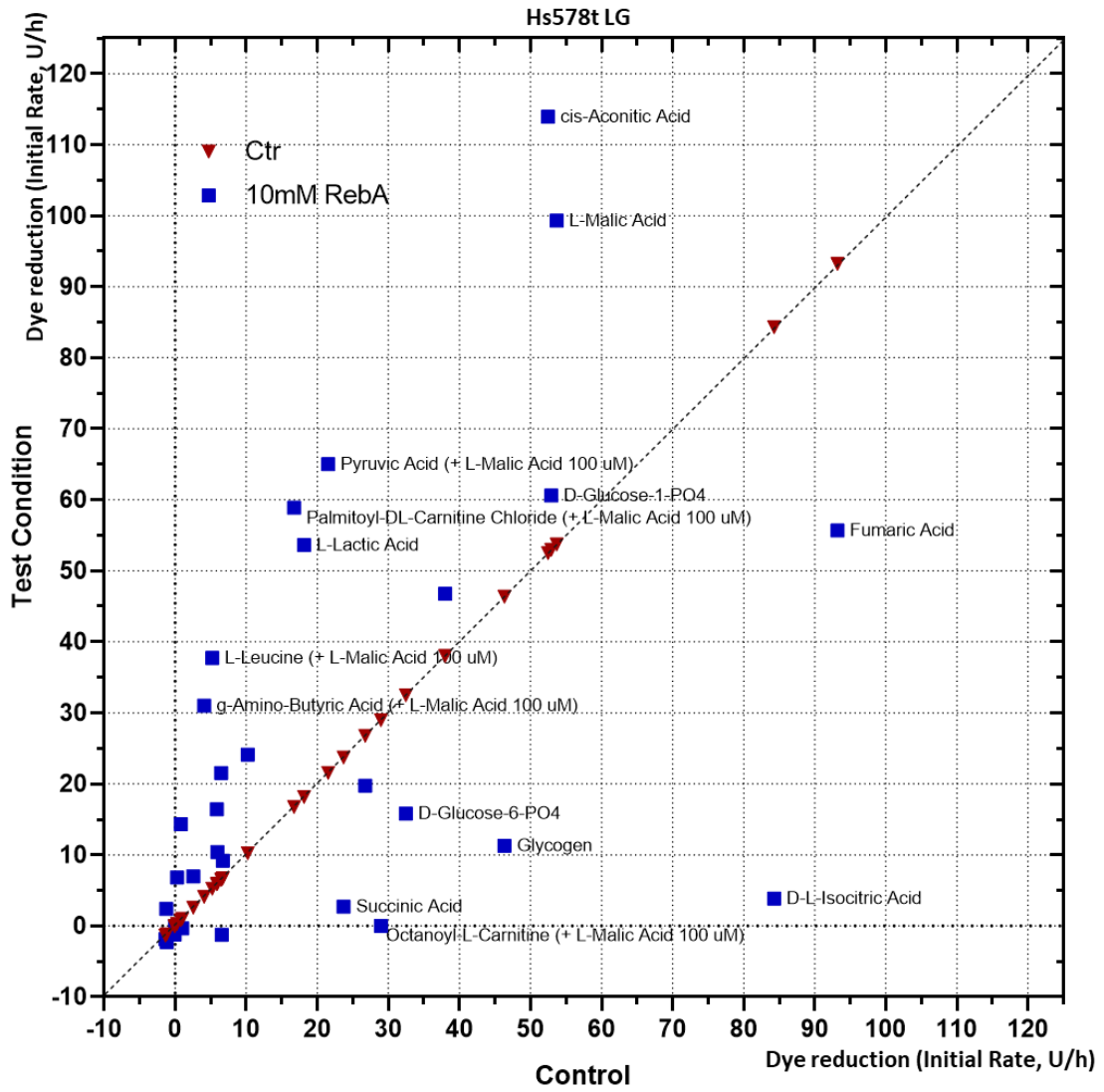


Figure 18: Scatter plot for the average of the results obtained through Mitoplate S-1 for Hs578t cells grown in LG medium in the presence of 10 mM of RebA plotted against the control condition. N=3 for each condition

3.2.2 Metabolic profiling through analysis of extracellular and intracellular metabolites

3.2.2.1 Details and objectives

¹H NMR analyses were made to measure the exact quantities of glucose that was being consumed and lactate that was being produced, as a way to characterize metabolic changes induced by RebA. Once this SG is described as insulin-mimetic by some authors, insulin was also tested, alone and in combination with RebA, to assess if the cells behaved in the same way regarding the measured parameters. Also, before the other assays, a commercial sample of RebA, sold as a sweetener and more available, with announced purity of 98%, was compared against an analytical sample of RebA with a purity of 98%. ¹H NMR spectra were acquired for both and comparisons performed. Results are shown in Figure 19.

¹³C NMR was performed to give further information about metabolism, studying intracellular concentration of key metabolites.

Insulin was also used along with RebA, not only to address the nature of the insulin-mimetic effect of this SG, but also because some SGs have been reported to enhance secretion of insulin in the β -Pancreatic cells (Jeppesen et al, 2000; Phillipaert et al, 2017). Eventual therapeutic uses of SGs would quite possibly be accompanied by raises in insulin concentration, so it would be interesting to know how those molecules act together and, also, to test the nature of its response and if the metabolic mechanisms that they induce are similar and synergetic, or if there is more to it.

3.2.2.2 Analysis of extracellular metabolites through ¹H NMR assays

3.2.2.2.1 The spectrum resolved for the commercial sample of RebA was similar to the one obtained for the analytical one, indicating high degree of purity

¹H NMR spectra for the samples of 10 mM of both the commercial and analytical RebA, dissolved in miliQ water, were obtained. Results show a high degree of similarity both in the resonances that appeared and their intensity. With this, it is conceivable that the commercial sample had, in fact, an apparent purity comparable to the one of the analytical sample. This excludes the fact that the results for the high IC₅₀ values of cell viability that were then achieved could be due to a possible lack of purity of the used sample.

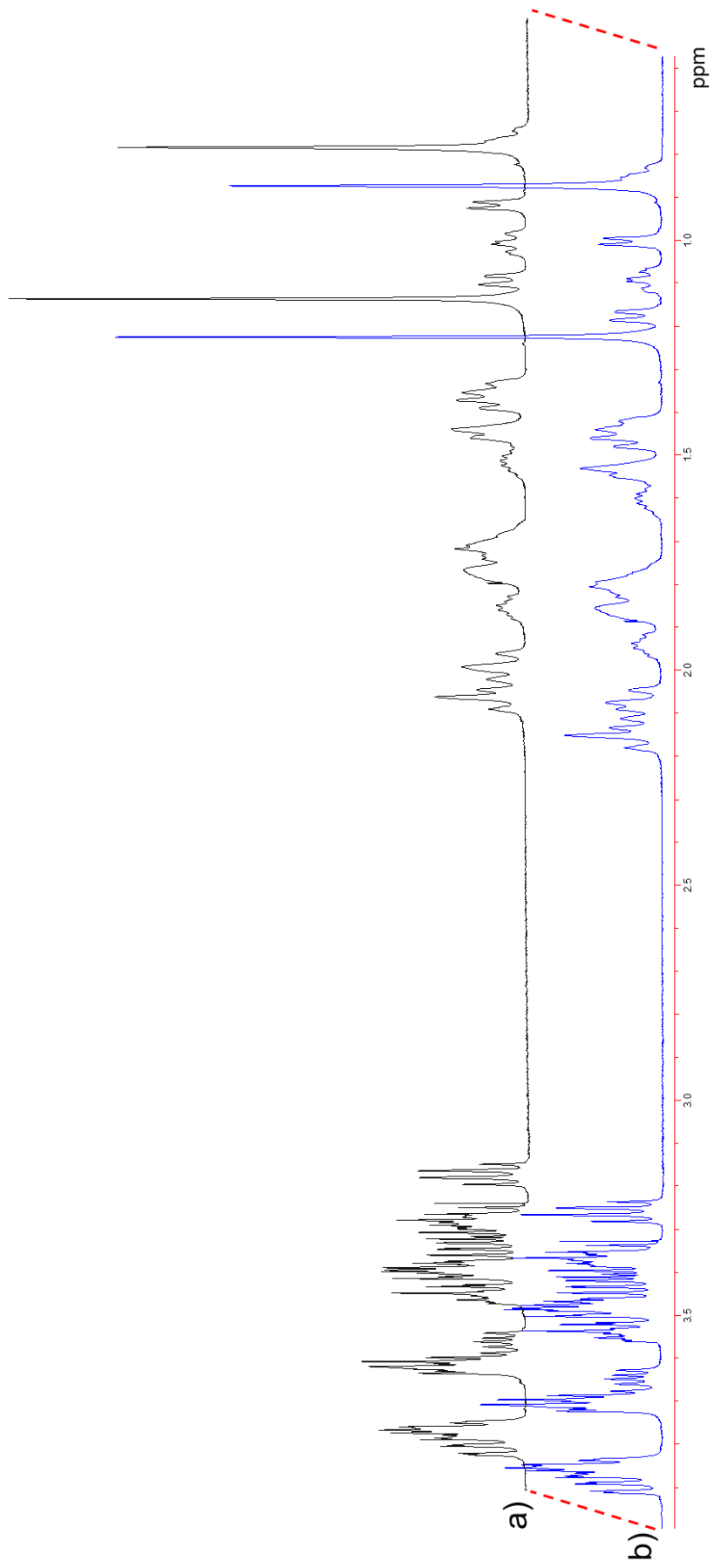


Figure 19 – a) ¹H Spectra for the commercial sample of RebA, sold as a sweetener; b) ¹H Spectra for the analytical sample of RebA, with a known purity of 98%

3.2.2.2.2 Increased glucose uptake and lower production of lactate hints at a shift towards a more oxidative phenotype in the presence of RebA

The areas below the peaks corresponding to ^{13}C lactate and ^{13}C glucose were integrated, giving the concentrations of those substrates at the moment of quenching. With this, the OXPHOS index could be calculated (Equation 1), giving an indication if the cells' metabolism tended towards a more oxidative or more glycolytic phenotype. Spectra were obtained for each experimental condition, being one example of each presented on Figure 20. Calculations of the concentrations of the desired metabolites were obtained through integration of the areas corresponding to their specific resonances. Values for all the different Ns were then grouped and plotted into Figure 21.

First of all, it is noteworthy to point out that, for some conditions, there were high discrepancies in the levels detected for the concentrations of some metabolites, leading to a low number of cases with statistically significant differences. So, further experiments would be beneficial in the future, to further consolidate the results. Possibly, a use of higher concentrations of glucose would be advisable by using, for example, HG medium instead of LG, so the peaks would be clearer, allowing for more precise readings. However, some consistent trends can still be noticed, allowing for analysis of this data.

For the NHDF cells, in the presence of RebA, there was a lower final concentration of glucose, indicating a higher rate of its uptake. However, insulin had a slightly opposite trend in this case. When both those molecules were present, the glucose uptake was further enhanced. Even if the results for insulin are not what was expected, a potential explanation was that the medium already contained insulin due to supplementation with FBS, with unknown concentration since it is dependent on the lot (although the same lot was used for all those assays), so the added insulin might not have been translated into a more accentuated response in this non-tumoral cell line. Regarding the levels of lactate, statistical significance can be observed between the control and the condition with 10 mM of RebA, with levels of lactate being less than half of those observed in the control condition. The condition containing added insulin produced levels of lactate similar to the control, while for the last condition with RebA combined with insulin the levels of lactate were, once again, below half of the control. With these values, the OXPHOS index was calculated, and a visible shift towards a more oxidative metabolism was observed for both conditions containing RebA, while for the case of insulin, the metabolic profile turned out to be more glycolytic. For the case of RebA and for RebA+Ins, while the glucose consumption was enhanced, the lower lactate levels suggest that glycolysis may not have been as active as in the control. Using the

information from the previous assays, it is possible that glucose was being converted into pyruvate and then into acetyl-CoA, powering the TCA cycle, associated with a higher reliance on mitochondria for obtention of energy. As cells were less glycolytic, they were also less proliferative, what was verified in our previous assays.

Analyzing the values obtained for Hs578t cells, a similar trend can be observed. The main differences come from the lower final concentration of glucose, indicating that it was more consumed, not only for both the conditions of RebA and RebA+Ins, but as well for Insulin alone, unlike what was observed for NHDF and, in this tumoral cell line, this condition with insulin was the one where the final glucose concentration was lower. Results for the final lactate concentration show that, once again, RebA was associated with lower levels of this metabolite. Insulin induced higher final levels of lactate than all the other conditions, while RebA+Ins showed results in between, suggesting that the response was averaged, with potential indication that RebA and insulin may induce contrary responses at a metabolic level. Regarding the OXPHOS index, once again it was significantly enhanced in the presence of RebA, in accordance with previous data, further indicating a shift towards a more oxidative metabolism. For the cases of insulin and RebA+Ins, the OXPHOS index appears to be slightly lower than the control, even if there is a big discrepancy in the individual values, making this comparison less reliable.

Finally, MCF7 cells were also studied. For this cell line, the final levels for the concentration of glucose were lower than for the other cell lines, making the areas below their peaks in the NMR spectra harder to integrate and, thus, less precise. Those cells appeared to be especially glycolytic even for the control condition. Apart from the control, the other conditions had a bigger error associated, making comparisons harder but, overall, RebA appears to have reduced the glucose uptake, while insulin averaged a small increase. RebA+Ins had intermediate results, but closer to those of RebA. The lactate levels, however, were clearer and in accordance with what was observed for the other cell lines, especially with Hs578t, where insulin appears to have increased the lactate levels by a considerable amount. For the OXPHOS index, once again, when compared with the control, RebA made the cells more oxidative, while insulin made them more glycolytic and the combination of both those molecules had results in between, but still making the cells more glycolytic than the control.

All in all, as described previously, RebA is inducing a more oxidative metabolism, unlike insulin, with special impact in the production of lactate, suggesting the activation of metabolic pathways other than glycolysis, quite possibly the TCA cycle, as it was suggested by the previous assays. Another remarkable factor is that there was a

tendency for the condition containing both RebA and Insulin to have results averaging those of these molecules when administered on its own. This suggests that, regarding their impact in metabolism, they may have even induced a different response. So, when they are referred as insulin mimetic, while they both may tendentially increase the glucose uptake, regarding the effective impact in metabolism, they are not so similar, inducing different kinds of responses.

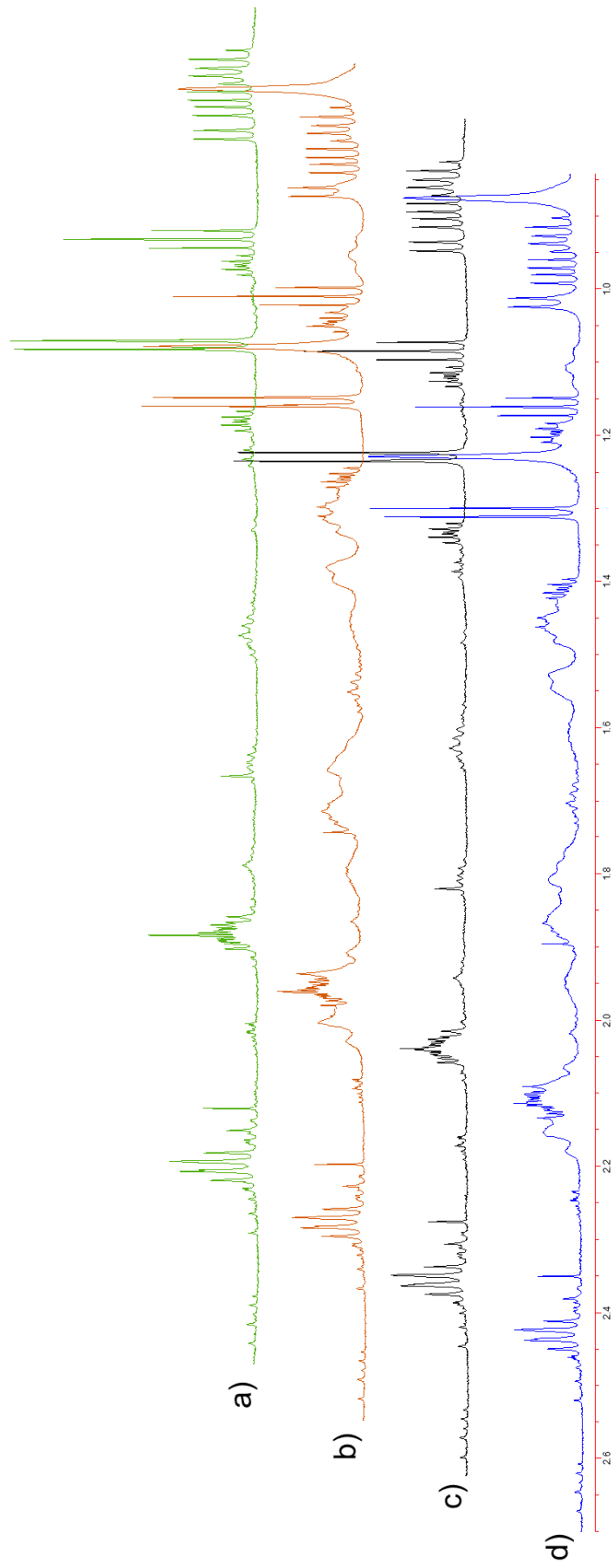


Figure 20 ^1H Spectra for the N=1 of NHDF cells, as a representation of the overall results. Cells were cultivated in LG medium containing $[\text{U-}^{13}\text{C}]\text{-Glucose}$, plus the drugs of interest. a) Control b) 10 mM of RebA; c) 3 nM of insulin d) 10 mM of RebA + 3 nM of insulin. Samples were dissolved in H_2O , with standard for calibration containing 2 mM of Fumarate

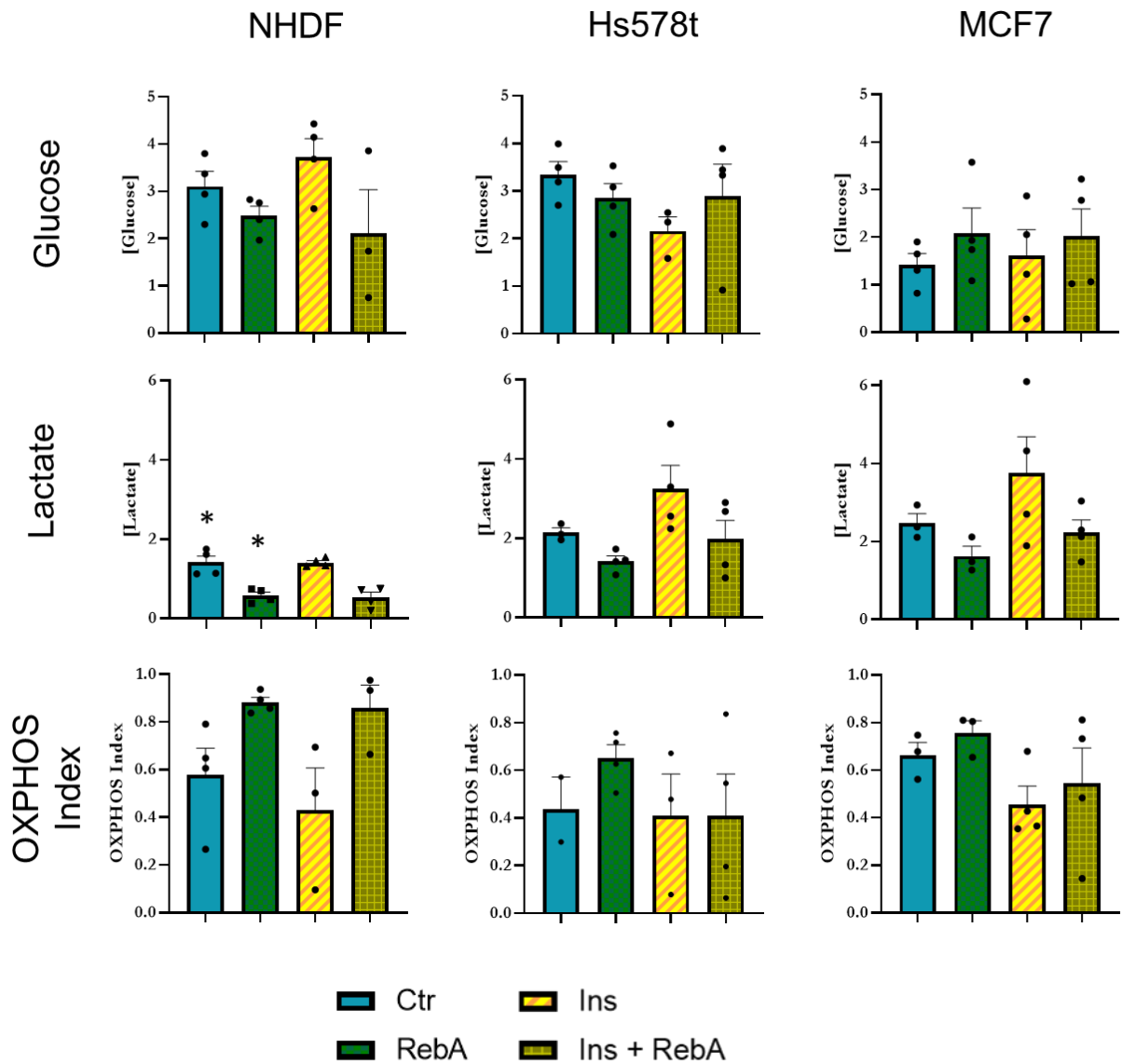


Figure 21: Extracellular final concentrations of ^{13}C -glucose and ^{13}C -lactate, in mM, obtained through reading of the culture medium collected immediately before the quenching process. N=4. Negative values were not considered. Non-parametric Kruskal-Wallis test followed by Dunn's post-test for multiple comparisons were performed, comparing each condition of the same cell line with its control, as to determine if there was statistical significance. *: $p < 0.05$. Results are expressed as a mean, with error bars for the SEM.

3.2.2.3 ¹³C NMR assays suggest an anabolic character of metabolism

Some ¹³C NMR spectra were obtained for evaluation of ¹³C incorporation in intracellular metabolites. It must be disclosed that only a small number of spectra were obtained, since acquisitions of ¹³C spectra require much longer times to obtain. This resulted in only N=1 readings for this particular assay, reducing the potential of the observed results. Despite this limitation, some simple inferences can be made.

In the available spectra, in figure 22, the presence of metabolites enriched with ¹³C can be observed. For cells exposed to RebA, there appears to be an increase in Ace-C2, specially in NHDF cells, and an expressive reduction of Glu-C4 for the non-tumoral cell line, not so evident for MCF7 and Hs578t cells. This would suggest, in the presence of RebA, that cells are not being able to fully oxidize acetyl-CoA by the TCA cycle. This hints that they possess a more anabolic phenotype, possibly in order to synthesize intermediates for the synthesis of biomolecules and also for cell proliferation. Once the results show the presence of Glu-C4 in the ¹³C NMR spectra from cells exposed to RebA, this suggests that the impairment in oxidizing acetyl-CoA is not total. The trend for reduced levels of Glu-C4 suggests a dilution of the TCA intermediaries in detriment of sources without ¹³C enrichment, such as amino acids or other molecules present in FBS. Still, these claims must be taken with caution due to the lack of replicas for each condition.

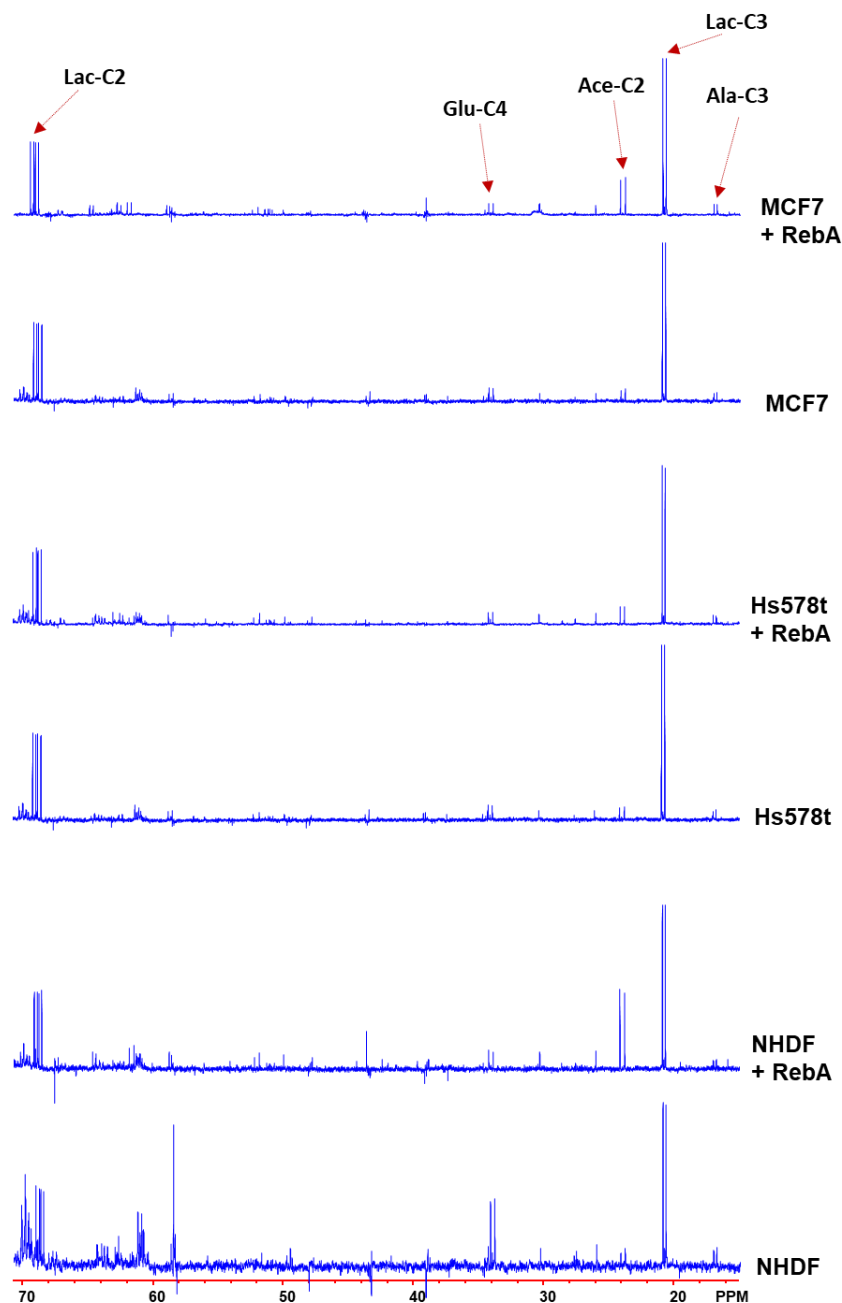


Figure 22: Expansions of ^{13}C NMR spectra from methanol: H_2O (80:20, v/v) extracts of cells cultured in media supplemented with $[\text{U}^{13}\text{C}]$ -glucose in the absence and presence of RebA. More abundant ^{13}C enriched metabolites include Lactate (Lac), Acetate (Ace), Glutamate (Glu) and Alanine (Ala). The presence of RebA leads to an increase in Ace-C2 concentration and a reduction in Glu-C4 in NHDF cells, suggestive of a partial inability of these to oxidize acetyl-CoA by the TCA cycle in the presence of RebA. In the other two cell lines the increase in Ace-C2 is less notorious and no effect is observed in Glu-C4 enrichment. These results reflect a limited oxidative character in the TCA cycle, being its activity partially embodied by an anabolic character which provides for the much-needed metabolic intermediates to sustain biosynthesis and cell proliferation. N=1

3.2.3 Impact of RebA for OCR and ECAR

Seahorse XFe96 assays using the Mito Stress kit were performed for the three cell lines, in LG and OX medium. Cells were exposed for 24 hours to 1 and 10 mM of RebA in its growth medium, then replaced with Mito Stress assay medium, without the presence of this SG, so any changes that occur are due to previous conditioning to the metabolism induced by it. OCR and ECAR were measured and, with their values, energy maps were drawn.

3.2.3.1 OCR values were higher in the presence of RebA for cells in LG medium. Spare respiratory capacity and non-mitochondrial respiration were tendentially enhanced

For the cells grown in LG medium, exposure to RebA caused some trends in the OCR, as can be seen in figure 23. Making a step-by-step analysis, looking at the values for the baseline, corresponding to the basal respiration, along with non-mitochondrial respiration, its noteworthy that for the NHDF and Hs578t cells exposed to RebA the values on OCR were higher, while on the MCF7 cells it remained similar to the control. After the injection of oligomycin, blocking ATP synthase, once again the values were higher for the RebA conditions than for the control for NHDF and Hs578t cells, and, as previously, there were no big differences in the MCF7 cancer cells. However, after the injection with FCCP, a consistent response can be seen for all the different cells, with increases in the OCR values when compared to the control. This change was more notorious in the NHDF cells, with the MCF7 showing the lowest response, but still noticeable for the 10 mM of RebA. After the last injection, with Rotenone + Antimycin A, the values of OCR lowered to levels indicative of non-mitochondrial oxygen respiration and returned to show little to no difference for the MCF7 cells. Though, a larger difference can be seen for Hs578t cells, suggesting increases in the levels of non-mitochondrial oxygen consumption. NHDF cells also had higher values for OCR after the last injection of this assay in the presence of RebA.

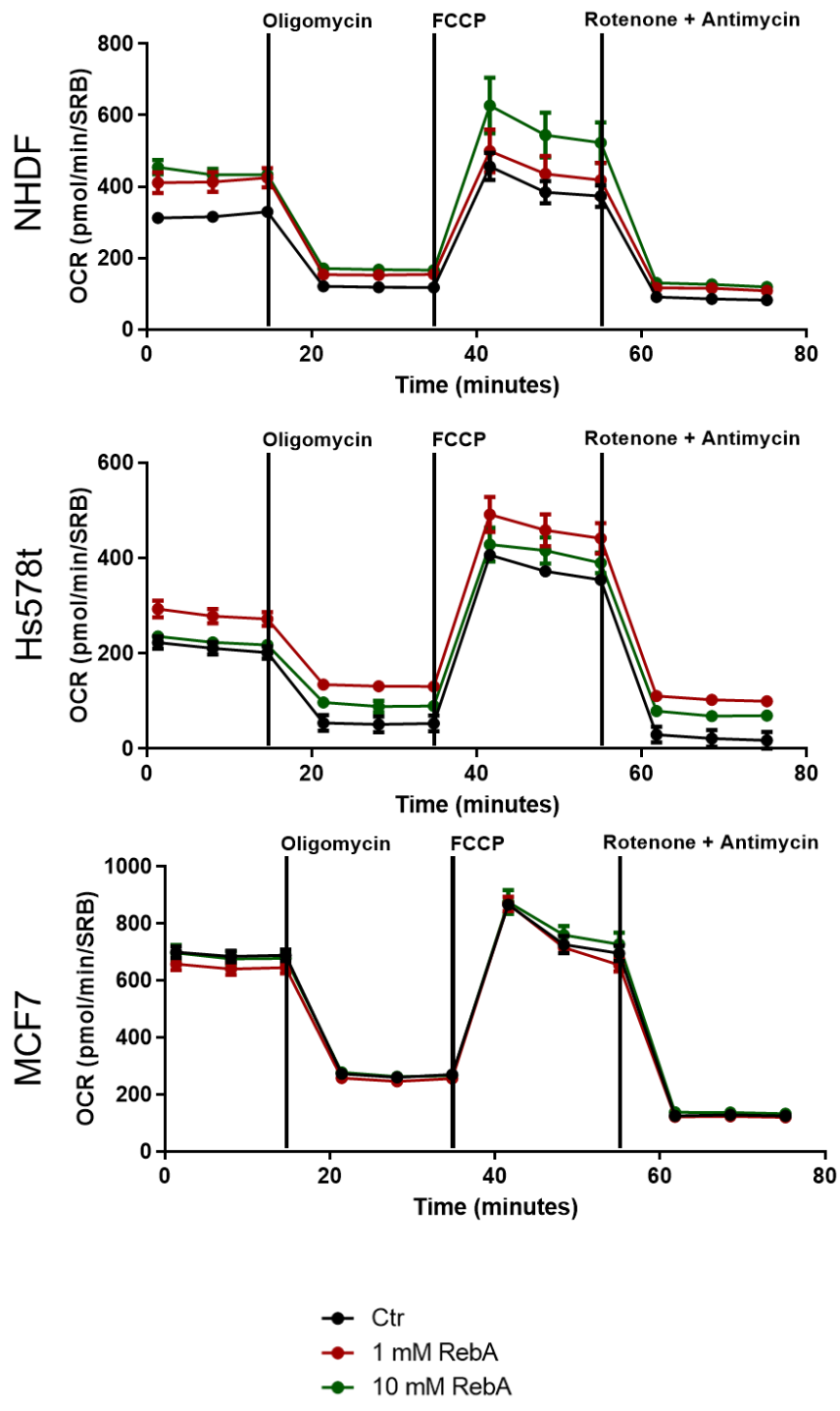


Figure 23: OCR values for NHDF, Hs578t and MCF7 cells, subjected to 24h of exposure to 0, 1 and 10 mM of RebA in LG medium. At intervals of 18 minutes, injections of oligomycin, FCCP and rotenone + antimycin A were performed, with final concentrations for NHDF cells of 2 μ M, 1 μ M, 1 μ M and 1 μ M, respectively. Concentration of FCCP for the tumoral cells was 0.25 μ M. NHDF cells were plated at a density of 8000 cells per well, Hs578t at 10000 cells per well and MCF7 at a density of 20000 cells per well. Values were chosen having in consideration previous optimization. Normalization was performed based on SRB analysis. Data expressed as mean \pm SEM of 4 N

The values for the ECAR were also plotted and can be seen in figure 24. For the NHDF cells, those that were exposed to RebA had higher values, especially for the ones exposed to 10 mM of this substance, in which the ECAR values almost doubled those of the control. In the other hand, Hs578t cells apparently showed a big difference for the lowest concentration of RebA, 1 mM, while for 10 mM the initial values for ECAR were lower than the control before the first 20 minutes, then tending to get higher. Results for MCF7 cells were more mixed, with those cells exposed to 1 mM of RebA having a lower ECAR than the control, while the ones exposed to 10 mM had higher values.

By plotting both those values of OCR and ECAR in energy maps (Figure 25), several trends can be observed. For NHDF cells, for the baseline conditions, results suggest a tendency for cells exposed to 1 mM of RebA to be more aerobic, while at 10 mM the cells were more glycolytic as well. After being subjected to the stress induced by oligomycin and FCCP, all conditions shifted towards a more energetic and glycolytic metabolism, with special emphasis for the cells treated with 10 mM of RebA.

Hs578t cells showed a similar trend to that of the non-tumoral cells for the condition of 1 mM of RebA, for both the baseline and stressed values. For the highest concentration of RebA, there appear to be less differences when compared with the control, moving towards a more glycolytic metabolism.

The energy map obtained for the MCF7 cells retrieved less expressive results. Comparing the control with the condition of 1 mM of RebA, the baseline values of those cells treated with the SG appear to be more glycolytic, and the same can be said for stressed results. However, when comparing the control with the higher concentration of RebA, 10 mM, the baseline values for the later had lower OCR values than the former, to a more quiescent state. Though, in the stressed condition, the OCR values match those of the control, indicating a bigger difference between the baseline and stressed states.

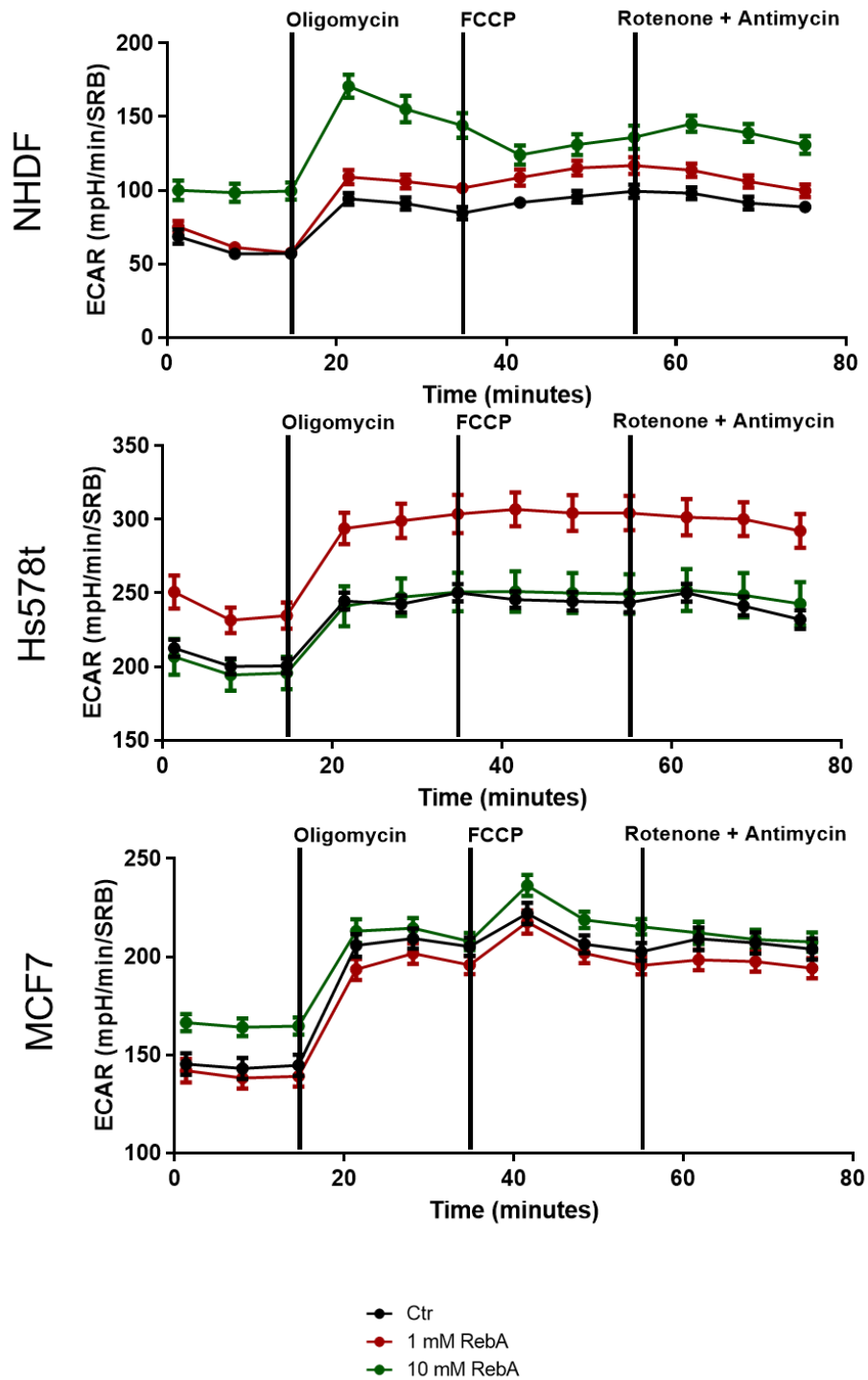


Figure 24: ECAR values for NHDF, Hs578t and MCF7 cells, subjected to 24h of exposure to 0, 1 and 10 mM of RebA in LG medium. At intervals of 18 minutes, injections of oligomycin, FCCP and rotenone + antimycin A were performed, with final concentrations for NHDF cells of 2 μ M for oligomycin and 1 μ M for the remaining inhibitors. Concentration of FCCP for the tumoral cells was 0.25 μ M. NHDF cells were plated at a density of 8000 cells per well, Hs578t at 10000 cells per well and MCF7 at a density of 20000 cells per well. Values were chosen having in consideration previous optimization. Normalization was performed based on SRB analysis. Data expressed as mean \pm SEM of 4 N

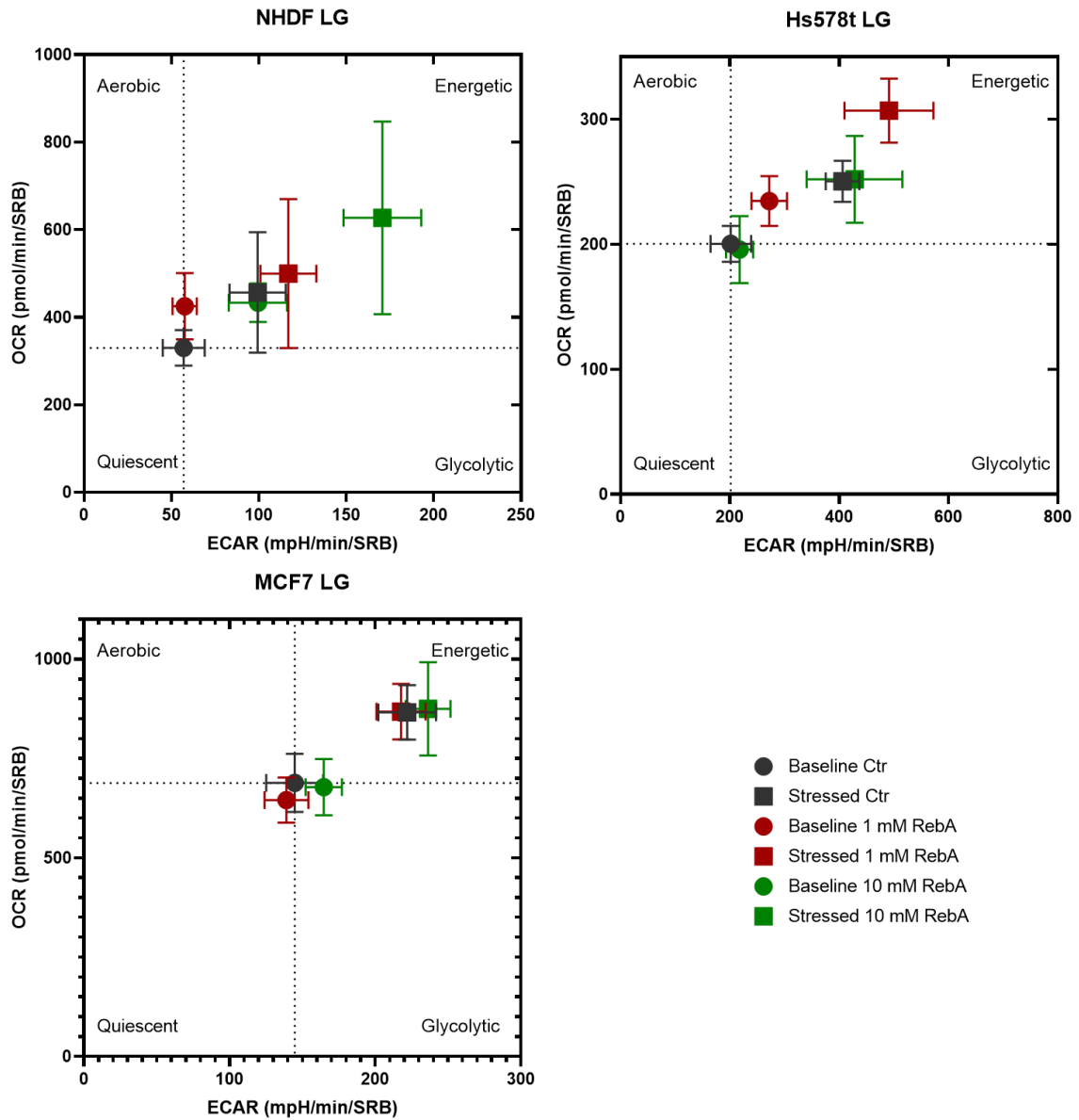


Figure 25: Energy maps obtained for NHDF, Hs578t and MCF7 cells, subjected to 24h of exposure to 0, 1 and 10 mM of RebA in LG medium, based in the OCR and ECAR data obtained in the previous two figures. Data expressed as mean \pm SD of 4 N

3.2.3.2 OCR values in the presence of RebA were lower in OX medium

The same set of experiments were performed also for OX medium. As it can be seen in the OCR graphs, in figure 26, the trends were the opposite as those verified for the LG grown cells, with the presence of 10 mM of RebA tending to cause a decrease in all the stages of the MitoStress protocol, for all the cell lines, while the lower concentration showed results very close to the control condition.

It is worth mentioning that for the Hs578t cells, the values of OCR after the injection of FCCP, corresponding to a maximal respiratory capacity, were lower than the basal levels. A possibility for this may be due to the concentrations of either Oligomycin or FCCP could have caused some type of damage to the cells, even though the concentration used of both inhibitors were the same as the ones used for the assays in LG and also for the other cell lines. With this occurring also for the control, this phenomenon was not due to RebA, and may be due to the fact that Hs578t cells are more susceptible to the effects of those inhibitors when grown in OX medium.

While in the LG medium, having in consideration all the different assays so far, RebA was possibly stimulating the oxidative phosphorylation and, thus, increased the values of OCR, in the case of OX medium, as this mitochondrial pathway was already stimulated due to the content of the medium, the effect previously mentioned may not have manifested. The decreases in OCR that were observed can be due to effects of different nature, such as some kind of impairment caused to these less proliferative cells.

Regarding the results for ECAR, in figure 27, a similar behavior is represented, with cells incubated with RebA tending to be associated with lower values of the acidification rate of the medium. While after the addition of oligomycin the ECAR values raised for both NHDF and MCF7, it decreased for the Hs578t cells, suggesting that the quantities of oligomycin injected may have had a negative impact in the metabolism of those cells.

Results from ECAR and OCR were plotted into the energy maps of figure 28. First of all, starting by the Hs578t cells, they had a opposite response to what was to be expected, possibly due to the problem mentioned previously, so no reliable conclusions can be made out of it. Looking at the values for the NHDF cells, the difference between the baseline and stressed states was bigger for the cells exposed to RebA when compared to the control, suggesting a higher potential to adopt a more energetic metabolism. A similar scenario was observed for the MCF7 cells, where for the case of the highest concentration of RebA, despite the OCR being lower than the control, in the stressed condition it became higher, along with a bigger delta in the ECAR values as well.

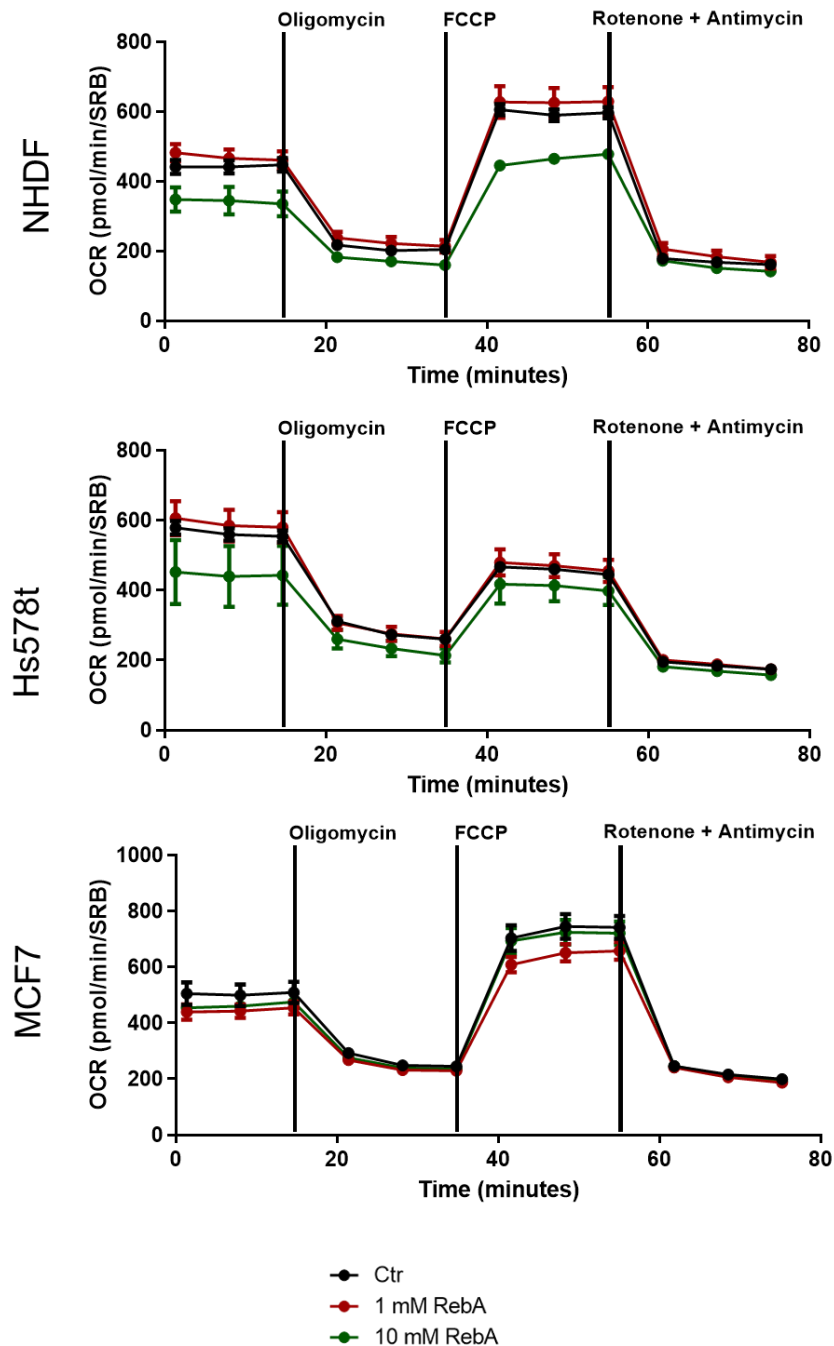


Figure 26: OCR values for NHDF, Hs578t and MCF7 cells, subjected to 24h of exposure to 0, 1 and 10 mM of RebA in OX medium. At intervals of 18 minutes, injections of oligomycin, FCCP and rotenone + antimycin A were performed, with final concentrations for NHDF cells of 2 μ M, 1 μ M, 1 μ M and 1 μ M, respectively. Concentration of FCCP for the tumoral cells was 0.25 μ M. NHDF cells were plated at a density of 8000 cells per well, Hs578t at 10000 cells per well and MCF7 at a density of 10000 cells per well. Values were chosen having in consideration previous optimization. Normalization was performed based on SRB analysis. Data expressed as mean \pm SEM of 4 N

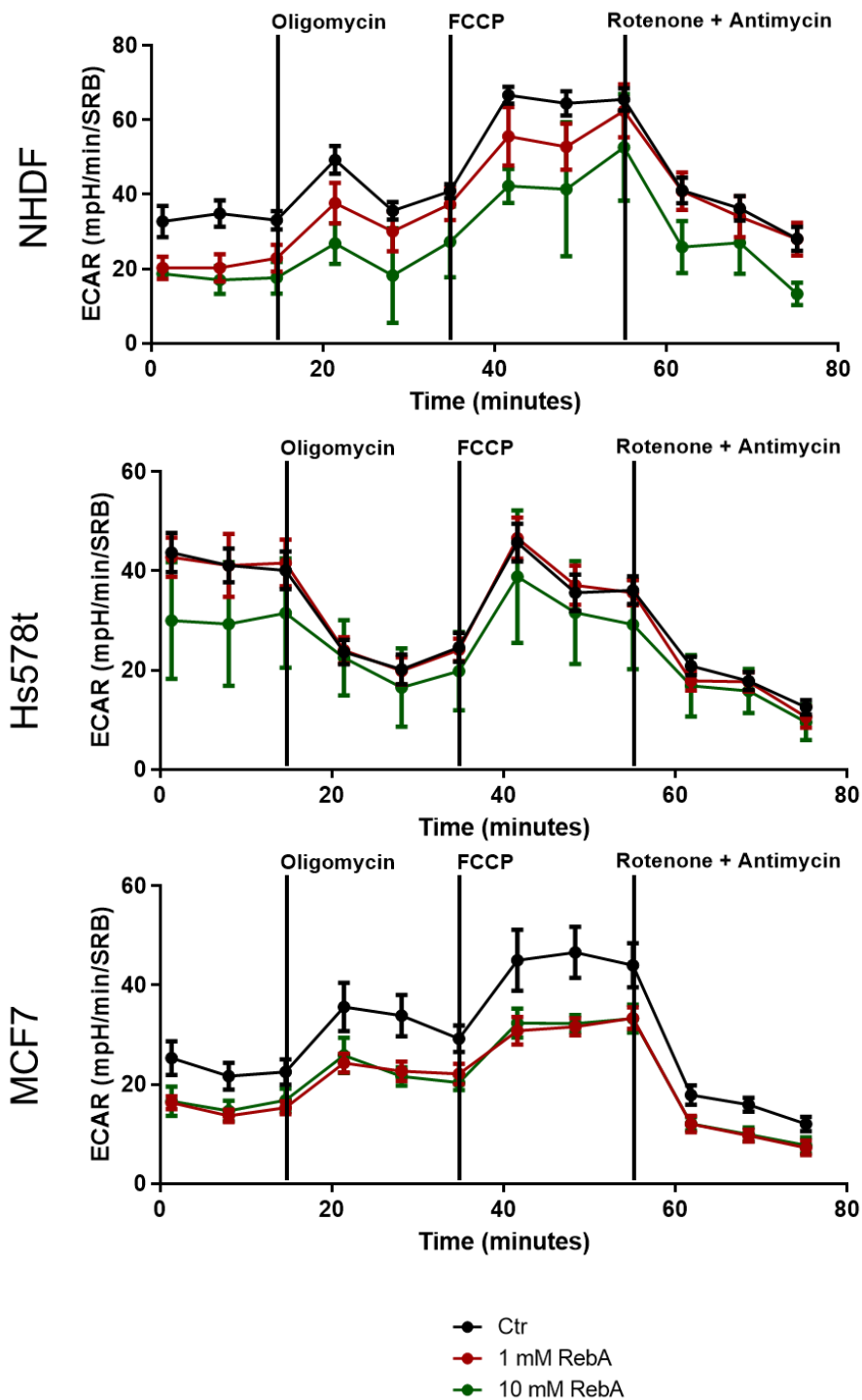


Figure 27: ECAR values for NHDF, Hs578t and MCF7 cells, subjected to 24h of exposure to 0, 1 and 10 mM of RebA in OX medium. At intervals of 18 minutes, injections of oligomycin, FCCP and rotenone + antimycin A were performed, with final concentrations for NHDF cells of 2 μ M for oligomycin and 1 μ M for the remaining inhibitors. Concentration of FCCP for the tumoral cells was 0.25 μ M. NHDF cells were plated at a density of 8000 cells per well, Hs578t at 10000 cells per well and MCF7 at a density of 10000 cells per well. Values were chosen having in consideration previous optimization. Normalization was performed based on SRB analysis. Data expressed as mean \pm SEM of 4 N

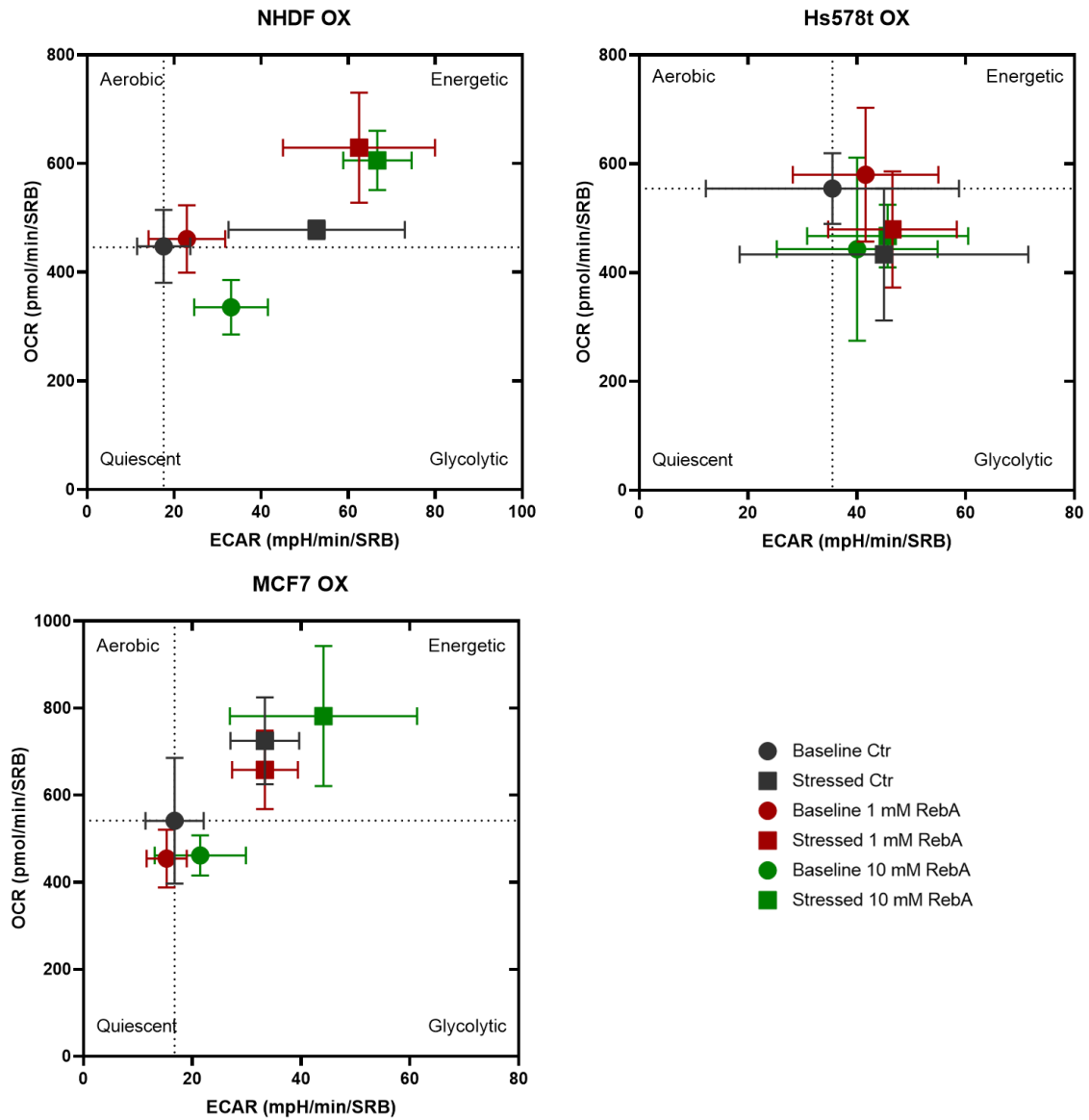


Figure 28: Energy maps obtained for NHDF, Hs578t and MCF7 cells, subjected to 24h of exposure to 0, 1 and 10 mM of RebA in OX medium, based in the OCR and ECAR data obtained in the previous two figures. Data expressed as mean \pm SD of 4 N

All the different parameters possible to be calculated by execution of the Mito Stress assay are presented in section 6, as supplementary data.

3.2.4 Study of the effect of RebA and correlation with changes in ROS levels

As it was indicated in the literature in previous articles, such as Afonso et al, 2020, there have been claims that RebA was associated with an increase in ROS levels, in this case, in murine brain slices, and also in cell lines, linked with ROS mediated apoptosis, as suggested by Paul et al, 2012. However, there are also other sources that claim that SGs have antioxidant properties, such as Bender et al, 2015. So, studies with H₂DCFDA were performed in NHDF, Hs578t and MCF7 cell lines, in LG medium, to see what of those outcomes would occur.

H₂DCFDA is converted into dichlorodihydrofluorescein (DCFH₂) that is then absorbed by the cells then oxidized into fluorescent dichlorofluorescein (DCF). It gives an indication about the levels of ROS in this system. However, it says nothing about its source, nor about what types of ROS are formed, so the results of other assays must complement this method. Cells were exposed to several concentrations of RebA for 24 hours. This medium was then removed and replaced by the assay medium, so there was no RebA present during the reading process. Thus, all the visible observations came for changes previously conditioned by RebA, indicating that those were not immediately irreversible. Samples were read for 160 minutes. However, only the 8 to 36 minutes were taken into consideration in the calculation of the linear regressions and their slopes. The first 8 minutes were discarded in order to allow the cells to stabilize from the change of medium, while after the 36th minute some of the curves lowered their slope, indicating a potential decrease of the available levels of the reduced form of the probe. This data is visible in Figure 29.

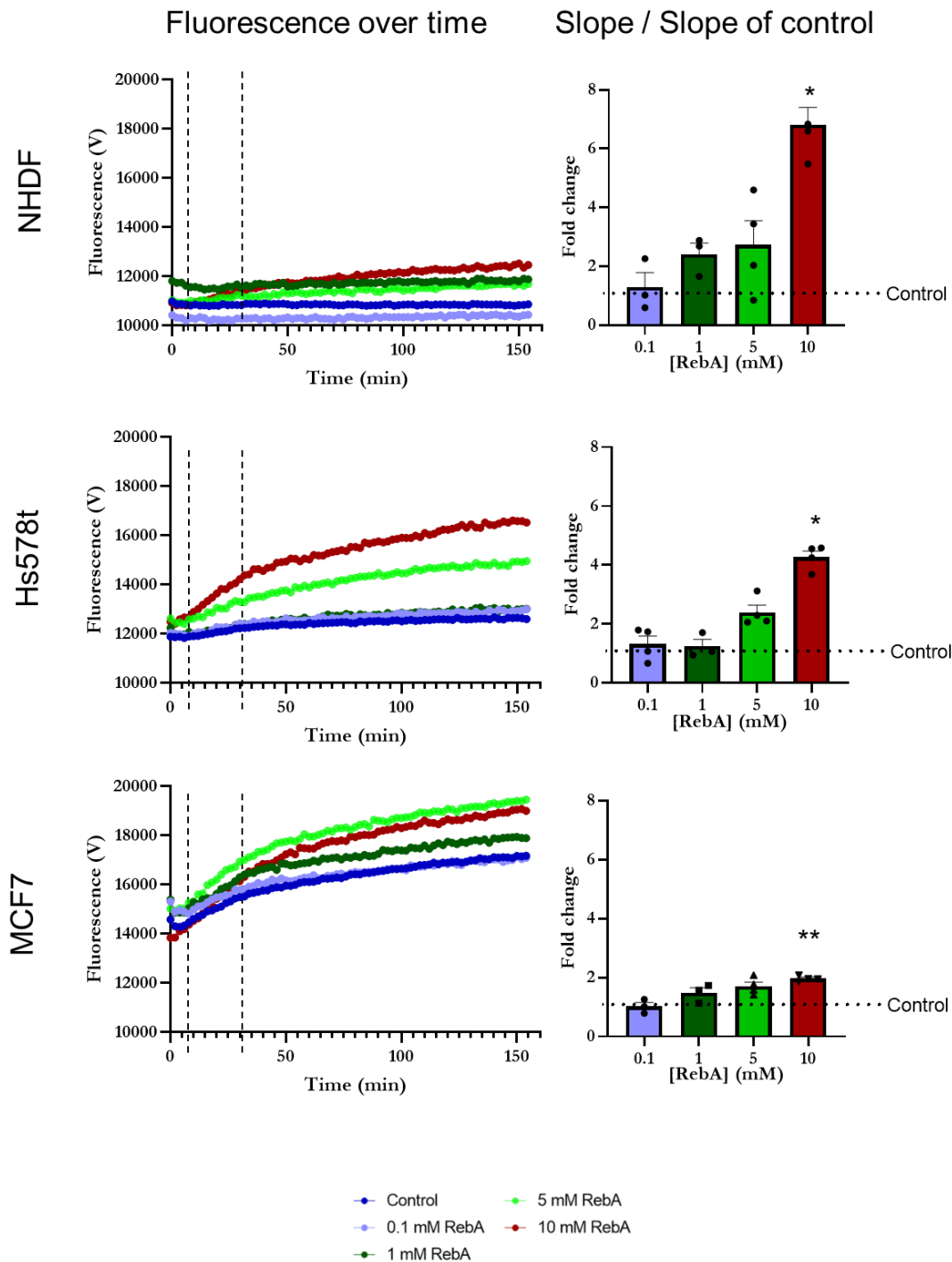


Figure 29: Values of variation of fluorescence over time for NHDF, Hs578t and MCF7, previously subjected to concentrations of RebA of 0, 0.1, 1, 5 and 10 mM, in LG medium, for 24 hours, then treated for 1h with H₂DCFDA. Wavelengths for excitation and emission were 485 and 528 nm. Linear regressions were performed as to obtain the slope of the curves from the variation of fluorescence between the 8 and 36 min, results then normalized by the control. Non-parametric Kruskal-Wallis test followed by Dunn’s post-test for multiple comparisons were performed, comparing each condition of the same cell line with its control, as to determine if there was statistical significance. *: $p < 0.05$; **: $p < 0.01$. Results are expressed as a mean, with error bars for the SEM. $N=3-4$

3.2.4.1 RebA significantly increased oxidation of DCFH into DCF

Exposure to RebA induced significant increases in the rate of oxidation of the probe. Statistical analysis pointed towards significant differences between the concentration of 10 mM and the control for all the cell lines. The most notorious increases in the levels of oxidation of the probe come for the NHDF cells, followed by Hs578t and MCF7, with the lesser fold change in the slope of the curve. Looking at the absolute values of fluorescence over time, especially looking at the controls, NHDF was associated with the lowest values of fluorescence and with less steep curves, while MCF7 had the highest values, factors that can influence the values of fold change in the slopes, as MCF7 were already associated with higher ROS levels and, possibly, higher basal ROS production.

There are several possible explanations for the increase in DCFH oxidation. One of them is related to the possible shift towards a more oxidative phenotype induced by RebA, as suggested by the results of the previous assays. During the process of oxidative phosphorylation in the inner mitochondrial membrane at the electron transport chain, in the complexes I and III, there occurs leakage of electrons that can lead to the formation of radicals, such as superoxide, due to partial reduction of oxygen. There are, however, mechanisms to avoid excessive oxidative stress, including through antioxidant enzymes, such as superoxide dismutases 1 and 2. However, at higher levels of ROS production, there can be an imbalance of this antioxidant mechanism, resulting in oxidative stress. With this, another possible explanation for the increase in the rate of oxidation of the probe can be connected to lower levels of the antioxidant defenses, but further experiments would be required to see how RebA or other SGs affect the expression of the proteins involved in this process. Finally, it is noteworthy to point out that one of the causes suggested for an eventual chemotherapeutic potential of other SGs, such as steviol and stevioside, was due to ROS mediated apoptosis. So, here the cells can also be headed towards this phenomenon, as at the higher concentrations of RebA a slight decrease in cell proliferation was observed. However, it cannot be said for sure if whether is the apparent increase in ROS levels the origin for this or is there other mechanism leading to this higher ROS production. The ROS can, however, have a non-mitochondrial origin, as the assays with H₂DCFDA does not allow for discrimination regarding the origin of this reactive molecules.

With this assay, it appears that RebA and, possibly by extension, other SG, may not be antioxidant. Probable reasons for the different outcomes of other papers could be due to the degree of purity of the samples, as in stevia there are found other types of molecules apart from SGs, and some of those happen to be linked with antioxidant properties, such

as phenolic compounds (Gawel-Bęben et al, 2015), that depending on their concentration may be inducing a net balance favoring an antioxidant response in those papers.

4 – Conclusions

SGs are molecules growing in importance in our society due to its sweetening properties, especially RebA, owing to its abundance in the plant and its taste quality, along with other properties that are being discovered and described in recent literature. However, unlike it was suggested for other SGs, such as steviol and stevioside, RebA appears to have no chemotherapeutic potential, at least for the conditions that were tested in this work, possessing IC50 values way higher than it was expected when compared with the results obtained for other molecules of its family, and without targeted toxicity towards cancer cells, with similar outcomes for the non-tumoral controls. In addition, RebA did not potentiated the cytotoxic effects of DOX – in fact, there was a slight trend towards the opposite effect. This could be due that at those concentrations, RebA may marginally lower cell proliferation, one of the factors that influence DOX's activity. This decrease in cell proliferation can have several origins, one of them being a potential shift towards a more oxidative metabolism, enhancing mitochondrial activity, consistent through most assays that were carried out, which can reflect a, at least partial, reversion of the Warburg effect. This, however, does not discard, in definitive, its use as chemotherapeutic adjuvant for other classes of chemotherapeutic drugs, where the effect it is having in metabolism can, in theory, still be exploited. As the outcomes for these effects were more expressive for high concentrations of this molecule, and having in consideration the lower IC50 observed for other SGs, if they happen to induce a stronger response, in the same proportion, at a metabolic level, they would have a better prospect for therapeutical use, as lower concentrations would be required to achieve a response. The only potentiation of the effects of DOX that was observed came from the effect of the media itself, with HG media, where cells conditioned to have a highly glycolytic profile, had enhanced proliferation and, thus, were more afflicted by DOX when compared to their counterparts in OX medium. This exposure to HG medium, interestingly, did not enhanced the toxicity of DOX towards non-tumoral cells, making it an attractive prospect for future studies.

Furthermore, despite being described as insulin-mimetic regarding the modulation of GLUT transporters, the results obtained in the present work suggest that there may be differences between those molecules beyond that point, as the outcomes from metabolic profiling assays suggest that insulin promotes a more glycolytic metabolism, as expected, while RebA promotes a more oxidative phenotype, as described previously.

Through analysis of alterations RebA caused in the values of OCR and ECAR, results suggest a consistent increase in the levels of non-mitochondrial oxygen consumption.

Spare respiratory capacity, basal respiration and proton leak were also enhanced for some conditions.

It was also observed that RebA appears to induce increases in the levels of ROS, with possible explanations for this being the enhancement of OXPHOS, or even possibly to sources other than the mitochondria. ROS-mediated apoptosis could also be occurring, but further studies are needed to further discriminate the origin of the observed response.

As the effects of RebA were registered for higher concentrations than those achieved in a balanced diet by its consumption as a sweetener, the present study does not argue against its safety for this application.

Overall, the results open the path for new studies regarding the properties of this natural molecule and, eventually, other SGs, as once these effects are fully understood they can be extrapolated into new applications far beyond their use as a sweetener.

5 – References

- AbdelKader, DH. 2016. "The Role of Insulin in Wound Healing Process: Mechanism of Action and Pharmaceutical Applications." *Journal of Analytical & Pharmaceutical Research*, 2 (1): 7-10. <https://doi.org/10.15406/japlr.2015.02.00007>.
- Abu-Eid, R., R. N. Samara, L. Ozbun, M. Y. Abdalla, J. A. Berzofsky, K. M. Friedman, M. Mkrtichyan, and S. N. Khleif. 2014. "Selective Inhibition of Regulatory T Cells by Targeting the PI3K-Akt Pathway." *Cancer Immunology Research*, 2(11):1080-9. <https://doi.org/10.1158/2326-6066.CIR-14-0095>.
- Adekola, Kehinde, Steven T. Rosen, and Mala Shanmugam. 2012. "Glucose Transporters in Cancer Metabolism." *Current Opinion in Oncology*, 24(6):650-4. <https://doi.org/10.1097/CCO.0b013e328356da72>.
- Afonso, G. J.M., J. B. Silva, R. M. Santos, L. M. Rosário, R. M. Quinta-Ferreira, and M. E. Quinta-Ferreira. 2020. "ROS Changes Evoked by the Natural Sweetener Rebaudioside A in a Neuronal System." In *Energy Reports*. Vol. 6:909-914. <https://doi.org/10.1016/j.egy.2019.12.003>.
- Agilent Seahorse XF Cell Mito Stress Test Kit, retrieved from https://www.agilent.com/cs/library/usermanuals/public/XF_Cell_Mito_Stress_Test_Kit_User_Guide.pdf. Date of assess: 30/10/2020
- Aghajanyan, Anush, Zaruhi Movsisyan, and Armen Trchounian. 2017. "Antihyperglycemic and Antihyperlipidemic Activity of Hydroponic *Stevia Rebaudiana* Aqueous Extract in Hyperglycemia Induced by Immobilization Stress in Rabbits." *BioMed Research International*, 2017:9251358. <https://doi.org/10.1155/2017/9251358>.
- Ashkenazi, Avi. 2015. "Targeting the Extrinsic Apoptotic Pathway in Cancer: Lessons Learned and Future Directions." *Journal of Clinical Investigation*, 125(2): 487–489. <https://doi.org/10.1172/JCI80420>.
- Babakhanyan MA, Kh Nahapetyan, Hovhannisyan LE, Simonyan KV, Avetisyan LG, Avetisyan RA, and Chavushyan VA. 2017. "Wound Healing Potential of Hydroponic *Stevia Rebaudiana* in Rats." *Physical Medicine and Rehabilitation Research*, 2 (3) 1-4. <https://doi.org/10.15761/PMRR.1000146>.

- Bhasker, Salini, Harish Madhav, and Mohankumar Chinnamma. 2015. "Molecular Evidence of Insulinomimetic Property Exhibited by Steviol and Stevioside in Diabetes Induced L6 and 3T3L1 Cells." *Phytomedicine*, 22(11):1037-44. <https://doi.org/10.1016/j.phymed.2015.07.007>.
- Bender, Cecilia, Sara Graziano, and Benno F. Zimmermann. 2015. "Study of *Stevia Rebaudiana* Bertoni Antioxidant Activities and Cellular Properties." *International Journal of Food Sciences and Nutrition*, 67(3):1-6 <https://doi.org/10.3109/09637486.2015.1038223>.
- Biolog user manual, MitoPlate™ S-1 and MitoPlate™ I-1 for Characterization of Mammalian Cell Mitochondria. Retrieved from <https://www.biolog.com/wp-content/uploads/2020/10/00P-273-Rev-C-MitoPlate-Instructions-For-Use.pdf>. Date of assess: 30/10/2020
- Boonkaewwan, Chaiwat, and Anyanee Burodom. 2013. "Anti-Inflammatory and Immunomodulatory Activities of Stevioside and Steviol on Colonic Epithelial Cells." *Journal of the Science of Food and Agriculture*, 93(15):3820-5 <https://doi.org/10.1002/jsfa.6287>.
- Boonkaewwan, Chaiwat, Chaivat Toskulkao, and Molvibha Vongsakul. 2006. "Anti-Inflammatory and Immunomodulatory Activities of Stevioside and Its Metabolite Steviol on THP-1 Cells." *Journal of Agricultural and Food Chemistry*, 54 (3) 785–789. <https://doi.org/10.1021/jf0523465>.
- Branco AF, Sampaio SF, Wieckowski MR, Sardão VA, Oliveira PJ. 2013 "Mitochondrial disruption occurs downstream from β -adrenergic overactivation by isoproterenol in differentiated, but not undifferentiated H9c2 cardiomyoblasts: differential activation of stress and survival pathways." *The International Journal of Biochemistry & Cell Biology*, 45(11):2379-91. doi: 10.1016/j.biocel.2013.08.006.
- Buppajarntham, Saranya, Parichart Junpaparp, Rami Salameh, and Catherine Anastasopoulou. 2019. "Insulin." , <https://emedicine.medscape.com/article/2089224>. Date of assess: 30/10/20
- Cai, Chuanxi, and Jianwen Chen. 2004. "Overexpression of Caveolin-1 Induces Alteration of Multidrug Resistance in Hs578T Breast Adenocarcinoma Cells." *International Journal of Cancer*, 111 (4) 522-9. <https://doi.org/10.1002/ijc.20300>.

- Cantor, Jason R., and David M. Sabatini. 2012. "Cancer Cell Metabolism: One Hallmark, Many Faces." *Cancer Discovery*, 2 (10) 881-98. <https://doi.org/10.1158/2159-8290.CD-12-0345>.
- Carew, Jennifer S, and Peng Huang. 2002. "Mitochondrial Defects in Cancer." *Molecular Cancer*, 1 (1) 1:9. <https://doi.org/10.1186/1476-4598-1-9>.
- Chavez KJ, Garimella SV, Lipkowitz S. "Triple negative breast cancer cell lines: one tool in the search for better treatment of triple negative breast cancer". *Breast Disease*. 2010;32(1-2):35-48. doi: 10.3233/BD-2010-0307.
- Chen, Chao, Lu Lu, Shichao Yan, Huimei Yi, Hui Yao, Di Wu, Guangchun He, Xiaojun Tao, and Xiyun Deng. 2018. "Autophagy and Doxorubicin Resistance in Cancer." *Anti-Cancer Drugs*, 29(1):1-9. <https://doi.org/10.1097/CAD.0000000000000572>.
- Chen, Jian Lin, Terry W.J. Steele, and David C. Stuckey. 2018. "Metabolic Reduction of Resazurin; Location within the Cell for Cytotoxicity Assays." *Biotechnology and Bioengineering*, 115(2) 351-358. <https://doi.org/10.1002/bit.26475>.
- Chen, Jiezhong, Xu-Feng Huang, Liang Qiao, and Andrew Katsifis. 2011. "Insulin Caused Drug Resistance to Oxaliplatin in Colon Cancer Cell Line HT29." *Journal of Gastrointestinal Oncology*, 2(1):27-33. <https://doi.org/10.3978/j.issn.2078-6891.2010.028>.
- Chen, Jun-Ming, Jue Zhang, Yong-Mei Xia, Xiao-Xia Wang, and Jian Li. 2018. "The Natural Sweetener Metabolite Steviol Inhibits the Proliferation of Human Osteosarcoma U2OS Cell Line." *Oncology Letters*, 15(4) 5250-5256. <https://doi.org/10.3892/ol.2018.7962>.
- Chen, Jun-ming, Yongmei Xia, Xiaochen Sui, Qingrui Peng, Tongtong Zhang, Jian Li, and Jue Zhang. 2018. "Steviol, a Natural Product Inhibits Proliferation of the Gastrointestinal Cancer Cells Intensively." *Oncotarget*, 9 (41) 26299-26308. <https://doi.org/10.18632/oncotarget.25233>.
- Coller, Hilary A. 2014. "Is Cancer a Metabolic Disease? 9582978472." *American Journal of Pathology*, 184(1): 4–17. <https://doi.org/10.1016/j.ajpath.2013.07.035>.
- Comporti, Mario. 1989. "Three Models of Free Radical-Induced Cell Injury." *Chemico-Biological Interactions*, 72 (1–2):1-56. [https://doi.org/10.1016/0009-2797\(89\)90016-1](https://doi.org/10.1016/0009-2797(89)90016-1).

- Comşa Ş, Cîmpean AM, Raica, M. 2015. "The Story of MCF-7 Breast Cancer Cell Line: 40 years of Experience in Research". *Anticancer Research*, 35(6):3147-54. PMID: 26026074.
- Costa, C., 2017, "Experimental enhancement of cellular OXPHOS reliance for mitochondrial health assessments: Development and characterization of a rapid and efficient method to induce OXPHOS in skin fibroblasts, for the assessment of mitochondrial toxicity and protection", Master's Thesis, University of Coimbra, 10316/86229
- Damyantov, Christo, Desislava Gerasimova, Ivan Maslev, and Veselin Gavrilo. 2012. "Low-Dose Chemotherapy with Insulin (Insulin Potentiation Therapy) in Combination with Hormone Therapy for Treatment of Castration-Resistant Prostate Cancer." *International Scholar Research Notes Urology*, 2012:140182. <https://doi.org/10.5402/2012/140182>.
- Das, Kuntal. 2013. "Wound Healing Potential of Aqueous Crude Extract of Stevia Rebaudiana in Mice." *Revista Brasileira de Farmacognosia*, 23 (2) 351-357. <https://doi.org/10.1590/S0102-695X2013005000011>.
- Djiogue, Sefirin, Armel Hervé Nwabo Kamdje, Lorella Vecchio, Maulilio John Kipanyula, Mohammed Farahna, Yousef Aldebasi, and Paul Faustin Seke Etet. 2013. "Insulin Resistance and Cancer: The Role of Insulin and IGFs." *Endocrine-Related Cancer*, 20(1):1-17 <https://doi.org/10.1530/ERC-12-0324>.
- Esen, F. 2016. "Steviol Glycosides from Stevia Rebaudiana Bertoni: Functional Properties, Safety and Application in Food Industry." *Journal of Molecular Biology and Genetics*, 93(9) 2121-2129 <https://doi.org/10.1002/jsfa.6016>
- Ferreira, Luciana L., Ana Raquel Coelho, Paulo J. Oliveira, and Teresa Cunha-Oliveira. 2018. "Mitochondrial Toxicity Induced by Chemotherapeutic Drugs.", *Mitochondrial Dysfunction Caused by Drugs and Environmental Toxicants*, 593-612 <https://doi.org/10.1002/9781119329725.ch40>.
- Gaweł-Bęben, Katarzyna, Tomasz Bujak, Zofia Nizioł-Łukaszewska, Beata Antosiewicz, Anna Jakubczyk, Monika Karaś, and Kamila Rybczyńska. 2015. "Stevia Rebaudiana Bert. Leaf Extracts as a Multifunctional Source of Natural Antioxidants." *Molecules*, 20(4):5468-5486 <https://doi.org/10.3390/molecules20045468>.

- Geeraert, L., 2019. "Insulin potentiation therapy".Cam-Cancer Consortium. URL <http://cam-cancer.org/en/insulin-potentiation-therapy> (accessed 30/10/2020).
- Geuns, Jan M.C. 2003. "Stevioside." *Phytochemistry*, 64 (5):913-21. [https://doi.org/10.1016/S0031-9422\(03\)00426-6](https://doi.org/10.1016/S0031-9422(03)00426-6).
- Gisbergen, M. W. van, A. M. Voets, M. H.W. Starmans, I. F.M. de Coo, R. Yadak, R. F. Hoffmann, P. C. Boutros, H. J.M. Smeets, L. Dubois, and P. Lambin. 2015. "How Do Changes in the MtDNA and Mitochondrial Dysfunction Influence Cancer and Cancer Therapy? Challenges, Opportunities and Models." *Mutation Research - Reviews in Mutation Research*, 764:16-30 <https://doi.org/10.1016/j.mrrev.2015.01.001>.
- Gupta, Ena, Shweta Kaushik, Shalini Purwar, Ramesh Sharma, AnilK Balapure, and Shanthi Sundaram. 2017. "Anticancer Potential of Steviol in MCF-7 Human Breast Cancer Cells." *Pharmacognosy Magazine* 13 (51) 345–350. https://doi.org/10.4103/pm.pm_29_17.
- Hawkins, P.T., and L.R. Stephens. 2015. "PI3K Signalling in Inflammation." *Biochimica et Biophysica Acta (BBA) - Molecular and Cell Biology of Lipids* 1851 (6) 882-897. <https://doi.org/10.1016/j.bbalip.2014.12.006>.
- Icard, Philippe, Seth Shulman, Diana Farhat, Jean-Marc Steyaert, Marco Alifano, and Hubert Lincet. 2018. "How the Warburg Effect Supports Aggressiveness and Drug Resistance of Cancer Cells?" *Drug Resistance Updates* 38 (May) 1-11. <https://doi.org/10.1016/j.drug.2018.03.001>.
- Jeppesen, P.B., S. Gregersen, C.R. Poulsen, and K. Hermansen. 2000. "Stevioside Acts Directly on Pancreatic β Cells to Secrete Insulin: Actions Independent of Cyclic Adenosine Monophosphate and Adenosine Triphosphate—Sensitvie K⁺ Channel Activity." *Metabolism*, 49 (2) 208-14. [https://doi.org/10.1016/S0026-0495\(00\)91325-8](https://doi.org/10.1016/S0026-0495(00)91325-8).
- Khan, Khurum H., Timothy A. Yap, Li Yan, and David Cunningham. 2013. "Targeting the PI3K-AKT-MTOR Singnaling Network in Cancer." 32(5): 253–265. *Chinese Journal of Cancer*. <https://doi.org/10.5732/cjc.013.10057>.
- Khare, Noopur, and Sheela Chandra. 2019. "Stevioside Mediated Chemosensitization Studies and Cytotoxicity Assay on Breast Cancer Cell Lines MDA-MB-231 and SKBR3." *Saudi Journal of Biological Sciences*, 7: 1596-1601. <https://doi.org/10.1016/j.sjbs.2018.10.009>.

- Koyama, Eriko, Norifumi Sakai, Yuji Ohori, Ken Kitazawa, Osamu Izawa, Kunio Kakegawa, Akiharu Fujino, and Michio Ui. 2003. "Absorption and Metabolism of Glycosidic Sweeteners of Stevia Mixture and Their Aglycone, Steviol, in Rats and Humans." *Food and Chemical Toxicology*, 41 (6) 875-83.
[https://doi.org/10.1016/S0278-6915\(03\)00039-5](https://doi.org/10.1016/S0278-6915(03)00039-5).
- Kuzniewska, B., Cysewski, D., Wasilewski, M., Sakowska, P., Milek, J., Kulinski, T. M., Winiarski, M., Kozielowicz, P., Knapska, E., Dadlez, M., Chacinska, A., Dziembowski, A., & Dziembowska, M., 2020. Mitochondrial protein biogenesis in the synapse is supported by local translation. *EMBO reports*, 21(8), e48882.
<https://doi.org/10.15252/embr.201948882>
- Leslie, N. R. 2003. "Redox Regulation of PI 3-Kinase Signalling via Inactivation of PTEN." *The EMBO Journal*, 22 (20) 5501–5510.
<https://doi.org/10.1093/emboj/cdg513>.
- Li, Shaoli, Yuhang Ren, Yingying Fu, Xingsheng Gao, Cong Jiang, Gang Wu, Hongqiang Ren, and Jinju Geng. 2018. "Fate of Artificial Sweeteners through Wastewater Treatment Plants and Water Treatment Processes." *PLoS ONE* 13(1):e0189867. <https://doi.org/10.1371/journal.pone.0189867>.
- Li, X., W. Lu, W. Shen, Y. Wu, Y. Liu, Y. Tuo, and Y. Liu. 2017. "Growth Inhibitory Effect of Stevioside on Ovarian Cancer through Akt/ERK Pathway." *Biomedical Research*, no. 28: 1820–27.
- Liu, Yong-Yu, Jing Yuan Yu, Dongmei Yin, Gauri Anand Patwardhan, Vineet Gupta, Yoshio Hirabayashi, Walter M. Holleran, et al. 2008. "A Role for Ceramide in Driving Cancer Cell Resistance to Doxorubicin." *The FASEB Journal*, 22(7):2541-51. <https://doi.org/10.1096/fj.07-092981>.
- Martínez-Rojo, Elizabeth, Raquel Cariño-Cortés, Laura Cristina Berumen, Guadalupe García-Alcocer, and Jesica Escobar-Cabrera. 2020. "Stevia Eupatoria and Stevia Pilosa Extracts Inhibit the Proliferation and Migration of Prostate Cancer Cells." *Medicina*, 56(2):90. <https://doi.org/10.3390/medicina56020090>.
- Mizushina, Yoshiyuki, Toshihiro Akihisa, Motohiko Ukiya, Yusuke Hamasaki, Chikako Murakami-Nakai, Isoko Kuriyama, Toshifumi Takeuchi, Fumio Sugawara, and Hiromi Yoshida. 2005. "Structural Analysis of Isosteviol and Related Compounds as DNA Polymerase and DNA Topoisomerase Inhibitors." *Life Sciences*, 77(17):2127-40 <https://doi.org/10.1016/j.lfs.2005.03.022>.

- Neve, Richard M., Kwei Chin, Jane Fridlyand, Jennifer Yeh, Frederick L. Baehner, Tea Fevr, Laura Clark, et al. 2006. "A Collection of Breast Cancer Cell Lines for the Study of Functionally Distinct Cancer Subtypes." *Cancer Cell*, 10(6):515-27 <https://doi.org/10.1016/j.ccr.2006.10.008>.
- Noh, Eun Mi, Young Rae Lee, Kee Oh Chay, Eun Yong Chung, Sung Hoo Jung, Jong Suk Kim, and Hyun Jo Youn. 2011. "Estrogen Receptor α Induces Down-Regulation of PTEN through PI3-Kinase Activation in Breast Cancer Cells." *Molecular Medicine Reports*, 4(2):215-9. <https://doi.org/10.3892/mmr.2011.412>.
- Paul, S., S. Sengupta, T. K. Bandyopadhyay, and A. Bhattacharyya. 2012. "Stevioside Induced ROS-Mediated Apoptosis Through Mitochondrial Pathway in Human Breast Cancer Cell Line MCF-7." *Nutrition and Cancer*, 64(7):1087-94. <https://doi.org/10.1080/01635581.2012.712735>.
- Philippaert, Koenraad, Andy Pironet, Margot Mesuere, William Sones, Laura Vermeiren, Sara Kerselaers, Sílvia Pinto, et al. 2017. "Steviol Glycosides Enhance Pancreatic Beta-Cell Function and Taste Sensation by Potentiation of TRPM5 Channel Activity." *Nature Communications*, 8 (1):14733. <https://doi.org/10.1038/ncomms14733>.
- Pothiwala, Pooja, Sushil K. Jain, and Subhashini Yaturu. 2009. "Metabolic Syndrome and Cancer." *Metabolic Syndrome and Related Disorders*, 7(4):279-88 <https://doi.org/10.1089/met.2008.0065>.
- Prata, Cecilia, Laura Zambonin, Benedetta Rizzo, Tullia Maraldi, Cristina Angeloni, Francesco Vieceli Dalla Sega, Diana Fiorentini, and Silvana Hrelia. 2017. "Glycosides from *Stevia Rebaudiana* Bertoni Possess Insulin-Mimetic and Antioxidant Activities in Rat Cardiac Fibroblasts." *Oxidative Medicine and Cellular Longevity*, 2017:3724545. <https://doi.org/10.1155/2017/3724545>.
- Porporato, Paolo Ettore, Nicoletta Filigheddu, José Manuel Bravo San Pedro, Guido Kroemer, and Lorenzo Galluzzi. 2018. "Mitochondrial Metabolism and Cancer." *Cell Research*, 28:265–280. <https://doi.org/10.1038/cr.2017.155>.
- Potter, Michelle, Emma Newport, and Karl J. Morten. 2016. "The Warburg Effect: 80 Years On." *Biochemical Society Transactions*, 44(5): 1499–1505 <https://doi.org/10.1042/BST20160094>.

- Ren, Hai-Peng, Xiao-Yan Yin, Hai-Ying Yu, and Hai-Feng Xiao. 2017. "Stevioside Induced Cytotoxicity in Colon Cancer Cells via Reactive Oxygen Species and Mitogen-Activated Protein Kinase Signaling Pathways-Mediated Apoptosis." *Oncology Letters*,13(4):2337-2343. <https://doi.org/10.3892/ol.2017.5744>.
- Redza-Dutordoir, Maureen, and Diana A. Averill-Bates. 2016. "Activation of Apoptosis Signalling Pathways by Reactive Oxygen Species." *Biochimica et Biophysica Acta (BBA) - Molecular Cell Research*, 1863(12):2977-2992. <https://doi.org/10.1016/j.bbamcr.2016.09.012>.
- Rizzo, Benedetta, Laura Zambonin, Cristina Angeloni, Emanuela Leoncini, Francesco Vieceli Dalla Sega, Cecilia Prata, Diana Fiorentini, and Silvana Hrelia. 2013. "Steviol Glycosides Modulate Glucose Transport in Different Cell Types." *Oxidative Medicine and Cellular Longevity*, 2013:348169. <https://doi.org/10.1155/2013/348169>.
- Rosignol R, Gilkerson R, Aggeler R, Yamagata K, Remington SJ, Capaldi RA. 2004 "Energy substrate modulates mitochondrial structure and oxidative capacity in cancer cells". *Cancer Research.*, 64(3):985-93. doi: 10.1158/0008-5472.can-03-1101.
- Sarker B, Singh R, Silva R, Roether JA, Kaschta J, Detsch R, Schubert DW, Cicha I, Boccaccini AR., 2014. "Evaluation of fibroblasts adhesion and proliferation on alginate-gelatin crosslinked hydrogel". *PLoS One*, 9(9):e107952. doi:10.1371/journal.pone.0107952.
- Sayed SM, Mahmoud AA, El Sawy SA, Abdelaal EA, Fouad AM, Yousif RS, Hashim MS, Hemdan SB, Kadry ZM, Abdelmoaty MA, Gabr AG, Omran FM, Nabo MM, Ahmed NS., 2013. "Warburg Effect Increases Steady-State ROS Condition in Cancer Cells through Decreasing Their Antioxidant Capacities (Anticancer Effects of 3-Bromopyruvate through Antagonizing Warburg Effect)." *Medical Hypotheses*, 81(5):866-70. <https://doi.org/10.1016/j.mehy.2013.08.024>.
- Serafim, T., 2011, "Mitochondria and Cancer: Opening Pandora's Box", PhD Thesis, University of Coimbra
- Silva FS, Starostina IG, Ivanova VV, Rizvanov AA, Oliveira PJ, Pereira SP, 2016. "Determination of Metabolic Viability and Cell Mass Using a Tandem Resazurin/Sulforhodamine B Assay". *Current Protocols in Toxicology*, 68:2.24.1-2.24.15. doi:10.1002/cptx.1

- Speelmans G, Staffhorst RW, de Kruijff B, de Wolf FA. "Transport studies of doxorubicin in model membranes indicate a difference in passive diffusion across and binding at the outer and inner leaflets of the plasma membrane", 1994. *Biochemistry*, 33(46):13761-8. doi: 10.1021/bi00250a029.
- Speth, P.A.J., van Hoesel, Q.G.C.M. & Haanen, C., 1988. "Clinical Pharmacokinetics of Doxorubicin". *Clinical-Pharmacokinetics*, 15:15–31
<https://doi.org/10.2165/00003088-198815010-00002>
- Srimaroeng, Chutima, Varanuj Chatsudthipong, Amy G. Aslamkhan, and John B. Pritchard. 2005. "Transport of the Natural Sweetener Stevioside and Its Aglycone Steviol by Human Organic Anion Transporter (HOAT1; SLC22A6) and HOAT3 (SLC22A8)." *Journal of Pharmacology and Experimental Therapeutics*, 313(2):621-8. <https://doi.org/10.1124/jpet.104.080366>.
- Sun, Qiang, Jia Li, and Feng Gao. 2014. "New Insights into Insulin: The Anti-Inflammatory Effect and Its Clinical Relevance." *World Journal of Diabetes*, 5(2):89-96 <https://doi.org/10.4239/wjd.v5.i2.89>.
- Tandel, Kirtida R. 2011. "Sugar Substitutes: Health Controversy over Perceived Benefits." *Journal of Pharmacology and Pharmacotherapeutics*, 2(4): 236–243. <https://doi.org/10.4103/0976-500X.85936>.
- Tavares LC, Jarak I, Nogueira FN, Oliveira PJ, Carvalho RA. 2015 "Metabolic evaluations of cancer metabolism by NMR-based stable isotope tracer methodologies". *European Journal of Clinical Investigation*, 45 Suppl 1:37-43. doi: 10.1111/eci.12358.
- Tsou, Shang-Hsun, Tzer-Ming Chen, Hui-Ting Hsiao, and Yen-Hui Chen. 2015. "A Critical Dose of Doxorubicin Is Required to Alter the Gene Expression Profiles in MCF-7 Cells Acquiring Multidrug Resistance." *PLoS ONE* 10 (1):e0116747. <https://doi.org/10.1371/journal.pone.0116747>.
- Vaupel, Peter, Heinz Schmidberger, and Arnulf Mayer. 2019. "The Warburg Effect: Essential Part of Metabolic Reprogramming and Central Contributor to Cancer Progression." *International Journal of Radiation Biology*, 95(7):912-919. <https://doi.org/10.1080/09553002.2019.1589653>.
- Wahrheit, Judith, and Elmar Heinzle. 2014. "Quenching Methods for the Analysis of Intracellular Metabolites." In *Methods in Molecular Biology*, 1104:211-21 https://doi.org/10.1007/978-1-62703-733-4_14.

- Wallace, Douglas C. 2012. "Mitochondria and Cancer." *Nature Reviews Cancer*, 12(10): 685–698. <https://doi.org/10.1038/nrc3365>.
- Wallace, Kendall B., Vilma A. Sardão, and Paulo J. Oliveira. 2020. "Mitochondrial Determinants of Doxorubicin-Induced Cardiomyopathy." *Circulation Research* 126(7):926-941. <https://doi.org/10.1161/CIRCRESAHA.119.314681>.
- Wang, Sheng Fan, Yueh Ching Chou, Nirmal Mazumder, Fu Jen Kao, Esly D. Nagy, Peter Guengerich, Cheng Huang, Hsin Chen Lee, Ping Shan Lai, and Yune Fang Ueng. 2013. "7-Ketocholesterol Induces P-Glycoprotein through PI3K/MTOR Signaling in Hepatoma Cells." *Biochemical Pharmacology*, 86(4):548-60. <https://doi.org/10.1016/j.bcp.2013.06.006>.
- Wang, Zilong, Jinpei Wang, Minhua Jiang, Yutuo Wei, Hao Pang, Hang Wei, Ribo Huang, and Liqin Du. 2015. "Selective Production of Rubusoside from Stevioside by Using the Sophorose Activity of β -Glucosidase from *Streptomyces* Sp. GXT6." *Applied Microbiology and Biotechnology*, 99(22):9663-74. <https://doi.org/10.1007/s00253-015-6802-z>.
- Wei, Zhao, Li Liang, Liu Junsong, Chen Rui, Chang Shuai, Qiu Guanglin, He Shicai, et al. 2015. "The Impact of Insulin on Chemotherapeutic Sensitivity to 5-Fluorouracil in Gastric Cancer Cell Lines SGC7901, MKN45 and MKN28." *Journal of Experimental & Clinical Cancer Research*, 34 (1):1303-1308. <https://doi.org/10.1186/s13046-015-0151-8>.
- Wu, Hao, Minfeng Ying, and Xun Hu. 2016. "Lactic Acidosis Switches Cancer Cells from Aerobic Glycolysis Back to Dominant Oxidative Phosphorylation." *Oncotarget*, 7(26):40621-40629 <https://doi.org/10.18632/oncotarget.9746>.
- Yasukawa, Ken, Susumu Kitanaka, and Shujiro Seo. 2002. "Inhibitory Effect of Stevioside on Tumor Promotion by 12-O-Tetradecanoylphorbol-13-Acetate in Two-Stage Carcinogenesis in Mouse Skin." *Biological & Pharmaceutical Bulletin* 25(11):1488-90. <https://doi.org/10.1248/bpb.25.1488>.
- Yu, T., M. Gao, P. Yang, Q. Pei, D. Liu, D. Wang, X. Zang, and Y. Liu. 2017. "Topical Insulin Accelerates Cutaneous Wound Healing in Insulin-Resistant Diabetic Rats." *American Journal of Translational Research*, 9:4682–93. <https://www.ncbi.nlm.nih.gov/pmc/articles/PMC5666074/>

Zhao, Na, Martin C Woodle, and A. James Mixson. 2018. "Advances in Delivery Systems for Doxorubicin." *Journal of Nanomedicine & Nanotechnology*, 9(5): 519. <https://doi.org/10.4172/2157-7439.1000519>.

Zong, Wei Xing, Joshua D. Rabinowitz, and Eileen White. 2016. "Mitochondria and Cancer." *Molecular Cell*. 61(5):667-676. <https://doi.org/10.1016/j.molcel.2016.02.011>.

6 – Supplementary data

In this section, there are present additional figures regarding the parameters of mitochondrial respiration calculated through the Seahorse Mitostress assay (Figures S1 and S2). Effect of RebA on cell proliferation are also shown (Figure S3), obtained through resazurin assays.

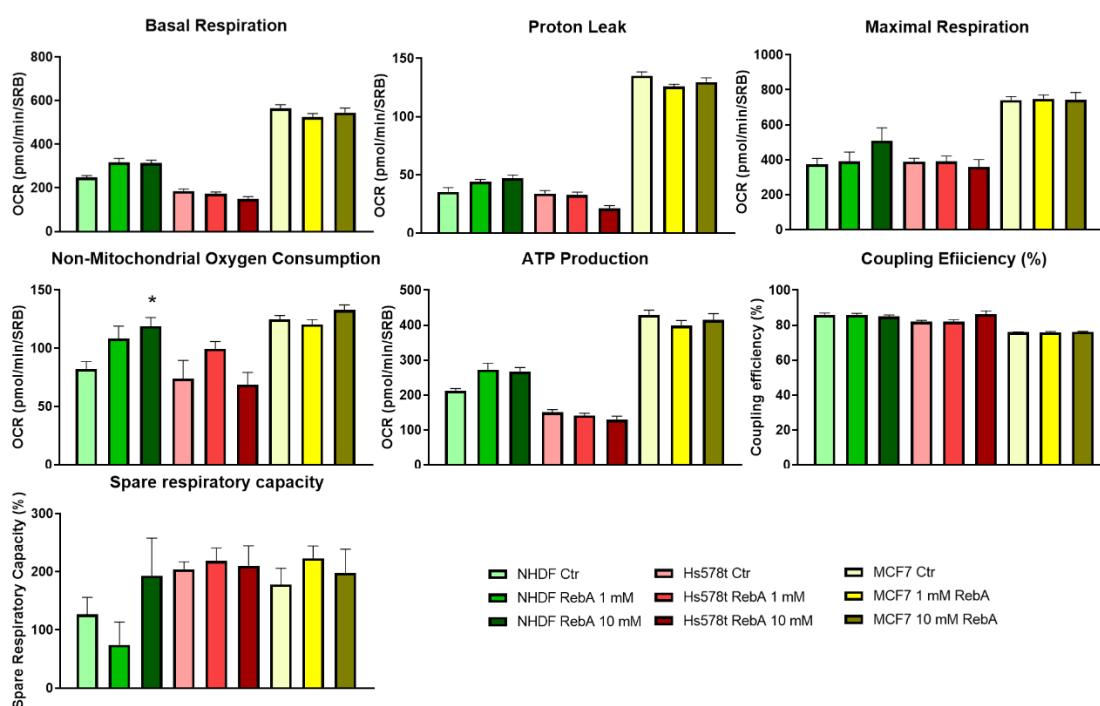


Figure S1: Changes in the different parameters measured through the Mito Stress assay for NHDF, Hs578t and MCF7 cell, grown in LG medium and treated for 24h with 1 and 10 mM of RebA. Non-parametric Kruskal-Wallis test followed by Dunn's post-test for multiple comparisons were performed, comparing each condition of the same cell line with its control, as to determine if there was statistical significance. *: $p < 0.05$. Results are expressed as a mean, with error bars for the SEM. N=4

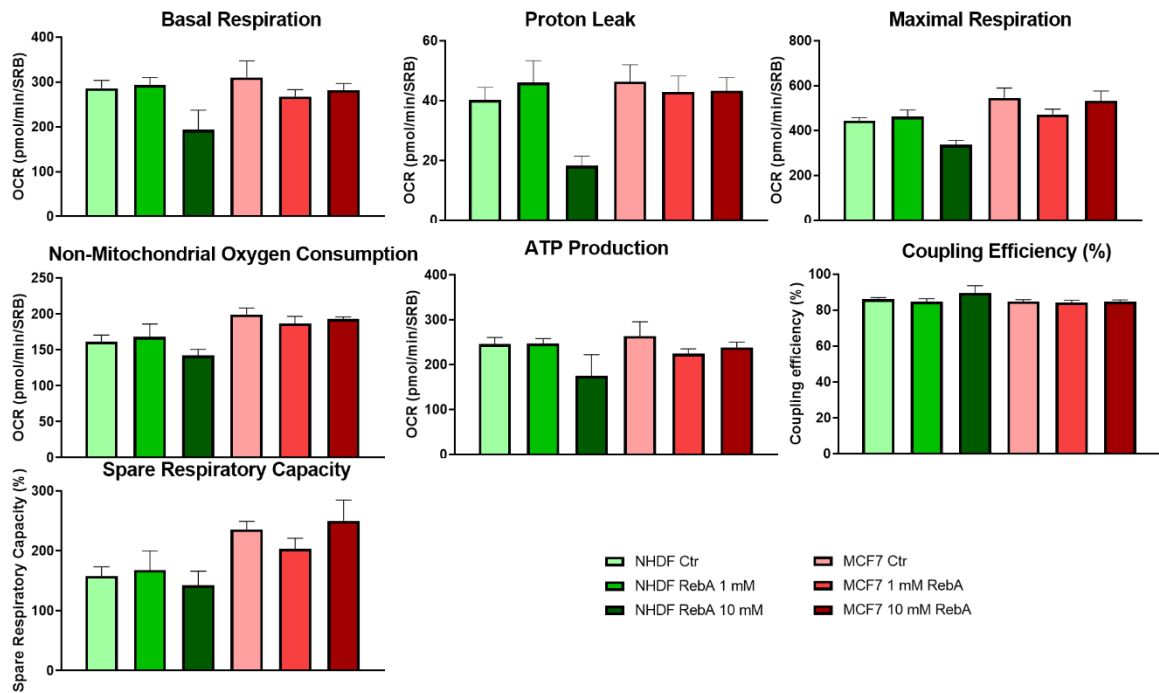


Figure S2: Changes in the different parameters measured through the Mito Stress assay for NHDF and MCF7 cells, grown in OX medium and treated for 24h with 1 and 10 mM of RebA. Non-parametric Kruskal-Wallis test followed by Dunn's post-test for multiple comparisons were performed, comparing each condition of the same cell line with its control, as to determine if there was statistical significance. *: $p < 0.05$. Results are expressed as a mean, with error bars for the SEM. N=4

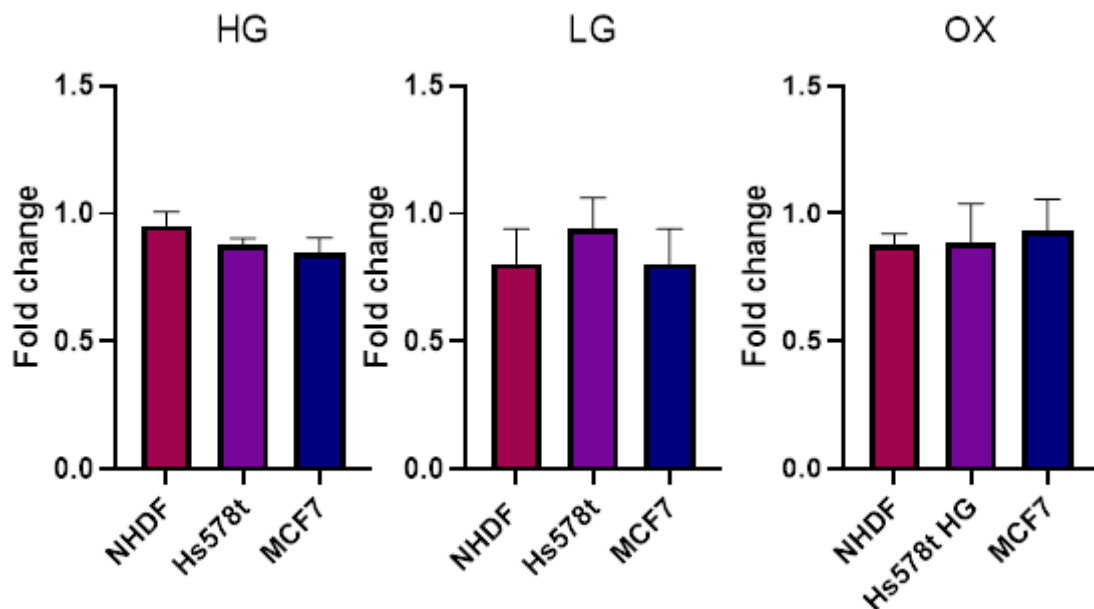


Figure S3: Resazurin assays suggesting decreases in cell proliferation induced by 5 mM of RebA, after 24h of exposure. Results were obtained for NHDF, Hs578t and MCF7 cells grown in HG, LG and OX. N=4